Dissertation

submitted to the
Combined Faculties for the Natural Sciences and for Mathematics
of the Ruperto-Carola University of Heidelberg, Germany
for the degree of
Doctor of Natural Sciences

presented by

Laura Hüser, Master of Science in Cell Biology and Physiology

born in: Essen, Germany

Oral-examination: 08.06.2018

The role of SOX2 in resistance towards targeted therapy

Referees: Prof. Dr. Viktor Umansky

Prof. Dr. Jochen Utikal

Declarations according to § 8 (3) b) and c) of the doctoral degree regulations:

b) I hereby declare that I have written the submitted dissertation myself and in this process have used no other sources or materials than those expressly indicated,

c) I hereby declare that I have not applied to be examined at any other institution, nor have I used the dissertation in this or any other form at any other institution as an examination paper, nor submitted it to any other faculty as a dissertation.

Heidelberg, 29.03.2018

(Laura Hüser)

This Thesis is dedicated to my parents who always supported me.

Parts of this thesis have been published in:

<u>Conferences and workshop presentations</u>:

Laura Hüser and Jochen Utikal

Poster presentation: "Investigating the role of SOX2 in TGF-β signaling andtherapy resistance in melanoma pathogenesis"

DKFZ PhD Retreat, July 2016, Weil der Stadt, Germany

Summerschool presentation: "Investigating the role of SOX2 in TGF-β signaling and therapy resistance in melanoma pathogenesis"

Anglo-German Research Training Initiative, July 2016, London, England

Laura Hüser, Sachindra, Lionel Larribere, Daniel Novak, Aniello Federico, Karol Grandos, Viktor Umansky, Peter Altevogt and Jochen Utikal

Poster presentation: "The role of SOX2 in therapy resistance in"

Summerschool in Translational Cancer Research, October 2017, Albufeira, Portugal

Laura Hüser, Sachindra, Karol Grandos, Lionel Larribere, Daniel Novak, Aniello Federico, Viktor Umansky, Peter Altevogt and Jochen Utikal

Poster presentation: "New mechanism of adaptive resistance towards targeted therapy in melanoma"

Hallmarks of Skin Cancer Conference, November, 2017

Laura Hüser, Sachindra, Karol Grandos, Lionel Larribere, Daniel Novak, Aniello Federico, Viktor Umansky, Peter Altevogt and Jochen Utikal

Poster presentation: "New mechanism of adaptive resistance towards targeted therapy in melanoma"

DKFZ PhD poster session, November 2017, Heidelberg, Germany

Within the thesis, works from the following publications were included:

Hüser L, Sachindra, Granados K, Federico A, Larribère L, Novak D, Umansky V, Altevogt P, and Utikal J (2018) SOX2-mediated upregulation of CD24 promotes adaptive resistance towards targeted therapy in melanoma. Resubmitted to IJC

Table of Contents

Abstract

Melanoma is often characterized by a constitutively active MAP kinase pathway. For inhibition of the aberrantly activated MAP kinase pathway targeted therapies with specific BRAF inhibitors are available that are very effective in the beginning but futile as soon as resistance occurs after a few months. Hence, a better understanding of the mechanisms mediating resistance is necessary to increase the success of the treatment. In this study I observed that SOX2 and CD24 were upregulated shortly after the BRAF inhibitor treatment was started. A similar upregulation was seen in melanoma-derived induced pluripotent cancer cells (iPCCs) which are resistant to targeted therapy. SOX2 and CD24 are known to promote an undifferentiated and cancer stem cell-like phenotype associated with resistance. Therefore, I elucidated the role of SOX2 and CD24 in resistance to targeted therapy in more detail. I found that the upregulation of SOX2 and CD24 required activation of STAT3. The STAT3 activation was caused by soluble factors which were at least partially cleaved by sheddases. Moreover, I detected that SOX2 induced the expression of CD24 by binding to its promoter. Additionally, I found that the overexpression of SOX2 significantly increased the resistance towards BRAF inhibitors, while SOX2 knockdown rendered the cells more sensitivity towards treatment. CD24 overexpression could mimic the effect of SOX2 overexpression while CD24 knockdown in SOX2 overexpressing cells re-established the sensitivity towards BRAF inhibitors. Furthermore, the overexpression of CD24 or SOX2 induced Src and STAT3 activity. Importantly, the more resistant SOX2 or CD24 overexpressing cells were still sensitive to Src/STAT3 inhibition. In contrast, in acquired resistance neither SOX2 nor CD24 played a major role. Here, other molecules and pathways mediate the cells' resistance to the treatment. Therefore, I suggest that the BRAF inhibitor induced activation of STAT3 and the resulting increased expression of SOX2 and CD24 work as an escape pathway to save some cancer cells from the BRAF inhibitor-induced cell death. In the long term these cells can then acquire other mechanisms to circumvent the BRAF inhibitor action and regrow. Thus, to prevent adaptive resistance it might be beneficial to combine Src/STAT3 inhibitors together with MAP kinase pathway inhibitors.

Zusammenfassung

Im malignen Melanom ist meistens der MAP Kinase Signalweg unverhältnismäßig stark aktiviert. Daher wurden zur Melanomtherapie Moleküle entwickelt, die diesen Signalweg inhibieren, z.B. BRAF Inhibitoren. Diese sind zu Beginn sehr effektiv, aber da sich meist recht schnell eine Resistenz ausbildet, stellt diese Therapie einen Zeitgewinn, aber keine dauerhafte Lösung dar. Deshalb ist es wichtig, die Mechanismen der Resistenzbildung zu erforschen und somit den Erfolg dieser Form der Therapie zu erhöhen.

In dieser Arbeit habe ich festgestellt, dass die SOX2 und CD24 Expression kurz nach der Behandlung von Melanomzellen mit BRAF Inhibitoren erhöht war. Eine ähnlich erhöhte Expression von SOX2 und CD24 konnte ich in induzierten, pluripotenten Krebszellen, die aus Melanomzellen gewonnen wurden, nachweisen. Deshalb habe ich die Rolle von SOX2 und CD24 in der Resistenzbildung gegen BRAF Inhibitoren genauer untersucht. Ich konnte feststellen, dass eine STAT3 Aktivierung für die durch BRAF Inhibitoren erhöhte Expression von SOX2 und CD24 notwendig ist. STAT3 wird durch Faktoren im Überstand aktiviert, welche nach der Behandlung mit BRAF Inhibitoren angereichert werden. Diese Faktoren werden zumindest teilweise von Sheddasen gespalten. Des Weiteren konnte ich zeigen, dass SOX2 direkt an den Promotor von CD24 bindet und somit für die erhöhte CD24 Expression verantwortlich ist. Außerdem konnte ich nachweisen, dass eine Überexpression von SOX2 zu einer signifikant erhöhten Resistenz gegen BRAF Inhibitoren führt, während SOX2 Knockdown die Zellen sensitiver gegenüber BRAF Inhibitoren macht. Eine CD24 Überexpression zeigt den gleichen Effekt wie eine SOX2 Überexpression, während CD24 Knockdown in den resistenteren SOX2 überexprimierenden Zellen zu einer Wiederherstellung der Sensitivität gegenüber dem BRAF Inhibitor führt. Des Weiteren führen sowohl SOX2 als auch CD24 Überexpression zur Aktivierung von Src und STAT3. Eine wichtige Beobachtung war, dass die resistenteren SOX2 oder CD24 überexprimierenden Zellen noch immer sensitiv gegenüber Src und STAT3 Inhibitoren waren. Im Gegensatz zur adaptiven Resistenz konnte ich zeigen, dass bei der erworbenen Resistenz weder SOX2 noch CD24 eine wichtige Rolle spielen. Dafür sind bei der erworben Resistenz andere Moleküle und Signalwege wichtig um den Effekten des Inhibitors zu entkommen.

Meine Arbeit gibt daher einen Hinweis darauf, dass die durch den BRAF Inhibitor ausgelöste Aktivität von STAT3 und die damit einhergehende erhöhte Expression von SOX2 und CD24 eine Art Fluchtweg darstellen, um so einige Zellen vor dem durch den Inhibitor hervorgerufen Zelltod zu schützen. Diese Zellen können dann mit der Zeit andere Mechanismen erwerben, um dem BRAF Inhibitor zu entkommen und weiter zu wachsen. Aus diesen Gründen wäre es vorteilhaft, Src oder STAT3 Inhibitoren zusätzlich zu den Inhibitoren des MAP Kinase Signalwegs zu verabreichen, da so eventuell die adaptive Resistenz verhindert werden kann.

List of Figures

Abbreviations

^{o}C	Degree Celcius
18S	18S ribosomal RNA
ABC	ATP-binding cassette
ADAM	a disintegrin and metalloproteinase
AGPAT9	1-Acyl-Sn-Glycerol-3-Phosphate O-Acyltransferase 9
AKT	v-akt murine thymoma viral oncogene
AXL	AXL receptor tyrosine kinase
bp	Base pair
BCA	Bichinonic Acid Protein Assay
BCL2	B-cell lymphoma 2
BRAF	B-Raf Proto-Oncogene, Serine/Threonine kinase
BRAFi	BRAF inhibitor
BSA	Bovine Serum Albumin
CD24	Cluster of differentiation 24
CDK	Cyclin-dependent kinase
CDK4	Cyclin-dependent kinase 4
CRAF	C-Raf Proto-Oncogene, Serine/Threonine kinase
CSCs	Cancer stem cells
CTC	Circulating tumor cells
CTLA-4	Cytotoxic T lymphocyte antigen 4
Ctrl	Control
Dab	Dabrafenib
DCT	Dopachrome Tautomerase
DDR1	Discoidin Domain Receptor Tyrosine Kinase 1

DKFZ	Deutsches Krebsforschungszentrum
DMSO	Dimethylsulfoxide
DMEM	Dulbecc's modified eagle's medium
DNA	Deoxyribonuleic acid
DRMs	detergent-resistant membrane domains
Dtk	TYRO3 protein tyrosine kinase
DUSP	Dual-specificity phosphatase
EGFR	Epidermal Growth Factor Receptor
EMT	Epithelial-to- Mesenchymal Transition
Eph	Ephrin receptor
ER	endoplasmic reticulum
ErbB3	v-erb-b2 avian erythroblastic leukemia viral oncogene homolog 3
ERK	Extracellular Signal Regulated Kinase
ESCs	Embryonic stem cells
EV	Empty vector
FACS	Fluorescence-activated cell sorting
FAK	Focal adhesion kinase
FDA	Food and Drug Administration
FOXD3	Forkhead Box D1
GAPDH	Glyceraldehyde 3-phosphate dehydrogenase
GPI	glycosyl-phosphatidylinositol
GTP	Guanosine triphosphate
H	hour
HMG	High-Mobility-Group
HMGS	human melanocyte growth supplement

IHC	Immunohistochemistry
IF	Immunoflurescence
IL	Interleukin
IP	Immunoprecipitation
iPCCs	induced Pluripotent Cancer Cells
JARID1B	lysine- specific demethylase 5B
KD	Knockdown
L1cam	L1 cell adhesion molecule
LB	lysogeny broth
MAPK	Mitogen Activated Protein Kinase
M-CSF R	monocyte colony stimulating factor receptor
MEK	Mitogen Activated Protein Kinase Kinase
MITF	Microphthalmia-Associated Transcription Factor
mRNA	Messenger Ribonuleic Acid
mTOR	mechanistic Target of Rapamycin
NC	Neural crest
NEAA	non-essential amino acids
NF-kappa B	nuclear factor kappa B
NHM	Normal Human Melanocytes
NRAS	Neuroblastoma RAS viral Oncogene Homolog
NURP1	Nuclear protein 1
OE	Overexpression
PBS	Phosphate buffered saline
PCR	Polymerase Chain Reaction
PD-1	Programmed death 1

PDGFRβ	platelet-derived growth factor receptor, beta polypeptide
PFA	Paraformaldehyde
PGC1α	peroxisome proliferator-activated receptor gamma coactivator 1 alpha
PI	Propidium Iodide
PI-3K	phosphatidylinositol 3-kinase
PIP3	Phosphatidylinositol phosphate
PTEN	Phosphatase and tensin homolog
PVDF	Polyvinylidenfluorid
qPCR	Quantitative real-time polymerase chain reaction
RAF	rat fibrosarcoma
RAS	Rat sarcoma
Res	Resistant
RNA	ribonucleic acid
RTKs	Receptor tyrosine Kinases
RUNX3	Runt-related transcription factor 3
SFRP1	Secreted frizzled-related protein 1
shRNA	short hairpin RNA
siRNA	small interfering RNA
SOB	Super optimal broth
SOS	son of sevenless
SOX	SRY (sex determining region Y)-box
SPRY	Sprouty
STAT3	signal transducer and activator of transcription 3
TGFβ	Transforming growth Factor β
TMA	Tissue Microarray

TNF	Tumor Necrosis Factor
Tra	Trametinib
UV	Ultraviolet
VEGF	Vascular Endothelial Growth Factor
vem	Vemurafenib
vs	Versus
WB	Western Blot
WT	Wild Type

1 Introduction

1.1 Melanoma

Melanoma is a skin cancer which arises from transformed melanocytes. The malignant degeneration of melanocytes in the epidermis is the most frequent form of this disease and is called cutaneous melanoma. The other, non-cutaneous melanomas, can arise from the choroidal layer of the eye or the mucosal surfaces of the respiratory, gastrointestinal, and genitourinary tract (Tsao et al. 2012). Melanoma is one of the most aggressive types of skin cancer as it only represents 4 % of the dermatological cancer cases but leads to 80 % of deaths caused by skin cancer (Miller & Mihm 2013). Melanoma incidences increase in many parts of the world where light-skinned people live. Now, melanoma is one of the most frequent cancers in light-skinned people. One risk factor for developing melanoma is the exposure to ultraviolet (UV) light, which is part of the solar radiation, as this can cause genetic mutations in melanocytes (Gandini et al. 2005; Rastrelli et al. 2014). The defensive mechanism to protect the skin from the UV damage is tanning. During tanning the melanocytes produce melanin which is transferred to keratinocytes and which absorbs and scatters the UV light (Miller & Mihm 2013). People with darker skin have a better protection from UV light and therefore have a lower risk of developing cutaneous melanoma in comparison to light-skinned people (Fajuyigbe & Young 2016). Other melanoma risk factors are immunosuppression, i.e. after organ transplantation (Moloney et al. 2006), a high number of congenital melanocytic nevi (Ribeiro et al. 2016) or a melanoma family history (Read et al. 2015).

1.1.1 Melanoma therapy

The mutations causing melanoma are diverse and during melanoma pathogenesis the tumors develop into a quite heterogeneous cell population. For this reason, the treatment of melanoma differs according to criteria as stage and mutational status. In primary stage tumors surgical excision is still the first-line treatment. After excision the thickness of the tumor and the result of the lymph node biopsy direct the next step of treatment. Before the age of targeted therapy, the most commonly used therapy for

metastatic melanoma was chemotherapy with drugs such as dacarbazine and immunotherapy mostly with interleukin-2 (IL-2). These were either given separately or in combination (Bhatia et al. 2009).

Nowadays, there are several therapeutic options for the treatment of patients with metastatic melanoma. These can be divided into two groups: the targeted therapies and the immune therapies.

1.1.1.1 Targeted Therapy

The most common mutation in melanoma is the BRAF^{V600E} mutation leading to a constitutive activation of the mitogen-activated protein Kinase (MAPK) pathway (Figure 1) which plays a major role in proliferation and survival of cells (Muñoz-Couselo et al. 2015). Therefore, cells with this mutation have a dramatic growth increase. Melanoma cells with this mutation can be treated with the FDA approved BRAF inhibitors dabrafenib (GSK2118436) or vemurafenib (PLX4032) (Samatar & Poulikakos 2014). Unfortunately, BRAF inhibitors only increase the lifespan of patients about 6-7 months since resistance occurs after a short period of treatment (Klinac et al. 2013).

Another possibility to target the MAPK pathway in patients with BRAF or NRAS mutation is to target MEK1/2 which is downstream of BRAF and NRAS. Trametinib (GSK1120212) which inhibits MEK1 and 2 and cobimetinib (GDC-0973, XL-518) which inhibits the catalytic activity of MEK1 were developed and approved by the FDA (Colombino et al. 2014), but also here resistance towards the inhibitor certainly occurs.

More recently, the FDA approved the combination of vemurafenib and cobimetinib as well as the combination of dabrafenib and trametinib for the treatment of patients with a BRAF^{V600E} mutation. These combination therapies result in a significantly longer survival than the monotherapy (Flaherty et al. 2012; Klinac et al. 2013; Long et al. 2017; Long et al. 2014). Furthermore, a second generation of vemurafenib (plx8394, plx7904) with less side effects and higher efficiency was developed (Zhang et al. 2015). Noteworthy, plx8394 is now in a clinical trial phase 1/2a with an estimated completion in the year 2020 (https://clinicaltrials.gov/ct2/show/NCT02428712).
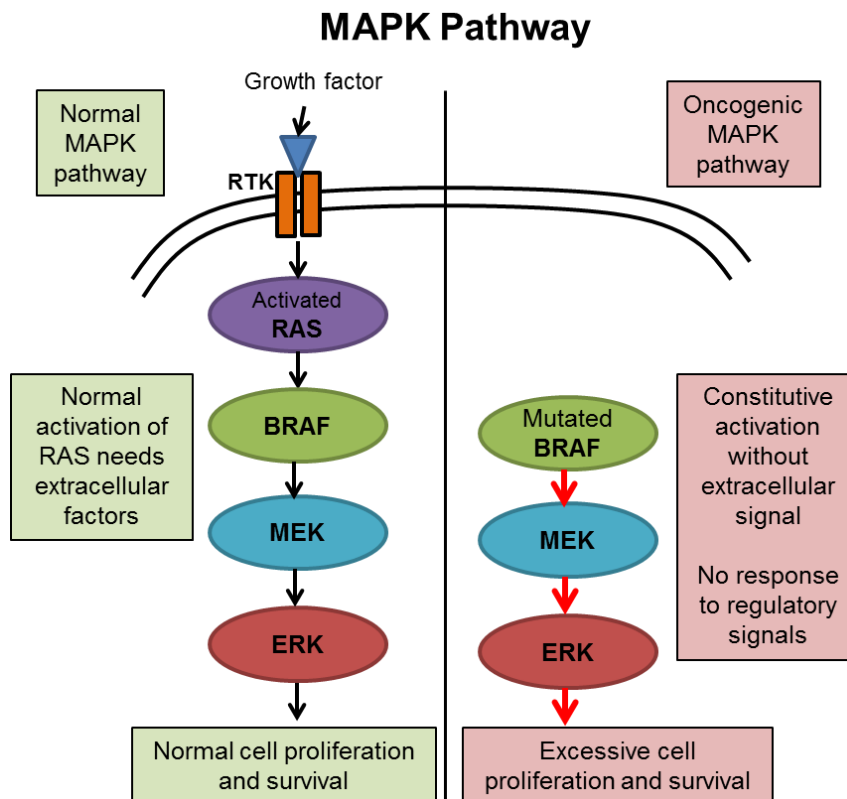
Figure 1: Normal vs oncogenic MAPK pathway. Mutation of BRAF leads to a constitutive activation of the MAPK pathway. No growth factors, which are usually essential for the activation of wild type BRAF, are needed anymore. BRAF mutation leads to an excessive cell proliferation and survival. This figure was adapted from Muñoz-Couselo et al. 2015.

1.1.1.2 Immunotherapy

As melanoma is a highly immunogenic tumor immunotherapy can be used to stimulate the immune system to attack the tumor. Formerly, for this purpose IL-2 or Interferon alpha (IFN-α) were utilized (Bhatia et al. 2009). But this approach had heavy side effects and was not as effective as the new immunotherapies which were developed after having a better understanding of the immune system. New immune checkpoint inhibitors developed in the last decade such as targeting cytotoxic T-lymphocyte-associated protein 4 (CTLA-4) and programmed cell death protein 1 (PD-1) showed very promising results and are therefore used in the clinics. CTLA-4 is a molecule which downregulates the response of T-cells. Tumor cells escape from the immune system by expressing high amounts of CTLA-4 and thereby inhibiting T-cell activity. Ipilimumab is a monoclonal antibody that blocks CTLA-4 and hence leads to an increase in cytotoxic T-cell activation. These T-cells can then kill the tumor cells (Sanlorenzo et al. 2014).

PD-1 is a receptor on T-cells which is activated by PDL-1 and PDL-2 leading to an inhibition of cytotoxic T-cells. In a healthy system this is used to avoid autoimmunity while cancer cells use PDL-1 to inhibit the immune system. Nivolumab and pembrolizumab are monoclonal antibodies that target PD-1 and block it. Hence, this treatment leads to an increased immune response also against the tumor (Topalian et al. 2017; Sanlorenzo et al. 2014).

1.1.2 Melanoma drug resistance

Due to the development of a new generation of drugs targeting the MAPK pathway, the overall survival of metastatic melanoma patients increased significantly. But as described in 1.1.1.1 resistance towards targeted therapy limits its therapeutic efficacy. Resistance can be divided into intrinsic, adaptive and acquired resistance. Intrinsic resistance is already present before the administration of a targeted therapy compound and hence these patients do not respond to therapy at all (Spagnolo et al. 2015). Adaptive resistance occurs shortly after the application of the drug to the tumor cells while acquired resistance develops after continuous inhibitor treatment (Kugel & Aplin 2014).

1.1.2.1 Intrinsic resistance

About 15 % of melanoma patients do not respond to BRAF inhibitor treatment due to intrinsic (primary) resistance (Spagnolo et al. 2015). The mechanisms of intrinsic resistance are highly studied. One know mechanism of resistance are mutations in RAC1, which plays an important role in cell proliferation and migration (Van Allen et al. 2014). Furthermore, it was demonstrated that the secretion of HGF/cMET is involved in primary resistance. HGF can be secreted by the cancer cells leading to a paracrine activation of PI3K which then promotes tumor cell growth and thereby circumvents the growth inhibitory effect of BRAF inhibitors (Manzano et al. 2016). Furthermore, mutation in the cyclin-dependent kinase 4 (CDK4) or amplification of cyclin D1 which are both important regulators of cell proliferation promotes intrinsic resistance (Smalley et al. 2008). Another mechanism is a loss of PTEN, a tumor suppressor and negative regulator of PI3K. It has been shown that patients with inactive PTEN are more resistant towards BRAF inhibitor treatment (Nathanson et al. 2013). Moreover, a loss of the tumor

suppressor NF1 causing an activation of RAS, PI3K and MAPK pathways has also been shown to play a role in primary resistance (Gibney & Smalley 2013).

1.1.2.2 Adaptive resistance

Adaptive resistance occurs rather fast after the application of the drug and is a mechanism to compensate for the action of the targeted therapy. Therefore, the tumor cells escape the inhibitor-induced cell death and can establish acquired resistance mechanisms allowing regrowth of the tumor (Kugel & Aplin 2014). The different known mechanisms of adaptive resistance towards BRAF inhibitors are summarized by Kugel & Aplin (2014) as shown in Figure 2. One possibility to overcome the inhibitory effect of the drug is to reactivate ERK1/2. This happens by downregulating the expression of DUSP and SPRY. DUSPs usually dephosphorylate ERK and thereby inactivate ERK. Hence, the lower expression of DUSPs causes a longer activation time of ERK. SPRY inhibits the activation of NRAS and if this inhibitor is downregulated, EGFR can easier activate NRAS resulting in an increased MAPK pathway activation. Another possibility is that MAPK inhibition leads to an increased AKT activation by an increase in PDGFRβ and ErbB3. The influence of PDGFRβ in adaptive resistance was also shown by Sun et al. (2014). Furthermore, a metabolic switch from glycolysis to oxidative phosphorylation, which favors the survival of the cells, can be the consequence of BRAF inhibitor treatment. This is due to an inhibitor induced expression of PGC1α and JARID1B which both favor oxidative phosphorylation (Kugel & Aplin 2014).
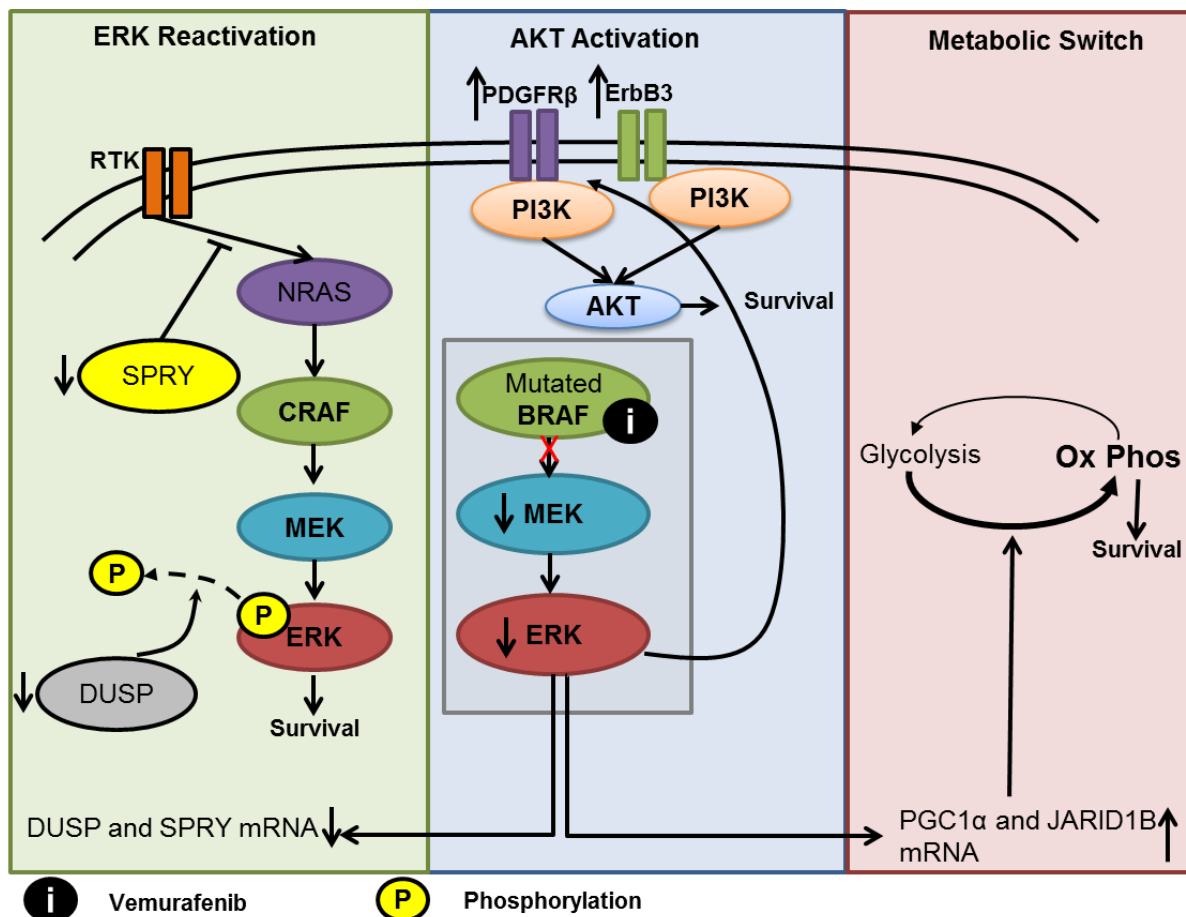
Figure 2: Mechanisms of adaptive resistance. Left: Reactivation of ERK1/2 by decreased expression of DUSP (Dual-specificity phosphatase) due to BRAF inhibitor treatment. DUSP facilitates the dephosphorylation of ERK (inactivation of ERK). Also SPRY (Sprouty) expression is downregulated. SPRY is an inhibitor of MAPK pathway activation. **Middle:** BRAF inhibition causes an increased expression of ErbB3 and PDGFRβ. ErbB3 and PDGFRβ are important players in AKT activation. **Right:** BRAF inhibition induces a metabolic switch from glycolysis to oxidative phosphorylation which facilitates cell survival. The switch is due to a BRAF inhibitor-induced upregulation of PGC1α which in addition to JARID1B (lysine- specific demethylase 5B) boosts oxidative phosphorylation. This figure was modified from Kugel& Aplin 2014.

1.1.2.3 Acquired resistance

In contrast to adaptive resistance acquired resistance appears after a longer period of continues treatment with an inhibitor but once it is established it can lead to a rapid relapse (Kugel & Aplin 2014). There are different known mechanisms of acquired resistance which are summarized in Figure 3. One possibility to overcome targeted therapy and to acquire resistance is a mutation in MEK leading to a reactivation of the MAPK pathway (Emery et al. 2009). Another possibility is a mutation in NRAS. An activating mutation in NRAS promotes RAF dimerization and activation (Nazarian et al.

2010). Furthermore, an overexpression of COT kinase which is able to reactivate the MAPK pathway in a RAF-independent way is a mechanism providing acquired resistance (Johannessen et al. 2010). In addition, different splice variants of BRAF can lead to a reactivation of the pathway (Poulikakos et al. 2011) as well as an amplification of BRAF (Shi et al. 2012). Also receptor tyrosine kinases (RTKs) like EGFR can be upregulated an thereby reactivate the survival and proliferation pathway either by signaling via PI3K or via CRAF to ERK (Nazarian et al. 2010; Spagnolo et al. 2015).
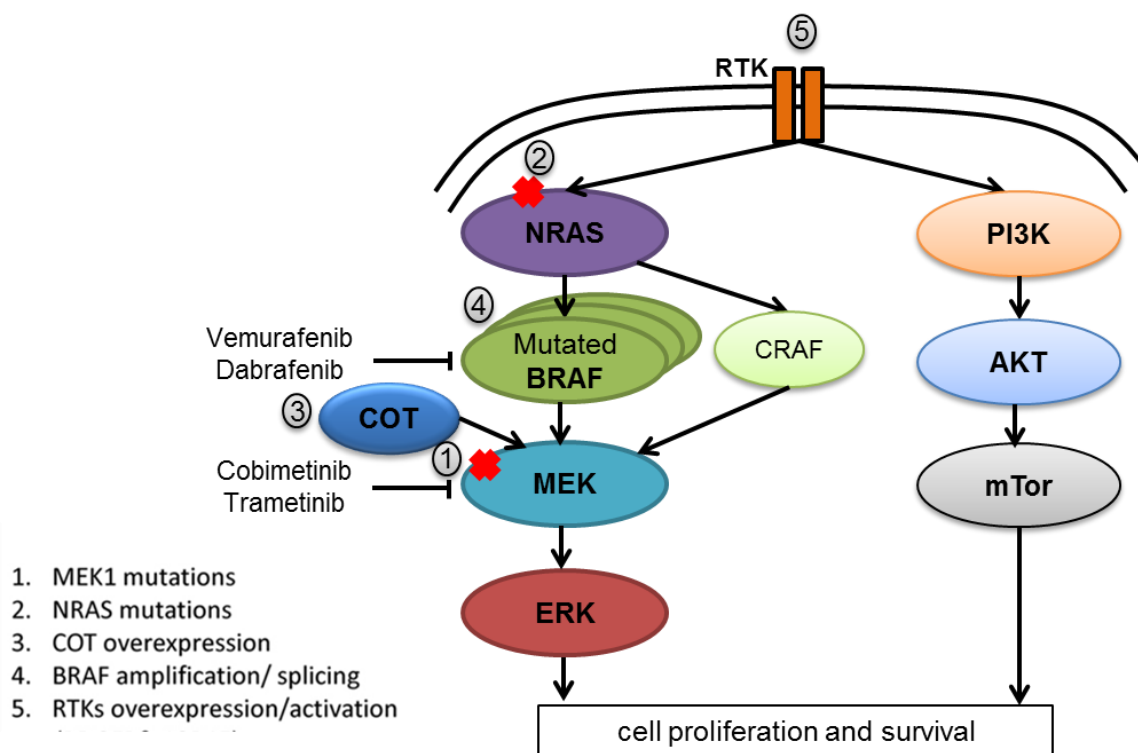
Figure 3: Mechanisms of acquired resistance. Resistance towards vemurafenib can result from MEK mutations, NRAS mutations, COT overexpression, BRAF amplification or splicing variants or receptor tyrosine kinase (RTK) upregulation. This figure was adapted from Kliniac et al. 2013.

1.2 SOX2

The SRY (sex determining region Y)-related HMG box (SOX) is named after the SRY, which is a critical gene for sex determination. As these proteins contain a high-mobility group (HMG) for DNA recognition and binding, all proteins with a similarity in the HMG domain of 50 % or higher are called SOX proteins. SOX2 has a molecular mass of around 35 kDa. It is located on chromosome 3q26.3-q27 and belongs together with SOX1 and SOX3 to the SOXB1 group within the SOX family. Within the SOXB1 group

there is a large homology and all proteins consist of an N-terminal domain, an HMG domain and a C-terminal domain (Figure 4A). The HMG domain is highly conserved between different species and the transactivation domain within the C-terminal domain binds to promotor sequences and thereby activates or represses transcription (Figure 4B) (reviewed by Weina & Utikal, 2014).

SOX2 plays an important role in lineage fate determination and in the maintenance of the stem cell status as well as in the development of the neuroectodermal lineage (Sarkar & Hochedlinger 2013; Adameyko et al. 2012). It is noteworthy that members of the SOX family have redundant function with respect to the maintenance of the stem cell phenotype of stem cells (i.e. SOX1, SOX2, SOX3 and SOX9) (Sarkar & Hochedlinger 2013). Furthermore, SOX2 is a major transcription factor in reprogramming somatic cells into pluripotent stem cells (Takahashi & Yamanaka 2006). Since SOX2 is an important player its dysregulation has been linked to different diseases as well as cancer (Sarkar & Hochedlinger 2013; Weina & Utikal 2014).
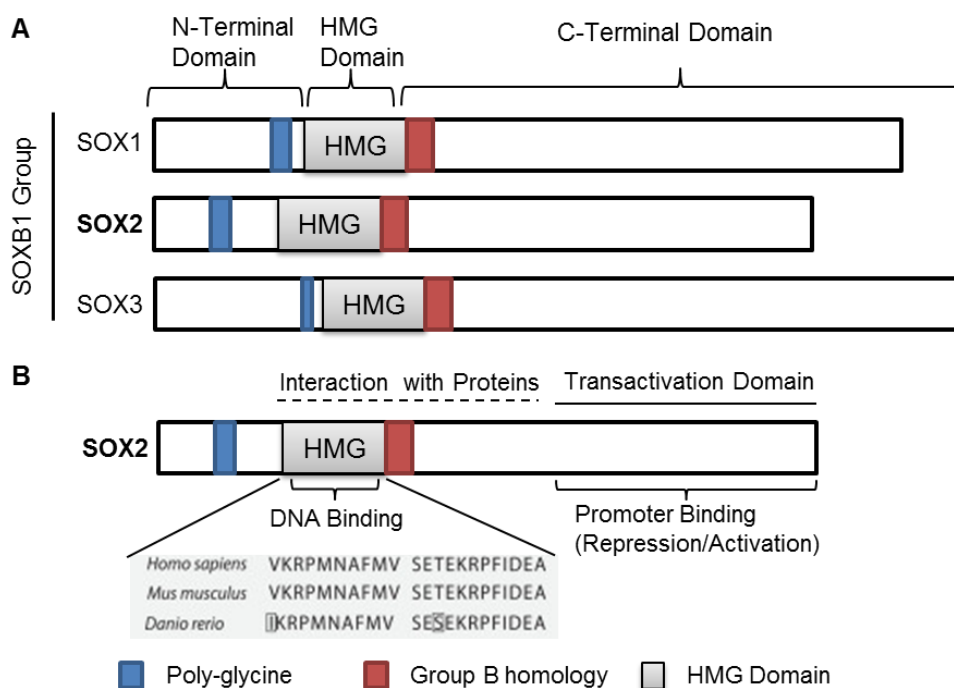
Figure 4: SOX2 structure and homology to members of the SOXB1 group. A: SOX2 belongs to the SOXB1 group of the SOX family together with SOX1 and SOX3. Each member of the family consists of an N-terminal domain, an HMG-domain and a C-terminal domain. **B:** The HMG domain is used for DNA recognition and binding and is conserved between different species. The transactivation domain can be used for promotor binding. This figure was modified from Weina & Utikal, 2014.

1.2.1 Role of SOX2 in cancer

Cancer can be characterized by the hallmarks of cancer: sustained proliferation, evasion of growth suppression, increased invasion and metastasis formation, immortality, induced angiogenesis and resistance to cell death (Hanahan & Weinberg 2011). Increased SOX2 expression or amplification in tumor tissue compared to healthy tissue has been reported for a variety of different cancer types (Wuebben & Rizzino 2017). Additionally, SOX2 expression has been related to some cancer-specific characteristics in different types of cancers and it is well known that it can regulate and also is regulated by signaling pathways involved in cancer pathogenesis (Figure 5). It has been shown that SOX2 promotes cancer cell invasion, migration and metastases formation in melanoma and various other cancer types (Alonso et al. 2011; Han et al. 2012; Weina et al. 2016; Girouard et al. 2012; Sun et al. 2013). Furthermore, SOX2 can lead to increased proliferation (Santini et al. 2014) and can help to overcome apoptotic signals (Chen et al. 2014; Jia et al. 2011). Moreover, SOX2 is associated with poor prognosis in some cancer cell types (Sun et al. 2013; Wang et al. 2009) while in other cancer types it is even associated with a better prognosis (Wilbertz et al. 2011). Hence, the role of SOX2 can differ according to cancer type. Beyond that, SOX2 has been shown to play a role in determining the tumor-initiating cell population (putative cancer stem cells (CSC)) in a number of studies (Wuebben & Rizzino 2017; Weina & Utikal 2014; Santini et al. 2014).
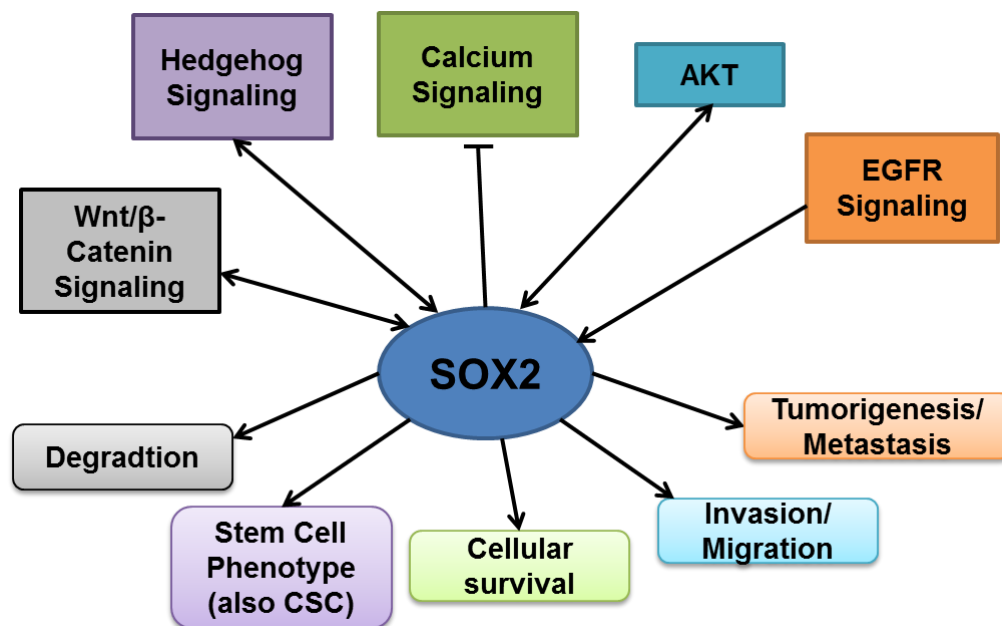
Figure 5: Role of SOX2 in cancer. SOX2 is involved in a lot of cellular processes. It is regulated by and regulates a variety of different signaling pathways. This figure was adapted from Weina and Utikal, 2014.

1.2.2 SOX2 in therapy resistance

A less differentiated cell state is associated with a higher resistance. As pluripotency markers like SOX2 typically promote an undifferentiated state of the cells, these pluripotency genes have been associated with resistance (Dogan et al. 2014). Furthermore, cancer cells that have been reprogrammed to pluripotency, the so-called induced pluripotent cancer cells (IPCCs), were shown to be more resistant towards targeted therapy (Bernhardt et al. 2017). A more undifferentiated state was also linked to adaptive resistance (Fallahi-Sichani et al. 2017). In breast cancer it was demonstrated that SOX2 promotes resistance towards tamoxifen as silencing SOX2 restored tamoxifen sensitivity (Piva et al. 2014). In glioblastoma cells it was shown that SOX2 was a necessary factor for the stem cell population and knockdown lead to reduced drug resistance (Song et al. 2016). There are a lot more studies addressing the role of SOX2 in promoting therapy resistance (reviewed by Wuebben & Rizzino, 2017). One other possible mechanism by which SOX2 promotes drug resistance is linked to its ability of regulating ATP-binding cassette (ABC) transporters i.e. a study where decreased SOX2 level reduces resistance by suppression of ABCG2 (S. H. Lee et al. 2014). Interestingly,

Pietrobono et al. (2016) demonstrated that the renewal and survival capacity of melanoma cells can be inhibited by indirectly targeting SOX2 using gentian violet. Although SOX2 seems to play an important role in therapy resistance, targeting SOX2 directly is not a good idea due to its very important roles in different cellular processes. Hence, targeting SOX2 could lead to a lot of unwanted side-effects. This points out the importance in finding possible targets up- or downstream of SOX2 to overcome therapy resistance.

1.3 CD24

CD24 which is also called HSA (heat stable antigen) in mouse is a highly glycosylated cell surface molecule with a molecular mass of 30-70 kDa. This range in size is due to different glycosylation patterns which are highly variable and cell type dependent. As demonstrated in Figure 6A it is attached to the membrane by a glycosyl-phosphatidylinositol-(GPI) anchor (Kay et al. 1991). Furthermore, the human CD24 gene is located on chromosome 6q21 while three intronless pseudogenes were found on chromosome 1, 15 and Y (Hough et al. 1994). The CD24 gene encodes for a protein of 80 amino acids. The first 26 amino acids serve as a signal peptide to process the GPI-anchor in the endoplasmic reticulum (ER) and are removed upon maturation of the protein. Without the GPI-anchor the mature human CD24 comprises only 31 amino acids and due to its O- and N-glycosylation sites it has mucin-like characteristics (Kay et al. 1991; Aigner et al. 1997; Kristiansen et al. 2004) (Figure 6). Due to its GPI-anchor, CD24 is preferentially located in lipid rafts which have been also termed detergent-resistant membrane domains (DRMs) as they are highly stabile against extraction with surfactants. Moreover, lipid rafts are considered to be important platforms for different signaling molecules for example Src family tyrosine kinases and G-proteins. Actually, it was already demonstrated in several studies that CD24 can physically interact with members of the Src-kinase family and can signal via them (Zarn et al. 1996; Baumann et al. 2012; Sammar et al. 1997; Bretz et al. 2012). Hence, CD24 serves as a signaling transducer in many different cellular processes and thus also its role in cancer is highly investigated. Additionally, CD24 glycans are able to interact with siglecs which are a class of sialic acid binding receptors on immune cells (Kristiansen et al. 2010; Chen et al. 2009). Therefore, CD24 is important in immune response as well as in syndromes

linked to immune response like autoimmune diseases (Fang et al. 2010). Furthermore, it was shown that due to its P-selectin binding site (Figure 6A) CD24 serves as a ligand for P-selectin which supports the adhesion of monocytes and neutrophils to activated endothelial cells and platelets (Aigner et al. 1997 and Aigner et al., 1995)
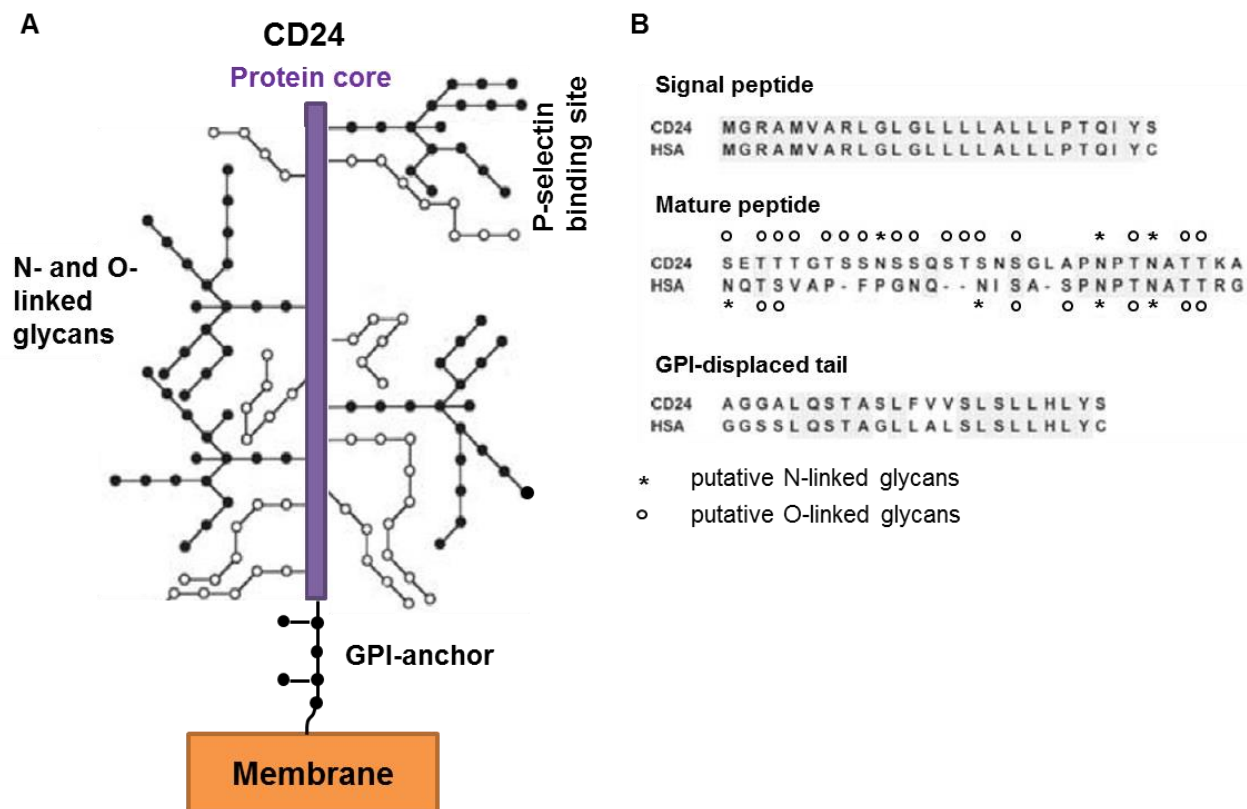
Figure 6: Schematic drawing and protein sequence of CD24. A: Display of a model of CD24, which is anchored by a GPI-anchor to the membrane. Furthermore, the core protein can be linked to N- and O-glycans and has a P-selectin binding site. **B:** Amino acid sequence of the signal peptide, the mature peptide and the GPI-tail of mouse HSA and human CD24. In the human CD24 there is a higher amount of serine and threonine residues in comparison to the murine protein. Additionally the putative N-linked and O-linked glycans are indicated. This figure was modified from Kristiansen et al. 2004.

1.3.1 CD24 in cancer

CD24 overexpression was reported for a lot of different tumor types (Fang et al. 2010). Additionally, also the functional role of CD24 in cancer has been studied and reveals an important function (Figure 7). For instance, it has been shown that due to its interaction with P-selectin CD24 can facilitate the adhesion of breast cancer cells to the endothelium and thereby promote metastatic tumor progression (Aigner et al. 1998). Since the tumor cells can bind via CD24 to P-selectin on the platelets, they can form tumor thrombi. Thus, the CD24-positive tumor can dissimilate faster (Kristiansen et al.

2004; Agrawal et al. 2007). Moreover, a study on bladder cancer showed that CD24 can serve as a therapeutic target as its expression is a requirement for the development of lung metastases (Overdevest et al. 2011). Furthermore, it was demonstrated that CD24 contributes to tumor cell proliferation while a depletion in CD24 leads to a stable growth inhibition (Sagiv et al. 2008). In addition, CD24 promotes FAK, Src and STAT3 signaling in cancer cells which are known to affect proliferation, adhesion and survival (Bretz et al. 2012; Baumann et al. 2012). Moreover, CD24 was shown to increase cell proliferation by activating the MAPK pathway in colorectal cancer (Wang et al. 2010). Another study also showed that doxycyclin-induced CD24 overexpression in breast cancer cells leads to an increase in proliferation. By activation of integrins it also leads to an adhesion to fibronectin, collagen I and IV and laminin (Baumann et al. 2005). Furthermore, also a more rapid cell spreading, induced motility and invasion upon increased CD24 expression was shown whereby the augmented proliferation and motility are integrin dependent (Baumann et al. 2005). Several other studies revealed the promoting role of CD24 in tumor cell adhesion, proliferation, cell motility, transmigration and invasion in different other tumor entities (Runz et al. 2008; Kitaura et al. 2011; Senner 1999; Mierke et al. 2011; Kim et al. 2007). Smith et al. (2006) pointed out the role of CD24 in cancer cell survival. Moreover, as described in 1.3, CD24 interacts with siglecs and could thereby inhibit the immune system. Cancer cells use this system to evade the immune system (Fang et al. 2010). Additionally, CD24 is a marker of CSC, in some tumor entities while in others CD24-low cells are supposed to be the CSCs (Yang et al. 2014; Keysar & Jimeno 2010; Ke et al. 2012; Jaggupilli & Elkord 2012). Overall, CD24 expression correlates with poor prognosis in cancer patients (Fang et al. 2010).
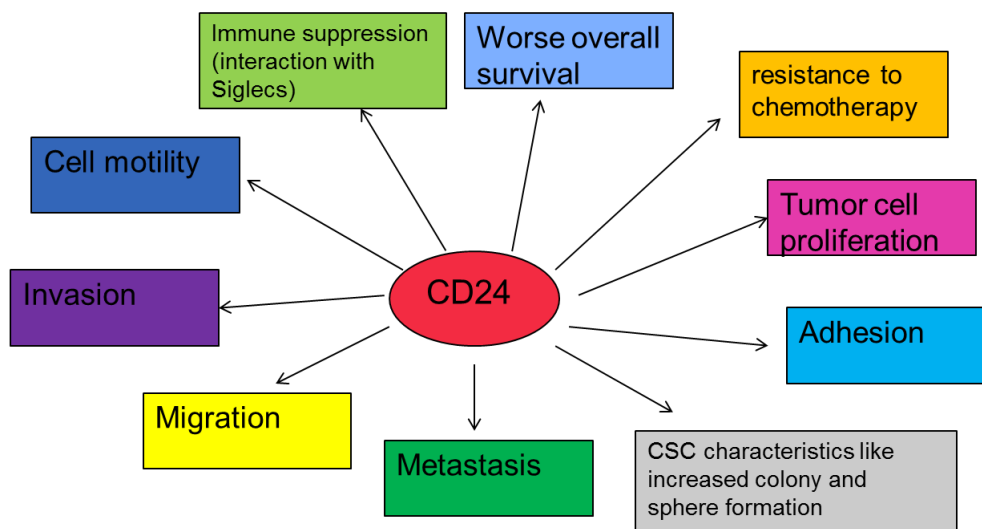
Figure 7: CD24 in cancer biology. Several studies show the involvement of CD24 in different processes related to cancer pathogenesis.

1.3.2 CD24 in therapy resistance

Several studies focused on the role of CD24 in therapy resistance. A study on breast cancer showed the effect of CD24 knockdown and overexpression on docetaxel and doxorubicin resistance. They could show that a CD24 knockdown leads to a higher sensitivity to docetaxel while the cells are more resistant to doxorubicin. CD24-overexpressing cells are more resistant to docetaxel but more sensitive to doxorubicin (Deng et al. 2017). Furthermore, another study on breast cancer showed that tamoxifen resistance is linked to CD24 (Surowiak et al. 2006). In agreement with this, the study of Goldman et al. (2015) on breast cancer matched CD24 expression to chemotherapy tolerance and revealed the CD24-triggered activation of the Src kinase as the reason for the resistance. Moreover, a study on gastric cancer showed that downregulation of CD24 enhances chemosensitivity (Jiao et al. 2013). Additionally, a study on endometrial cancer demonstrated that CD24 leads to drug resistance by the increased recruitment of phospho-Met to lipid rafts (Ono et al. 2015). On the opposite site, there are also several studies showing that a low amount of CD24 favors resistance. The study of Wang and collegues (2012) revealed that cells with high CD44 but low CD24 are more resistant. Moreover, it was shown that repressed expression of CD24 promotes resistance to radiation by controlling the proliferation rate as well as reactive oxygen species levels (Bensimon et al. 2016). Additionally, the study of Cufí et al. (2012) showed that the

CD24^{low} population in breast cancer is more resistant. Therefore, the role of CD24 in therapy resistance seems to be drug and cell type-specific.

2 Aim of the study

The most severe problem in metastatic melanoma treatment is the occurrence of resistance. The initially very effective treatment with inhibitors fails due to resistance towards these compounds. Therefore, getting a better insight into the underlying mechanisms of resistance could improve the therapeutic options and the chances for a cure for patients with metastatic melanoma. While huge effort has been made to understand acquired resistance, still very little is known about the mechanism of adaptive resistance in melanoma. Hence, studying these mechanisms of adaptive resistance is the primary aim of this thesis. Moreover, it has been shown in several studies that dedifferentiation goes along with therapy resistance. Thus, investigating the genes upregulated in undifferentiated and more therapy resistant induced pluripotent cancer cells (iPCCs) and uncovering how these genes are upregulated during inhibitor treatment might help to understand the underlying mechanisms.

Taken together, there are four specific questions that should be answered in this study:

1. Which genes are upregulated in iPCCs derived from melanoma cells as well as after a short-time BRAF inhibitor treatment?
2. Does up- or downregulation of these genes change the sensitivity towards BRAF inhibitors?
3. Are these genes connected and how do they lead to a survival benefit in the presence of the inhibitor?
4. Finally, how are these genes upregulated in the presence of the inhibitor?

3 Materials and Methods

3.1 Materials

3.1.1 Reagents and Kits

Product	Company	Catalog No.
Agarose NEEO Ultra Qualität	Carl Roth	2267.4
Alamar Blue®	Invitrogen	DAL1100
Ammonium persulfate solution (APS)	Carl Roth	9592
Ampicillin	Carl Roth	HP62.1
ARCTURUS PicoPure RNA Isolation Kit	Life Technologies	KIT0204
Complete Mini Protease Inhibitor Cocktail	Roche Diagnostics	04693159001
Dual-Glo® Luciferase Assay System	Progema	E2920
Endofree Plasmid Maxi Kit	Qiagen	12362
FITC Annexin V Apoptosis Detection Kit	BD Biosciences	556547
Fluorescence Mounting Medium	Dako	S3023
High Performance Chemiluminescence Film	GE healthcare	28906836
HumanHT-12 v4 Expression BeadChip Kit	Illumina	BD-103-0204
Immobilon PVDF membrane, 0.45µM	Merck Millipore	IPVH00010
Luminata Forte Western HRP Substrate	Merck Millipore	WBLUF0500
Pierce BCA Protein Assay Kit	Thermo Fisher Scientific	23225
Proteome Profiler Human Phospho-RTK Array Kit	R&D systems	ARY001B
Proteome Profiler Human Cytokine Array Kit	R&D systems	ARY005B
PhosSTOP^{TM} Phosphatase inhibitor Cocktail	Roche Diagnostics	04906845001
PageRuler Plus Prestained Protein Ladder	Life Technologies	26619
Qiaprep Spin Miniprep Kit	Qiagen	27106
Rnase-Free Dnase Set	Qiagen	79254

RNeasy Plus Mini Kit	Qiagen	74136
RevertAid First strand cDNA Synthesis Kit	Thermo Fisher Scientific	K1622
Skim milk powder	Gerbu Biotechnik	1602,1000
SYBR Green PCR Master Mix	Applied Biosystems	4309155
TEMED	Carl Roth	2367.3
Human TNF alpha ELISA Kit	Abcam	ab181421
Tween® 20	Applichem	A13890500
TritonX-100	Carl Roth	3051.4
X-treme GENE® 9 DNA Transfection Reagent	Roche Diagnostics	06365787001

3.1.2 Reagents for cell culture

Product	Company	Catalog No.
2-Mercaptoethanol	Gibco®Life Technologies	31350010
Blasticidin	Sigma Aldrich	15205
DMSO	Carl Roth	A994.2
DMEM AQ media^{TM}	Gibco®Life Technologies	41965-039
Fetal Calf Serum (FCS)	Biochrom	S0115
Human melanocyte growth supplement (HMGS) 100x	Gibco® Life Technologies	S002-5
Lipofectamine® RNAiMAX Transfection Reagent	Life Technologies	13778075
Lipofectamine 2000	Life Technologies	11668030
Medium 254	Gibco® Life Technologies	M254500
Non-essential amino acids	Sigma-Aldrich	M7145
Opti-MEM®	Gibco® Life Technologies	31985062
PBS	Sigma-Aldrich	D8537
Penicillin/Streptomycin	Sigma-Aldrich	P4333
Puromycin	Carl Roth	240.1
Trypan blue solution	Sigma-Aldrich	93595
Trypsin	Sigma-Aldrich	T3924
TNFα	PeproTech	300-01A

3.1.3. Human cell lines

Cell Line	Source	Cell type	Mutation
A375	ATCC	Melanoma cell line	BRAF V600E
HT144	ATCC	Melanoma cell line	BRAF V600E
SK Mel 28	ATCC	Melanoma cell line	BRAF V600E
HEK293T	ATCC	embryonic kidney	WT

cells

3.1.4. Antibodies

Specificity	Source	Company	Catalog No.
SOX2	Rabbit	Cell signaling	23064S
SOX2	Rabbit	Abcam	ab97959
Src	Rabbit	Cell signaling	36D10
pScr (Tyr416)	Rabbit	Cell signaling	D49G4
Stat3	Mouse	Cell signaling	9139S
pStat3	Mouse	Cell signaling	4113S
α-actinin	Mouse	Santa Cruz	sc-17829
AKT	Mouse	Cell signaling	2920S
pAKT (Thr 308)	Rabbit	Cell signaling	4056S
p21	Rabbit	Cell signaling	2947S
p27	Rabbit	Cell signaling	2552S
CD24	Mouse	NON commercial	clone SWA11
CD24	Mouse	Thermo Fisher scientific	MA5-11833
SOX10	Mouse	Abcam	ab181466
MITF	Mouse	Abcam	ab80651
Axl	Rabbit	Cell signaling	4566
ERK	Rabbit	Cell signaling	4695
pERK (T202/Y204)	Mouse	Cell signaling	9106S
GAPDH	Rabbit	Cell signaling	CST2118
NF-kappa p65	Rabbit	Cell signaling	3034
phospho NF-kappa p65 (Ser536)	Rabbit	Cell signaling	3033

3.1.5 Small molecule inhibitors

Product	Company	Catalog No.
Trametinib (GSK1120212)	Selleckchem	S2673
Vemurafenib (PLX4032)	Selleckchem	S1267
Dabrafenib (GSK2118436)	Selleckchem	S2807
BP-1-102	Sigma-Aldrich	573132-M
PP2	Selleckchem	S7008
Dasatnib	BioVision	1586-25
TAPI-2 (CAS 187034-31-7)	Biomol	Cay14695-500

3.1.6 siRNAs

Product	Sequence	Company
si-GFP	5'-GGC CAG GUC CAG CAG CGC ACC UU-3'	Eurofins
si-CD24	5'-ACA ACA ACU GGA ACU UCA AUU-3'	Eurofins
siSOX2	5'GCGUGAACCAGCGCAUGGACAGUUA-3'	Invitrogen
si-STAT3	5´-UGA AAG UGG UAG AGA AUC UUU-3´	Eurofins
si-Src	5´-UCA AGC AGA CAU AGA AGA GUU-3´	Eurofins

3.1.7 Plasmids

Name	Source
renilla plasmid pAAV psi2	Holger Sültmann (NCT, Heidelberg, Germany)
pCMV-dR8.91 (Packaging)	Konrad Hochedlinger (Harvard, Bosten, USA)
pCMV-VSV-G (Packaging)	Addgene #8454
pGL4.10	Holger Sültmann (NCT, Heidelberg, Germany)
pCD24-1896	Dan Theodoresu (UC Denver, Colorando, USA)
pGL4.51	Dan Theodoresu (UC Denver, Colorando, USA)
SOX2 OE	Addgene #16577
SOX2 KD1	TRCN0000231642 (Sigma-Aldrich)
SOX2 KD2	TRCN0000257314 (Sigma-Aldrich)
SOX2 KD3	TRCN0000355694 (Sigma-Aldrich)
SOX2 KD4	TRCN0000231642; TRCN0000257314 TRCN0000355694 (Sigma-Aldrich)
CD24 OE	HsCD00418330 (Harvard PlasmID Database)

3.1.8 Primer

Amplification target	Forward Sequence	Reverse Sequence
SOX2	GCCGAGTGGAAACTTTTGTCG	GGCAGCGTGTACTTATCCTTCT
CD24	TGCTCCTACCCACGCAGATT	GGCCAACCCAGAGTTGGAA
18S	GAGGATGAGGTGGAACGTGT	TCTTCAGTCGCTCCAGGTCT
SOX10	GGCTTTCTGTCTGGCTCACT	TAGAGGGTCATTCCTGGGGG
MITF	GCTCACAGCGTGTATTTTTCC	TCTCTTTGGCCAGTGCTCTT
EGFR	TCCTCTGGAGGCTGAGAAAA	GGGCTCTGGAGGAAAAGAAA
Src	TACTGCTCAATGCAGAGAACCCGA	TGTCCAGCTTGCGGATCTTGTAGT
STAT3	ATGGAAGAATCCAACAACGGCAGC	AGGTCAATCTTGAGGCCTTGGTGA
p75	CGACAACCTCATCCCTGTCT	GCTGTTCCACCTCTTGAAGG
Axl	CCGTGGACCTACTCTGGCT	CCTTGGCGTTATGGGCTTC

3.1.9 Solutions and Buffers

Transfer buffer (pH 8.3)	**Running buffer (pH8.3)**
25mM Glycine	25mM Glycine
190mM Tris	190mM Tris
20% SDS	0.1% SDS
20% Methanol	dH2O
dH$_2$O	
TBS 10X (pH 7.6)	**Washing buffer (TBST)**
150mM NaCl	0.02% Tween® 20
50mM Tris	1X TBS
dH$_2$O	
Blocking buffer (milk)	**Blocking buffer (BSA)**
5% Skim milk powder	5% BSA
1x TBS	1x TBS

Cell lysis buffer for protein isolation	**LB Medium**
1X PhosphoStop	20g LB-Medium (Carl Roth, X964.2)
1X Complete mini protease inhibitor cocktail	1l H_2O
1% Triton-X in TBS	
SOC Outgrowth Medium	
New England BioLabs (B9020S)	

3.1.9 Devices

Product	Company
AB 7500 Real-Time PCR Machine	Applied Biosytems
Classic E.O.S. Developer	AGFA Mortsel, Belgium
Nanodrop Spectophotometer ND-1000	Peqlab Biotechnologie GmbH
Nikon Eclipse Ti Fluorescence Microscope	Nikon
FacsCanto II	BD Biosciences
Tecan Infinite F200 PRO	Tecan
Leica DM LS light microscope	Leica

3.1.10 Software

Software name	Source
7500 Software v2.0.5	Applied Biosystems
ApE	M. Wayne Davis (Open Source)
Chipster	Chipster Open source
FlowJo 7.2.2	FlowJo
GraphPad PRISM	GraphPad software
i control 1.10	TECAN
Image J	NIH
Mendeley	Mendeley
NIS-Element	Nikon

3.2 Methods

3.2.1 Cell culture

All cell lines except normal human melanocytes (NHM) were cultured in DMEM (Gibco, Life Technologies) supplemented with 10 % heat-inactivated FCS (Biochrom), 0.1mM β-mercaptoethanol (Gibco, Life Technologies), 1% non-essential amino acids (NEAA) and 1% penicillin/streptomycin (Sigma-Aldrich). IPCCs were generated and cultured as described before (Bernhardt et al. 2017). All cell lines were cultured in a humidified incubator at 37°C and 5 % CO_2. Cell lines were sub-cultured every 3-5 days as soon as they reached around 80 % confluency.

NHM were isolated from the foreskin of donors in accordance to the ethical regulations (Ethics committee II, University Medical Centre Mannheim, Germany) and were afterwards cultivated in medium 254 (Gibco, Life Technologies) supplemented with human melanocyte growth supplement (HMGS) (Gibco, Life Technologies).

3.2.2 Resistant cell lines

Resistant cells were generated by gradually increasing the concentration of the inhibitor in the culture medium. A375 res cells (5 µM vem-resistant cells) were kindly provided by Prof. Dr. David Proia (Synta Pharmaceuticals Corp., Lexington, Massachusetts) and SK Mel 28 res cells were a kind gift from Prof. Dr. Joon Kim (Graduate School of Medical Science and Engineering, KAIST, Daejeon, Korea).

3.2.3 Cell viability assay

Melanoma cells were seeded in flat bottom 96-well plates (Gibco Life Technologies) at a density of 2500-5000 cells/well depending on the cell line and growth properties. The following day, the cells were treated with different concentrations of vemurafenib (plx4032), plx8394 or plx7904 (all Selleckchem), respectively, in the indicated doses. To compare the sensitivity to vemurafenib with the sensitivity to a combination of vemurafenib and PP2 (Src kinase inhibitor dissolved in DMSO), 50 µM of PP2 or the same volume of DMSO were added to the different concentrations of vemurafenib. After 72h of treatment, Alamar blue (10 % of the culture medium volume) was added and after 3,5h of incubation at 37°C the fluorescence was measured at an emission wavelength of

535 nm and an excitation wavelength of 590 nm, using a Tecan Infinite F200 PRO (Tecan, Männedorf, Switzerland).

3.2.4 Inhibitor treatment

$2x10^5$ cells (for SK Mel 28 $5x10^4$ were used) were seeded in flat bottom 6-well plates (Gibco Life Technologies) and after attaching (within hours) they were treated with the inhibitor as indicated or the respective volume of solvent for control. The cells were incubated for 6h, 24h, 48h, 72h and 96h and afterwards RNA was isolated for qPCR or proteins for western blot analysis.

In case of the Src inhibitor PP2 (Selleckchem, Munich, Germany) the cells were seeded one day before the 72h treatment with 50 µM PP2 or DMSO as control.

For the STAT3 inhibitor BP-1-102 (Merck Millipore) $1x10^6$ cells were seeded in a 10 cm dish one day prior to treatment. After 24h of treatment with either DMSO, vemurafenib [3 µM], BP-1-102 [15 µM] or vemurafenib [3µM] + BP-1-102 [15 µM] or PP2 [50 µM] or PP2 [50 µM] + vemurafenib [3 µM] the cells were harvested and lysed.

For TAPI-2 (Biomol) treatment cells were seeded at a density of $2x10^5$ cells/well in a 6-well plate. The next day, the cells were treated with 10 µM TAPI-2. After 24h the cells were treated again with 10 µM TAPI-2. After a total of 48h the cells were harvested.

3.2.5 TNFα stimulation

Cells were seeded at a density of $2x10^5$ cells/well in a 6 well plate one day prior treatment. At the next day the cells were treated with 10 nM TNFα. After 48h of treatment the cells were harvested.

3.2.6 Puls experiment

$1x10^6$ cells were seeded in a 10 cm dish. The next day, the cells were treated for 6h with vemurafenib [3 µM] or DMSO as control. Next, the cells were washed twice with pre-warmed (37°C) medium before fresh medium was added. After overnight incubation with fresh medium the supernatant was transferred to naive cells seeded the day before at a density of $2x10^5$ cells/well in a 6-well plate. These cells were treated with the overnight

supernatant for 2h, 4h, 6h and 8h and were then harvested to perform a western blot analysis.

3.2.7 Transduction with lentiviral particles

HEK293T cells were used for lentiviral particle production. The cells were grown to approximately 60 % confluency before transfection. For transfection, 11 µg of the plasmid containing the gene/shRNA of interest were mixed with the packaging plasmids pCMV-VSV-G (5.5 µg) and pCMV-dR8.91 (8.25 µg) and X-treme GENE® (Roche) solution in DMEM. After 30 min of incubation at room temperature, the mixture of DNA, X-treme GENE and DMEM was added to the HEK293T producer cells. After 12h, the supernatant was discarded. After another 12, 24, and 36 h the supernatant containing the virus particles was collected and the virus particles were concentrated by ultracentrifugation. The concentrated virus was used to infect the melanoma cells. 24h after the first infection the melanoma cells were re-infected with the same virus in fresh medium and after 48h of transduction, the cells were washed twice with PBS and then cultured in their culturing medium. In order to select for transduced cells, cells were selected for 3 days in medium containing 0.8 µg/ml of puromycin or 15 µg/ml blasticidin.

3.2.8 Lipofectamine transfection

Cells were seeded to 60-80 % confluency and the siRNA transfection using Lipofectamine™ RNAiMAX Transfection Reagent (Thermo Fisher Scientific) was performed according to the manufacturer's protocol. The cells were incubated for 72h before use in further experiments. Transduction efficacy was monitored by qPCR and western blot analysis.

3.2.9 Luciferase assay

CD24 promoter constructs pCD24-1896 and the respective pGL4.51 control vector were a kind gift from Dan Theodoresu (UC Denver, Colorando, USA). The renilla plasmid pAAV psi2 (Börner et al. 2013) and the empty vector control pGL4.10 were a kind gift from Holger Sültmann (NCT, Heidelberg, Germany). In addition to these plasmids, the cells were co-transfected with the SOX2 OE construct (Addgene #16577) or empty vector as control. One day before transfection $5x10^3$ cells were seeded in flat bottom 96-

well plates. The next day, the cells were transfected with 100 ng total plasmid DNA. Thus, 66 ng of the firefly plasmids as well as 33 ng of the SOX2 OE or EV plasmid were transfected. Co-transfection with 1 ng renilla luciferase plasmid served as a transfection efficiency control. After 48h, firefly and renilla luciferase levels were determined with the Dual-Glo® Luciferase Assay System (Promega) according to the manufacturer's instructions. Luciferase activity was normalized to renilla activity. Activities were calculated as the relative response ratio (RRR) whereby the positive control pGL4.51 was 100 %.

3.2.10 Immunoprecipitation (IP)

Immunoprecipitation of CD24 was performed by lysing the cells of interest with 1x NP40 lysis buffer for 30 min on ice followed by 10 min centrifugation at 14 000 rpm. The antibody (SWA11, 5 µg) was added to the supernatant and incubated for 1h on a rotating wheel at 4 °C. Next, agarose G beads were added to the antibody lysate mix to and incubated for 30 min at 4 °C under rotation. After washing the beads, sample buffer was added and the samples were cooked for 5 min at 95 °C. A western blot was run to visualize the result. To ensure an equal input, a small aliquot of the lysate was saved to serve as loading control.

3.2.11 TMA staining

Tumor samples from melanoma patients were used to prepare TMA-slides as reported before (Wagner et al. 2015). After overnight incubation with primary antibody, the slides were washed in TBS-T and secondary antibody staining (Dako EnVisionTM + System-HRP; AEC K4009) was performed according to the manufacturer's protocol. The samples were counterstained with H&E and mounted (Dako S3025). To ensure that the analyzed regions contained tumor cells, the tumor cells were stained against S100β. The sections were examined in a blinded setup by two individuals.

3.2.12 Immunofluorescence

20 000 cells were seeded in 8-well chamber slides (Falcon) in 400 µl medium. The next day, the cells were treated for 24h with vemurafenib [3µM] or DMSO as control. After 24h, the cells were washed for 5 min in PBS on a shaker. Next, the cells were fixed

using 4% paraformaldehyde (PFA) for 5 min on ice and 10 more minutes on room temperature. After 5 min washing with PBS the cells were permeabilized with methanol for 1 min at -20°C. Followed by 5 min wash in PBS and blocking in 1% BSA/ 0.3 % Triton X-100 in PBS for 30 min, the cells were incubated overnight at 4 °C in a humid chamber with the primary antibody diluted in 1% BSA/ 0.3 % Triton X-100 in PBS (here pSTAT3 (cell signaling) 1:100). The next day, the cells were washed 3 times with PBS and afterwards incubated with the secondary antibody coupled to a fluorophore (here Alexa fluor 488 goat anti mouse (Invitrogen)) diluted 1:1000 in 1% BSA/ 0.3 % Triton X-100 in PBS for 120 min protected from light in a humid chamber under constant agitation. After removing the antibody dilution, DAPI diluted 1:5000 in 1% BSA/ 0.3 % Triton X-100 in PBS was added for 10 min to the cells to visualize the nucleus. After 3 more washes with PBS in the dark the cells were rinsed with water. Lastly, the chamber was removed and the slide was mounted with fluorescence mounting medium (Dako). The next day the cells were analyzed with fluorescence microscopy.

3.2.13 RNA isolation and cDNA synthesis

Total RNA was isolated using the RNeasy Mini Kit (Qiagen). The isolation was performed according to the manufacturer's protocol. If the number of cells was too small to use the RNeasy Kit the PicoPure RNA Isolation Kit (Thermo Fisher Scientific) was used. In any case, on-column DNase digestion was performed. Before further experiments, the RNA was quantified by using a NanoDrop ND1000 spectrophotometer (PEQLAB Biotechnologie GmbH, Erlangen, Germany). cDNA was transcribed using the Revert Aid First Strand cDNA Synthesis Kit (Thermo Fisher scientific) following the manufacturer's instructions.

3.2.14 qPCR

To determine the expression level of mRNA quantitative real-time PCR (qPCR) was used. Therefore the SYBR Green Master Mix (Applied Biosystems, Life technologies) was mixed with cDNA and the primer of interest and the qPCR was run on a 7500 Real-Time PCR System (Applied Biosystems, Life Technologies). As an endogenous control in all experiments, 18S was used. All CT values were normalized to 18S to calculate the $2^{-\Delta\Delta Ct}$ to obtain the relative gene expression. All qPCRs were run in technical triplicates

and the mean of the technical triplicates of at least 3 independent experiments was used to calculate the mean and the SEM as well as the statistical significance.

3.2.15 Protein isolation

After harvesting the cells were washed once with PBS and proteins were solubilized using lysis buffer with Complete Mini Protease Inhibitor Cocktail (Roche) and 1% Triton-X-100. In order to maintain the phosphorylation of proteins, 1x of PhosSTOP (Roche) was added to the lysis buffer. The cells were lysed for 20 minutes on ice and afterwards centrifuged at 14 000 rpm for 15 minutes at 4 °C. The supernatant containing the proteins was transferred to a fresh Eppendorf tube. For the determination of the protein concentration, the Pierce BCA Protein Assay Kit (Thermo Fisher Scientific) was used following the manufacturer's instructions.

3.2.16 Western blot

30 µg of protein from each sample were loaded on a 10 % SDS gel and the proteins were resolved according to their size by SDS-PAGE gel electrophoresis. Afterwards the proteins were transferred to a PVDF membrane (Merck Millipore). After blocking in blocking buffer, the membrane was incubated overnight at 4 °C with predetermined primary antibody dilution followed by washing and detection of bound antibody using HRP-conjugated secondary antibody for 1 hour at room temperature. To visualize the HRP-bound antibody, Luminata Forte Western HRP Substrate (Merck Millipore) was used according to the manufacturer's instructions.

3.2.17 Fluorescence-activated cell sorting (FACS)

$2x10^5$ cells were seeded in 6- well plates. The next day, the cells were treated with 3 µM vemurafenib or DMSO as control. After 24h the cells were washed and trypsinized and after centrifugation resuspended in FACS buffer (PBS + 0.5 % BSA). Afterwards, the cells were incubated with mAb CD24 (SWA11) for 1 h. After washing, cells were incubated with a PE-conjugated IgG secondary antibody (Jackson ImmunoResearch) for 30 minutes. PI and Annexin V staining were performed using the FITC Annexin V Apoptosis Detection Kit (BD Biosciences) following the manufacturer's instruction. The

cells were analyzed by using a FacsCanto II (BD Biosciences). The acquired data were analyzed with the FlowJo software.

3.2.18 Proteome Profiler Human Phospho-RTK Array Kit

$1x10^6$ cells were seeded in a 10 cm dish. After attachment the cells were treated for 24h with vemurafenib [3 µM] or DMSO as control. After 24h the cells were lysed and the array was performed according to the manufacturer's instructions.

3.2.19 Proteome Profiler Human Cytokine Array Kit

The cells were seeded in a 10 cm dish ($1x10^6$ cells/dish) and after they attached they were treated with vemurafenib [3 µM] or DMSO as control for 24h. The supernatant was harvested and processed according to the manufacturer's instructions.

3.2.20 TNFalpha Elisa

Supernatant after DMSO, vemurafenib [3µM], TAPI-2 [10 µM], vemurafenib [3 µM] and TAPI-2 [10 µM] and TNFα [10 nM] treatment for 48h were used to perform the Elisa after the manufacturer's instructions.

3.2.21 Microarray gene expression profiling

Total RNA isolation was performed using the RNeasy Mini Kit (Qiagen, Hilden Germany). After labelling, the RNA was hybridized to whole-genome BeadChips using the HumanHT-12 v4 Expression BeadChip Kit from ILLUMINA (Santa Clara, CA, USA) according to the manufacturer's instructions. The procedure was carried out by the core facility of the DKFZ. Statistical analyses of hybridization data were performed using Chipster. To compare two groups of interest for significant differences, a Bayes test was used on the bead expression values of the two groups. The mean of the measured expressions of beads together with the standard deviation of the beads were used to calculate the average expression value. Only p-values lower than 0.05 were assumed as significantly different. Furthermore, the fold change (FC) was calculated and only genes with a FC outside of 1 or -1 were considered as genes whose expression changed between the two groups (FC is shown as log2-expression values of the differentially expressed genes). Some microarray data are accessible via the GEO database (iPCC

and HT144 data: accession number GSE95281; A375 24h DMSO/vemurafenib data: accession number GSE106321) others on demand.

3.2.22 Bacterial transformation and plasmid isolation

DH5α competent Escherichia coli (E.coli) bacteria were used for transformation and plasmid isolation. Therefore, 100 µl of DH5α were thawed on ice and maximum 10 µl DNA were added and the mix was incubated for 40 min on ice. Afterwards, the bacteria got a 3 min 42°C heat shock and returned in the next step for 10 min on ice. Next, 500 µl of SOC Medium were added and incubated for 1 hour at 37 °C under constant agitation. For a retransformation 50 µl were platted out on drug selection agarose plates containing an antibiotic for selection. Next, the plates were incubated over night at 37 °C. On the following day, 5-6 clones were picked and were incubated over night at 37 °C under constant agitation in LB-medium supplemented with the antibiotic for selection. The next day, the plasmid was isolated by using the Qiaprep Spin Miniprep Kit (Qiagen) according to the manufacturer's instructions. To determine if the isolated plasmid was correct a restriction digestion was performed. Afterwards, the bacteria carrying the correct plasmid were cultivated over night at 37 °C in 200 ml of LB-medium containing the antibiotic for selection. Next, the Endofree Plasmid Maxi Kit (Invitrogen) was used following the manufacturer's description to isolate the plasmid DNA. In the last step the Nanodrop ND-1000 was used to determine plasmid DNA concentration and quality.

3.2.23 Statistical analysis

All statistics were performed using GraphPad Prism (GraphPad Software) and statistical tests were performed on at least 3 independent experiments if not indicated differently. T-Test was used when 2 groups were compared while two-way-anova was utilized for more than two groups. Only the microarray data were statistically analyzed using Chipster.

4 Results

4.1 SOX2 and CD24 are upregulated in melanoma-derived iPCCs and after treatment with MEK/BRAF inhibitors

A previous study from our lab showed that induced pluripotent cancer cells (iPCCs) generated from melanoma cells by stable reprogramming with the transcription factors OCT4, KLF4, and SOX2 are more resistant towards targeted therapy (MEK and BRAF inhibitors) than their parental counterpart (Bernhardt et al. 2017). Using microarray expression data of these iPCCs and their parental counterpart, a significant increase of SOX2 and CD24 expression was observed in HT144-iPCCs in comparison to the parental HT144 cells (Figure 8A). Due to the ectopic overexpression of SOX2 during reprogramming a high expression level of SOX2 was expected. Notably, when comparing this data set with genes changed in A375 cells after 24h of vemurafenib (vem) treatment, SOX2 and CD24 were also significantly upregulated (Figure 8B). The microarray data were further confirmed by qPCR and western blot (WB) to ensure that the increase is also detectable with other methods than microarray expression analysis (Figure 8). Since SOX2 and CD24 expression was increased in BRAF inhibitor (BRAFi) and MEK inhibitor resistant melanoma-iPCCs as well as in melanoma cells treated for a short time with the inhibitor, the role of SOX2 and CD24 in adaptive resistance became the focus of attention of this work.
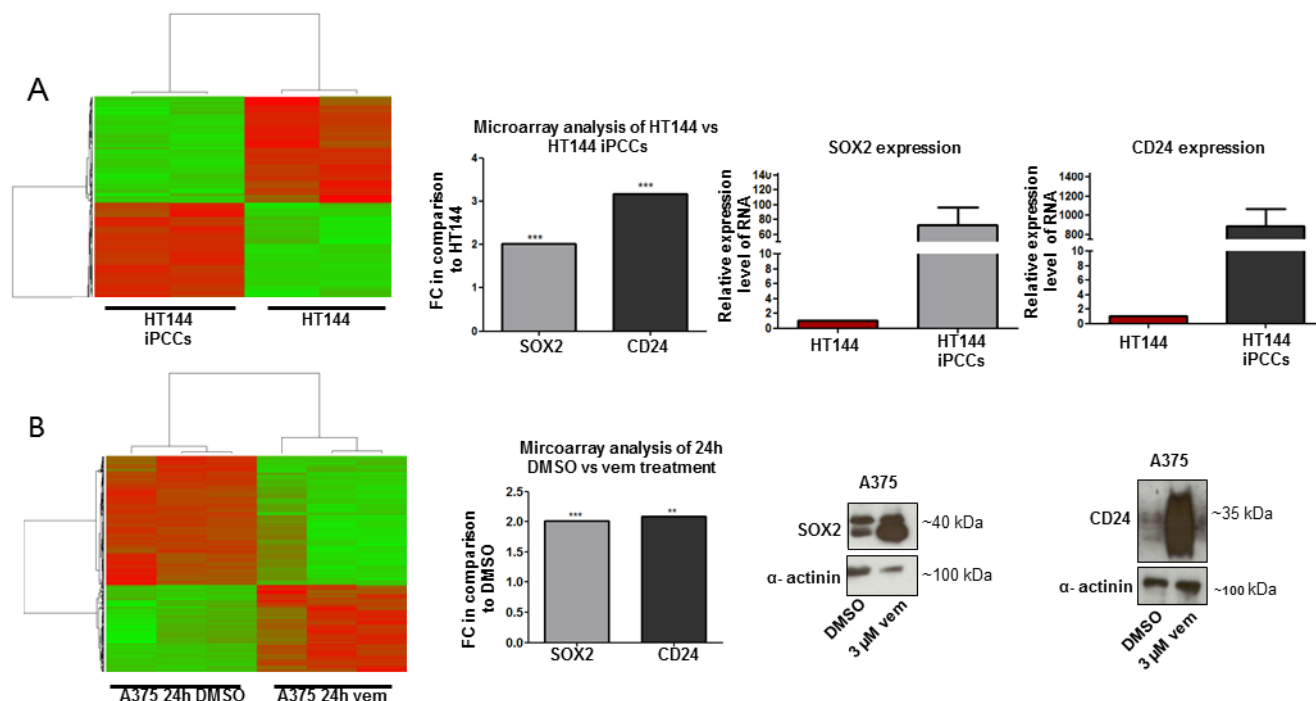
Figure 8: SOX2 and CD24 are highly upregulated in BRAFi-resistant melanoma iPCCs and in short-time BRAFi-treated melanoma cells. A: Microarray data from HT144-iPCCs in comparison to the parental HT144 cells show a significant upregulation of SOX2 and CD24 in the iPCCs (FC= fold change in log2 scale). The two graphs on the right show validation of microarray data by qPCR. qPCR data are shown as the relative expression level of mRNA, normalized to 18S (n=2). **B:** Microarray data from A375 treated for 24h with 3 μM vemurafenib or the corresponding amount of DMSO show significant upregulation of SOX2 and CD24 after vemurafenib treatment. This was also validated by western blot (WB). α-actinin served as loading control.

To determine the time of treatment which is necessary to observe an upregulation of CD24 and SOX2, different BRAF-mutated melanoma cell lines (A375, HT144, SK Mel 28) were treated for various time periods with BRAFis (vemurafenib, plx8394, plx7904). All melanoma cell lines showed a significant upregulation of SOX2 and CD24 on the mRNA level after BRAFi treatment. The time periods, however, varied from cell line to cell line (Figure 9A-F).

Since MEK and BRAF inhibitors are used in combination with each other in melanoma therapy, A375 melanoma cells were treated simultaneously with the BRAFi vemurafenib and the MEK inhibitor trametinib. As demonstrated in Figure 9G, again, a significant increase in SOX2 and CD24 expression was determined by qPCR.
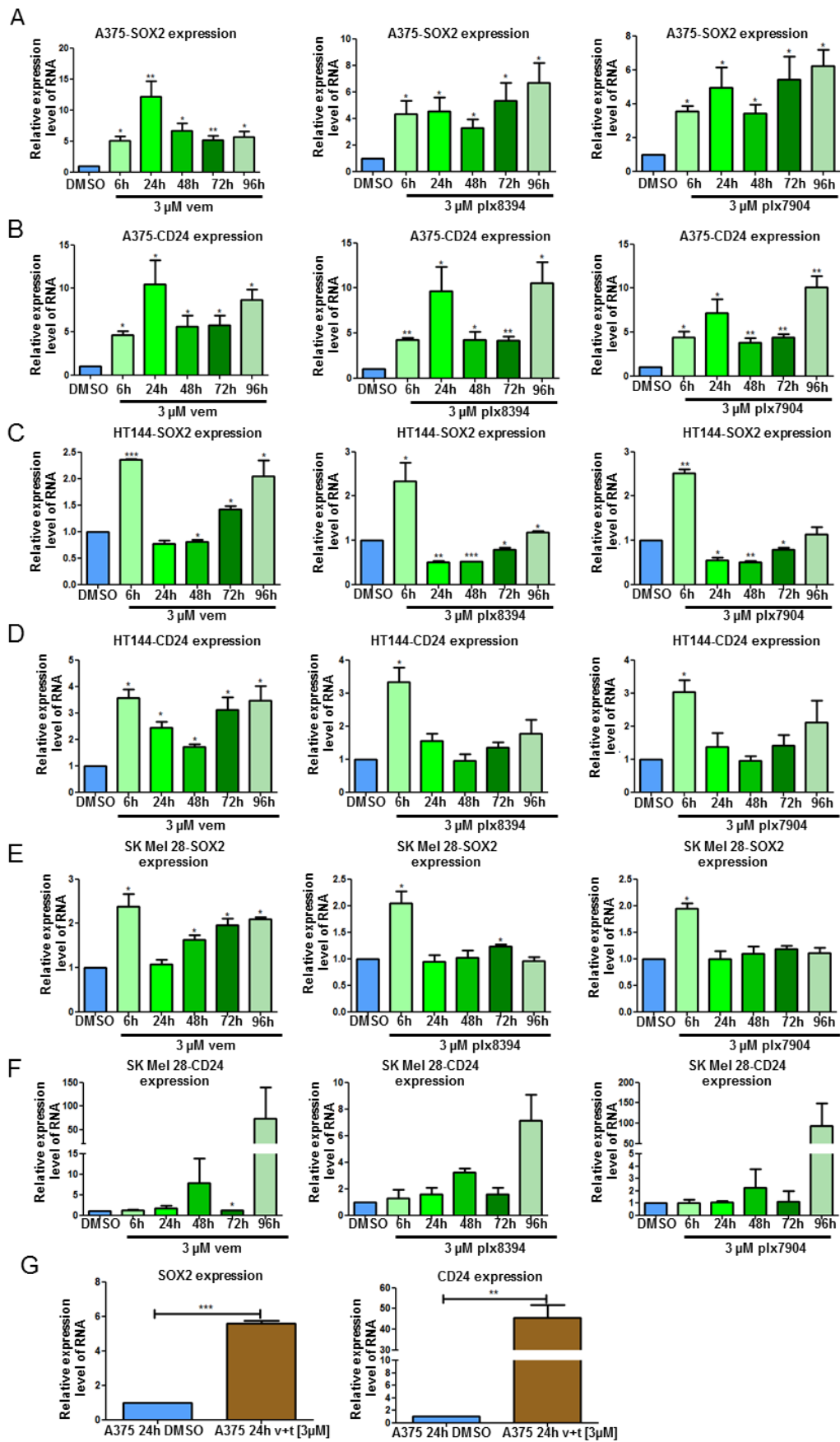
Figure 9: Short-time treatment with BRAFis as well as with a combination of MEK and BRAFis resulted in an upregulation of SOX2 and CD24 expression. A: SOX2 is significantly upregulated after different time periods of BRAFi (vemurafenib, plx8394, plx7904) treatment [3 µM] in A375 cells. **B:** CD24 is significantly unregulated after treatment with BRAFi in A375 cells. **C:** HT144 cells show increased level of SOX2 after short-time BRAFi treatment [3 µM]. **D:** CD24 is upregulated in HT144 cells after short-time treatment with BRAFi. **E:** SK Mel 28 cells show an increase in SOX2 expression after short-time of BRAFi treatment. **F:** CD24 is upregulated in SK Mel 28 cells after different time periods of treatment with BRAFi. **G:** A375 cells were treated for 24h with a combination of vemurafenib (v) and trametinib (t) (each 3 µM). SOX2 and CD24 are higher expressed in the treated cells in comparison to DMSO control cells. All data are shown as relative expression level of mRNA, normalized to 18S (p < 0.05 *; p < 0.01 **; p < 0.001 ***)

Moreover, to ensure that the increased expression is due to an upregulation of the protein rather than the result of selective killing flow cytometric analysis after PI and Annexin-V staining was performed to detect apoptotic cells. This experiment revealed that the vemurafenib-mediated upregulation of CD24 was due to induction of expression and not the result of selective cell death of CD24-negative cells (Figure 10). Together, these data suggest that SOX2 and CD24 might play a role in adaptive resistance.
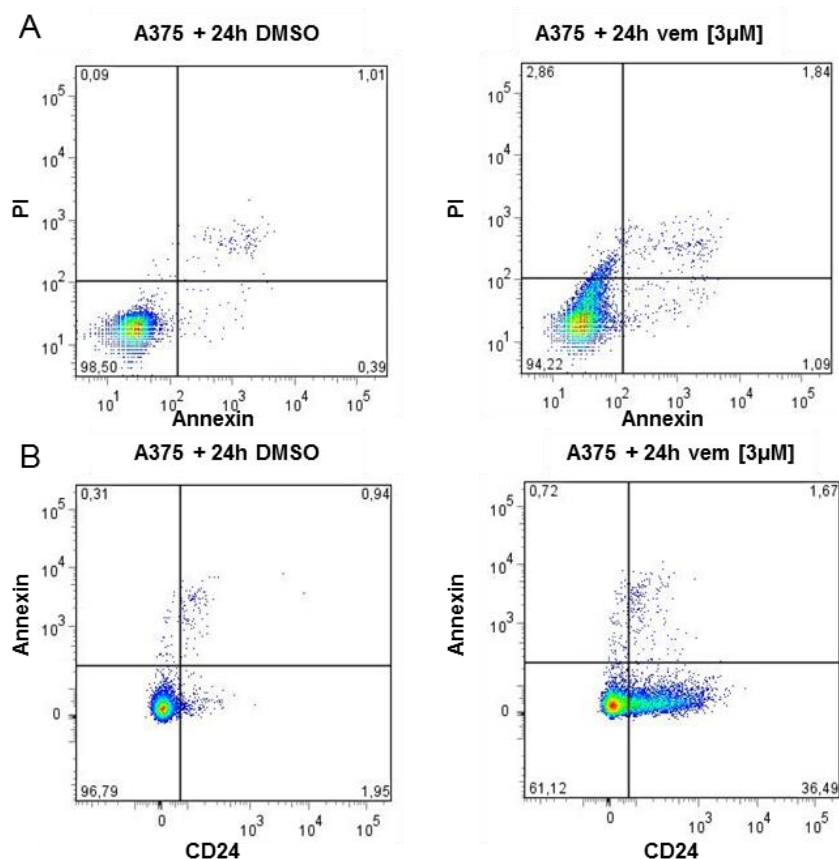
Figure 10: Elevated number of CD24-positive cells is due to increase of CD24 expression and not due to selection. A: Double staining with PI and AnnexinV combined with FACS analysis show that the apoptotic cell population is increased after 24h of vemurafenib treatment (3 µM). **B:** Double staining of CD24 and AnnexinV in FACS shows that vemurafenib treatment increases the amount of apoptotic cells and the amount of living CD24-positive cells.

4.2 Vemurafenib treatment or overexpression of SOX2 show a more neural crest cell like phenotype

To investigate if the vemurafenib treated cells have a more dedifferentiated phenotype the microarray data of vemurafenib-treated as well as DMSO-treated cells were compared to microarray data of normal human melanocytes (NHM) and neural crest (NC) cells. Interestingly, the DMSO-treated A375 cells clustered in a heat map together with NHMs while A375 cells treated with vemurafenib were more close to NC cells which represent a more undifferentiated phenotype (Figure 11). Noteworthy, SOX2-overexpressing (OE) A375 cells were more close to vemurafenib-treated and NC cells while A375 cells transduced with an empty vector (EV) control clustered together with DMSO-treated cells and NHMs (Figure 11). Hence, it can be concluded that melanoma cells treated with vemurafenib as well as cells overexpressing SOX2 have a more undifferentiated phenotype.
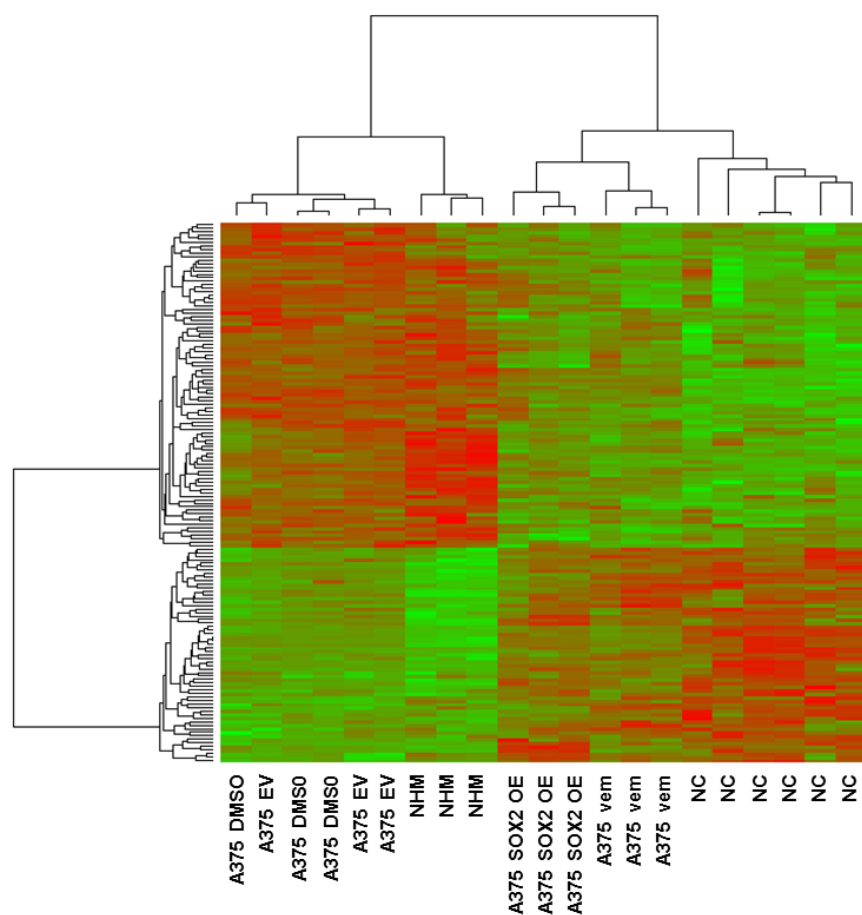
Figure 11: SOX2 overexpression or vemurafenib treatment favors a more undifferentiated phenotype. Heat map representation of microarray data shows clustering of A375 empty-vector control cells (EV) with DMSO–treated control cells and normal human melanocytes (NHMs) while SOX2-overexpressing cells (OE) cluster with vemurafenib-treated [3 µM 24h] and neural crest cells (NCs).

4.3 SOX2 regulates the expression of CD24

To investigate if there is connection between the SOX2 and the CD24 expression or if they are independently upregulated, SOX2 was overexpressed in the melanoma cell lines A375 and SK Mel 28. Subsequently, the level of CD24 expression was examined. A significant increase of CD24 expression on both mRNA and protein level was observed (Figure 12A&B) while no increase in SOX2 expression was noticed upon CD24 OE (data not shown).

To corroborate these data in clinical samples of metastatic melanoma patients, a TMA of 60 tissues stained by IHC was analyzed for SOX2 and CD24 expression. A significant positive correlation (r=0.4; p=0.004) between SOX2 and CD24 expression was observed using pearsons correlation (Figure 12C).

Next, it was investigated if SOX2 regulates CD24 at the transcriptional level. Therefore, the CD24 promotor was examined for potential SOX2 binding sites. By using the JASPAR prediction tool (http://jaspar.genereg.net) 6 putative binding sites for SOX2 were identified in the CD24 promoter as displayed in Figure 12D. The luciferase assay was utilized to measure if SOX2 directly binds to the CD24 promotor at these sites. The assay was performed by using the CD24-promoter luciferase construct published elsewhere (Overdevest et al. 2012). This luciferase construct includes the whole promoter upstream of the luciferase gene. For this assay SOX2 was transiently overexpressed in HEK293T cells as well as in A375 cells (Figure 12E&G) whereby the overexpression in HEK293T cells was more effective than in A375 cells. The plasmids for transient overexpression were co-transfected with the CD24 promotor-luciferase reporter plasmid as well as with a CMV promotor driven Renilla plasmid as control. This resulted in an increased luciferase activity compared to the control cells that had been transfected with an empty control vector instead of the SOX2 OE construct (Figure 12 F&H).

These data are consistent with published CHIP-Seq data on the overexpression of SOX2 in human embryonic stem cells and human skin fibroblasts. These data reveal a

binding of SOX2 to the CD24 promotor at position -1342 with reference to the transcription start site (Tsankov et al. 2015; Soufi et al. 2012; GEO acession number: GSM1505768; GSM896986). Hence, the most likely binding site of SOX2 in the CD24 promotor is the one indicated by a circle in Figure 12D.
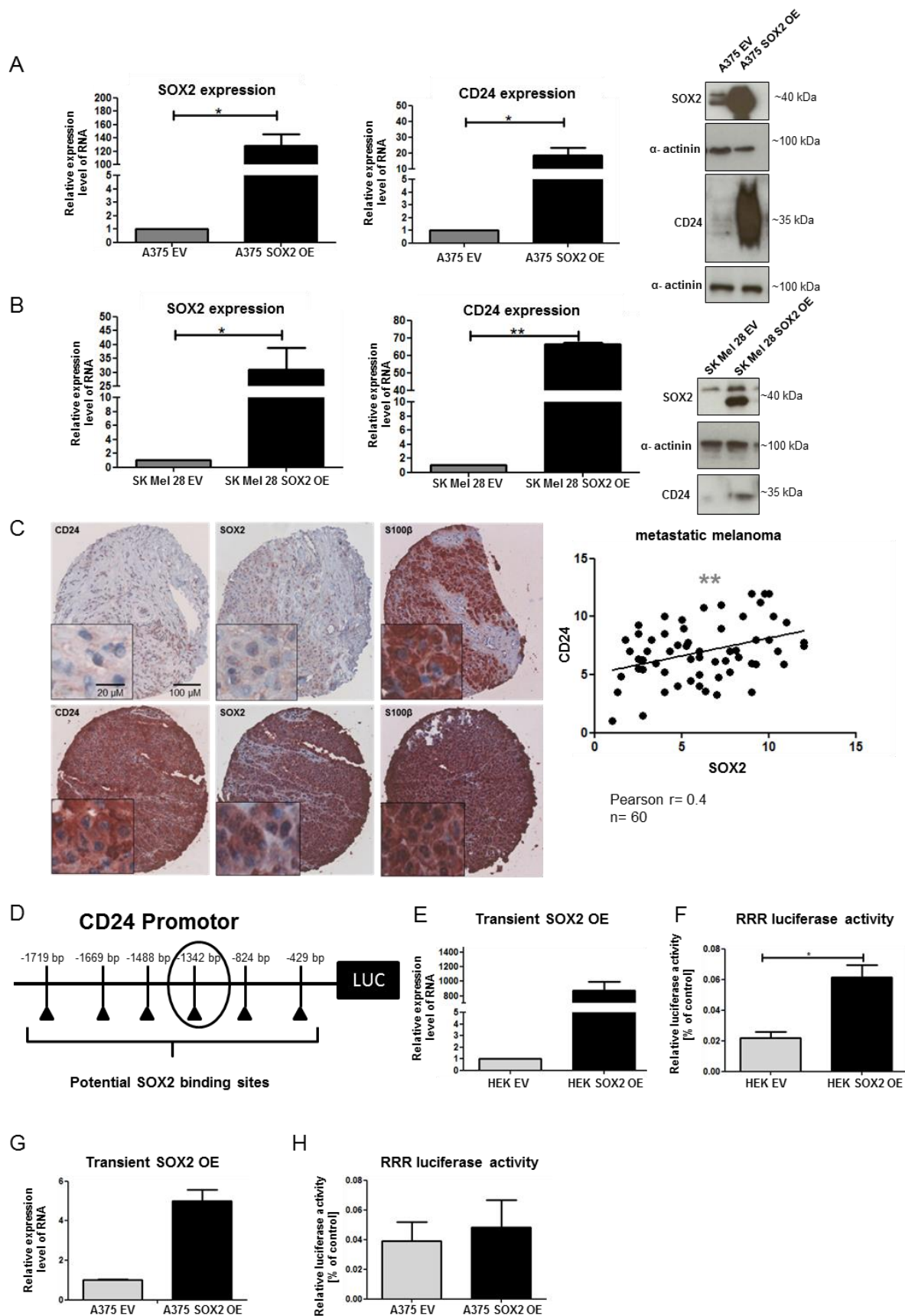
Figure 12: CD24 is regulated by SOX2 and their levels are correlated in metastatic melanoma patient samples. A: Left: Validation of SOX2 overexpression (OE) in A375 cells by qPCR showing relative expression level of mRNA, normalized to 18S, EV= empty vector. Middle: qPCR Data showing increase of CD24 expression in SOX2 OE in comparison to EV A375 cells. Right: Confirmation of qPCR data by WB **B:** Left: SOX2 OE in SK Mel 28 cells was validated by qPCR. The SOX2 OE cells have a significantly higher expression level of SOX2. Middle: qPCR data showing a significant increase in CD24 expression in SK Mel 28 SOX2 OE cells in comparison to EV control cells. Right: WB analysis of the CD24 level after SOX2 OE. An immunoprecipitation against CD24 in lysate of the same protein concentration was performed to enrich the amount of CD24. CD24 is highly increased in the SK Mel 28 SOX2 OE cells. **C:** Left: IHC staining of a TMA of metastatic melanoma patient samples stained for SOX2, CD24 and S100β as indicated. The top row shows an example for a low score of SOX2, CD24 while the sample for sure contains tumor cells as demonstrated by the marker S100β. The lower row shows a TMA sample highly positive for SOX2 and CD24. S100β serves as a marker for tumor cells. Right: Pearson's correlation analysis of CD24 and SOX2 IHC reveals positive correlation of SOX2 and CD24 expression levels in metastatic melanoma samples of patients. **D:** Schematic drawing of CD24 promotor with its potential SOX2 binding sites followed by the luciferase reporter as it is used in the luciferase assay. The most likely binding site due to ChIPseq data is highlighted with a circle. The plasmids were transiently transfected into HEK and A375 cells either together with a SOX2 OE plasmid or an EV control for 48 h. The CMV promotor served as positive control and the pGL4.10 empty vector was used as negative control. **E:** Transient OE of SOX2 in HEK cells validated by qPCR. **F:** The luciferase activity dependent on the SOX2 expression level was measured and all were normalized to the Renilla luciferase activity. The Relative Response Ratio (RRR) is significantly higher in the SOX2-overexpressing HEK cells. **G:** Validation of transient SOX2 OE in A375 cells by qPCR, showing increased SOX2 expression upon overexpression. **H:** Luciferase assay reveals a slight increase of the luciferase activity upon transient SOX2 OE as demonstrated by the increased RRR. (p < 0.05 *; p < 0.01 **; p < 0.001 ***)

4.4 SOX2 or CD24 overexpression augments resistance towards vemurafenib and induces activation of Src and STAT3

Next, it was elucidated whether an increased expression level of SOX2 would influence the resistance towards vemurafenib treatment. Two different melanoma cell lines (A375 and SK Mel 28) either transfected with a constitutively active SOX2 OE construct or an EV as control were treated with increasing concentrations of vemurafenib to determine the IC50. This experiment revealed a significant increase in the IC50 value in SOX2-overexpressing cells compared to empty vector control cells (i.e.: A375: EV mean IC50= 165 nM, SOX2 OE mean= 269 nM; p value= 0.045) (Figure 13A). In accordance with this also an overexpression of CD24 resulted in an increased resistance towards BRAFi treatment when compared to empty vector control cells (Figure 13B). Hence, CD24 OE can mimic the effect of SOX2 OE.

To investigate which downstream pathways could be important for the increased resistance induced by SOX2 or CD24 OE we investigated the change in activity of Src and STAT3. These were shown before in other human carcinoma cells to have an

increased activity upon CD24 OE (Bretz et al. 2012). Thus, it might be possible that the SOX2-mediated upregulation of CD24 cause a similar effect in melanoma cells. Indeed, an increased phosphorylation of Src, STAT3 and ERK was observed upon SOX2 OE in A375 and SK Mel 28 melanoma cell lines that could be related to the increased resistance towards vemurafenib (Figure 13C). CD24 OE in A375 cells led to comparable results (Figure 13D). Therefore, Src and STAT3 activity might play an important role in the SOX2 and CD24-mediated resistance.
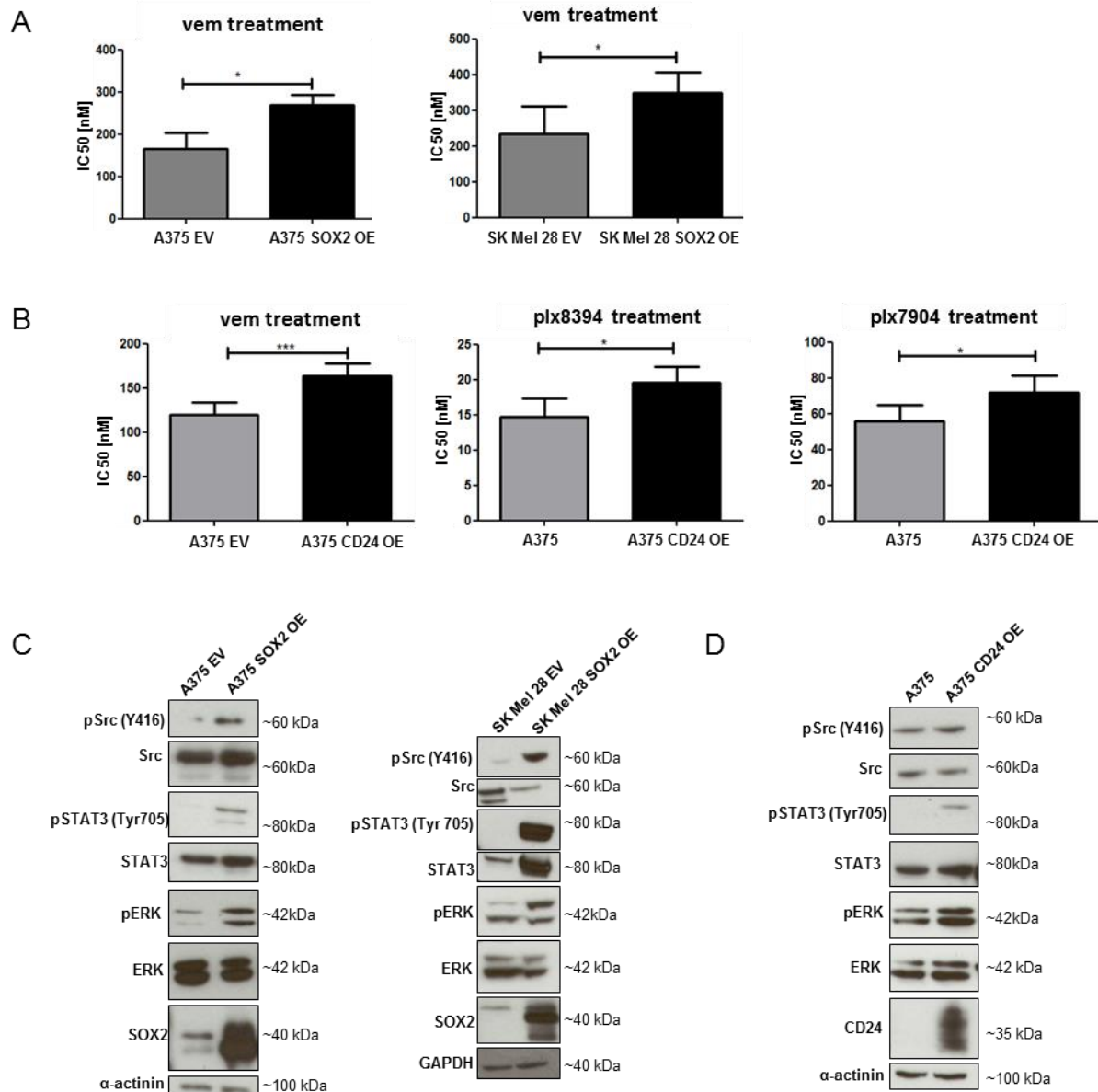
Figure 13 Upregulation of SOX2 or CD24 goes along with increased resistance towards BRAFi and activation of Src, STAT3 and ERK. A: SOX2-overexpressing (OE) A375 and SK Mel 28 cells showed a higher IC50 than empty vector (EV) control cells and were therefore less sensitive towards vemurafenib. **B:** CD24 OE A375 cells showed a higher IC50 when compared to EV control cells. Therefore these cells could tolerate a higher concentration of vemurafenib, plx8394, plx7904. **C:** WB showing an increased activation of Src, STAT3, and ERK in SOX2-overexpressing A375 and SK Mel 28 cells **D:** CD24 OE in A375 cells resulted in an increased activation of Src, STAT3 and ERK.

4.5 Src or STAT3 inhibition is still effective in SOX2 OE and CD24 OE cells

To investigate if the more resistant SOX2 and CD24 OE cells can still be targeted by using Src or STAT3 inhibitors viability assays were performed where the cells were treated with Src or STAT3 inhibitors in addition to vemurafenib.

Figure 14A shows that PP2 is an effective inhibitor of Src but has no effect on STAT3 activity. When SOX2 OE or CD24 OE A375 cells were treated with PP2 in addition to vemurafenib the cells showed a significantly lower IC50 compared to treatment with vemurafenib and DMSO control (Figure 14B&C).

Interestingly, vemurafenib-induced phosphorylation of STAT3 was blocked in the presence of the STAT3-specific inhibitor BP-1-102 but was not affected in the presence of the Src inhibitor PP2 (Figure 14D). Similar results were obtained with another Src inhibitor, dasatinib (data not shown). When SOX2 or CD24 OE cells were treated with BP-1-102 in addition to vemurafenib a decreased IC50 was determined (Figure 14E&F). Hence, these data are comparable with data obtained in the vemurafenib and PP2 treatment experiment (Figure 14B&C).

Thus, the results obtained here suggest that the activation of STAT3 is not dependent on Src phosphorylation and that SOX2 and CD24 might induce adaptive resistance via Src and STAT3 activation. For this reason, targeting Src or STAT3 might be beneficial to overcome adaptive resistance.
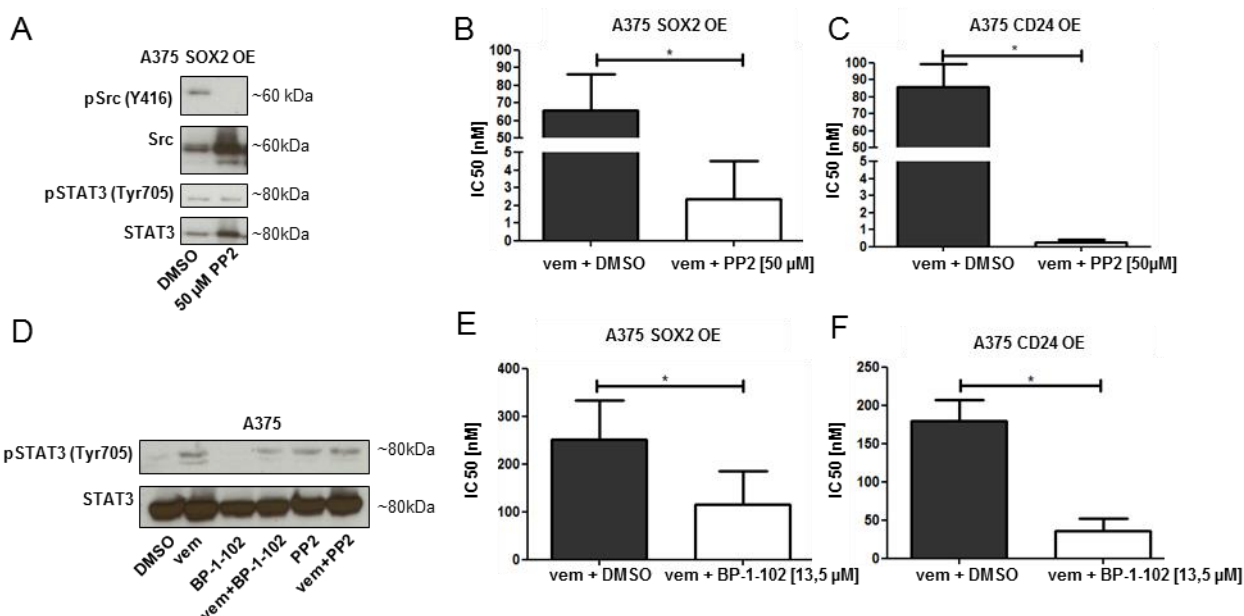
Figure 14: Inhibition of Src or STAT3 is still effective in the more resistant SOX2 or CD24-overexpressing cells. A: SOX2-overexpressing (OE) A375 cells were treated with PP2 [50 μM], an inhibitor of Src. WB showing Src inactivation but no changes in STAT3 activation. **B, C:** Treatment of SOX2 OE or CD24 OE A375 cells with PP2 [50 μM] in addition to vemurafenib leads to a decreased IC50. **D**: STAT3 is activated by vemurafenib [3 μM] and can be inhibited by BP-1-102 [15 μM] but not by PP2 [50 μM]. **E, F**: the more resistant SOX2 OE/ CD24 OE A375 cells can still be killed by the STAT3 inhibitor BP-1-102 as demonstrated by the lower IC50 value of the cells treated with BP-1-102 in addition to vemurafenib. ($p < 0.05$ *; $p < 0.01$ **; $p < 0.001$ ***)

4.6 SOX2 or CD24 knockdown result in a higher sensitivity towards BRAFis

To further analyze the impact of SOX2 on cell viability and BRAFi resistance, a stable knockdown (KD) of SOX2 via shRNA was used. Several clones (KD1-4) showing SOX2 depletion were established (Figure 15A-C). SOX2 KD in A375 (Figure 15A), HT144 (Figure 15B) or SK Mel 28 (Figure 15C) which all represent BRAF mutant cell lines, led to a higher sensitivity towards BRAFis indicated by the lower IC50 values than the respective scramble control cells. Additionally, the effect of CD24 KD on cell viability was examined. To check if knockdown of CD24, which is a downstream effector of SOX2, can hamper the cells resistance, the more resistant SOX2 OE cells were transiently transfected with siRNA targeting CD24. As demonstrated in Figure 15D the KD of CD24 in SOX2-overexpressing cells resulted in an increased sensitivity towards BRAFis. To confirm earlier results for melanoma, the effect of CD24 KD on activation of Src and STAT3 was studied (Bretz et al. 2012). As expected the KD of CD24 resulted in a decreased activity of Src and STAT3 (Figure 15E) in melanoma cells and therefore confirmed the results obtained from other carcinoma cells. Interestingly, CD24 seems to play an important role in melanoma patient survival (Figure 15F). The data revealed that CD24 expression negatively influences patient survival since a higher expression of CD24 can be found in short-time survivors in comparison to long-time survivors. Taken together, these results suggest that in melanoma cells SOX2 and CD24 play an important role in conferring BRAFi resistance and possibly other tumor feature via regulating Src and STAT3 activity.
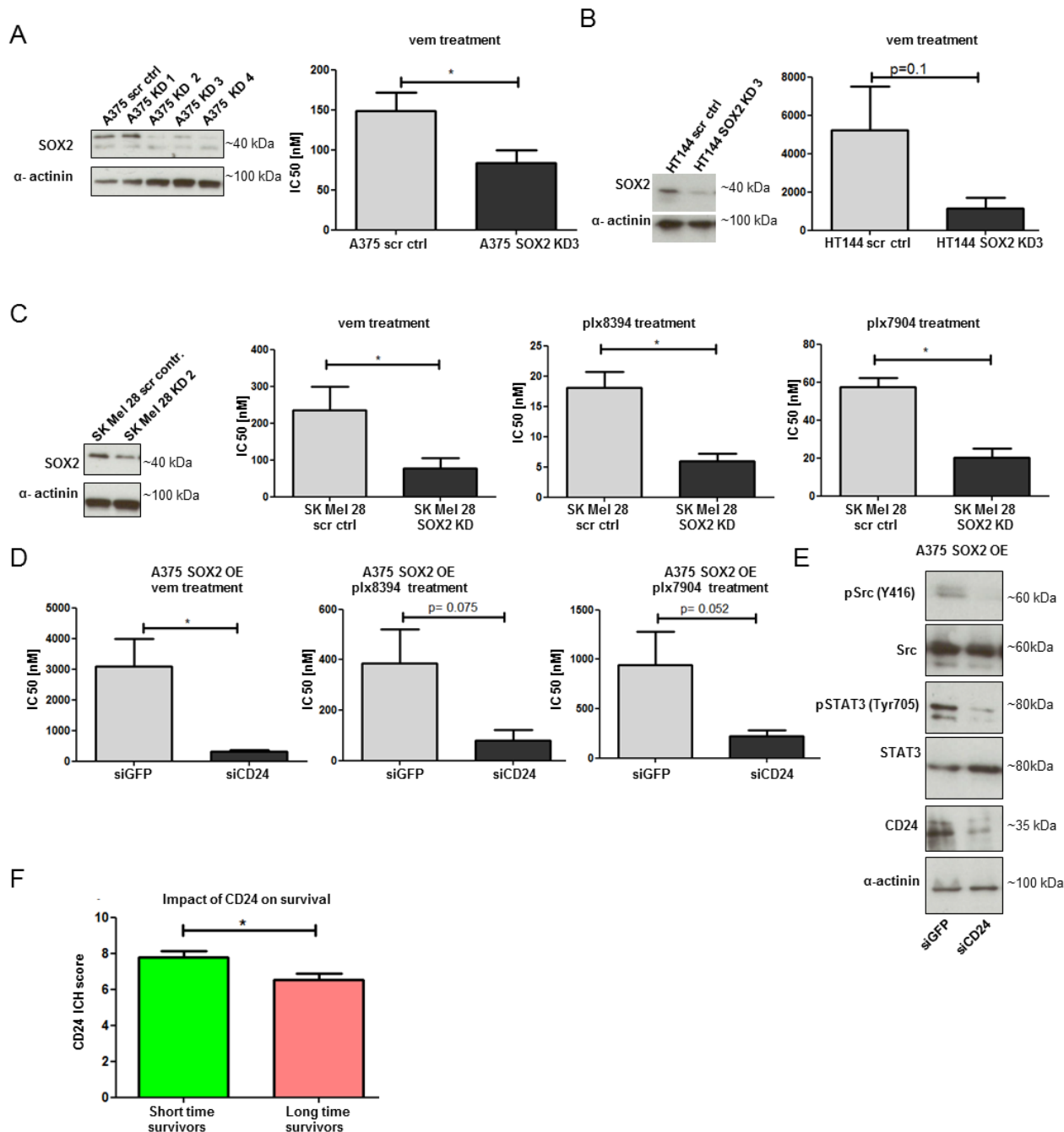
Figure 15: KD of SOX2 or CD24 causes a higher sensitivity towards BRAFi treatment. A: WB demonstrating that the shRNA-mediated knockdown (KD) of SOX2 in A375 cells is effective. A375 cells with a KD of SOX2 show a higher sensitivity towards vemurafenib. **B:** WB to validate shRNA-mediated KD of SOX2 in HT144 cells and the effect of SOX2 KD on the viability of HT144 cells. **C:** KD of SOX2 makes the SK Mel 28 cells more sensitive towards BRAFi treatment. **D:** siRNA KD of CD24 in SOX2-overexpressing A375 cells results in a decreased resistance towards BRAFi treatment as shown by the lower IC50 in the CD24 KD cells. **E:** siRNA-mediated KD of CD24 leads to a decreased activation of Src and STAT3 in SOX2 OE A375 cells. **F:** TMA staining of melanoma patient specimens were analyzed for the CD24 expression and classified into short-time survivors (<12 months; n=57) and long-time survivors (>12 months, n=41). The results revealed a significantly higher CD24 expression in short-time survivors in comparison to long-time survivors. (p < 0.05 *; p < 0.01 **; p < 0.001 ***)

4.7 STAT3 activation is required for SOX2 and CD24 induction

To examine the upstream regulators of SOX2 and CD24 during vemurafenib treatment, the SOX2 and CD24 expression in dependence of STAT3 activity was investigated. STAT3 is a transcription factor that after being phosphorylated at tyrosine 705 dimerizes and translocates to the nucleus, where it binds to target genes and promotes transcription (Darnell 1997). Figure 16 shows that upon vemurafenib treatment phosphorylated STAT3 was increased and translocated to the nucleus where it can regulate its target genes. It could be shown that the increase of SOX2 and CD24 expression upon vemurafenib treatment was linked to STAT3 activation (Figure 17A-C). Figure 17 illustrates that inhibiting STAT3 by the STAT3-specific inhibitor BP-1-102 during vemurafenib treatment diminished the vemurafenib-induced increase of SOX2 and CD24 expression on protein and mRNA level. Furthermore, an early activation of STAT3 was noticed. It was detectable already 6 h after onset of treatment (Figure 17D). Moreover, SOX2 and CD24 were upregulated upon vemurafenib treatment when STAT3 was activated. Src on the other hand showed only a slight increase in activity after 24h of vemurafenib treatment (Figure 17D). Additionally, siRNA KD of STAT3 or Src was used to investigate their influence on SOX2 and CD24 expression. Indeed, siRNA-mediated STAT3 KD resulted in a decrease of SOX2 and CD24 expression while Src KD showed no effect (Figure 17E). These data clearly suggest that STAT3 activation is required for the induction of SOX2 and CD24 expression in A375 melanoma cells upon vemurafenib treatment. A similar regulation of SOX2 by STAT3 in neural precursor cells (Foshay & Gallicano 2008) and the binding of STAT3 to the SOX2 promoter in melanoma cells were shown before (Pietrobono et al. 2016).
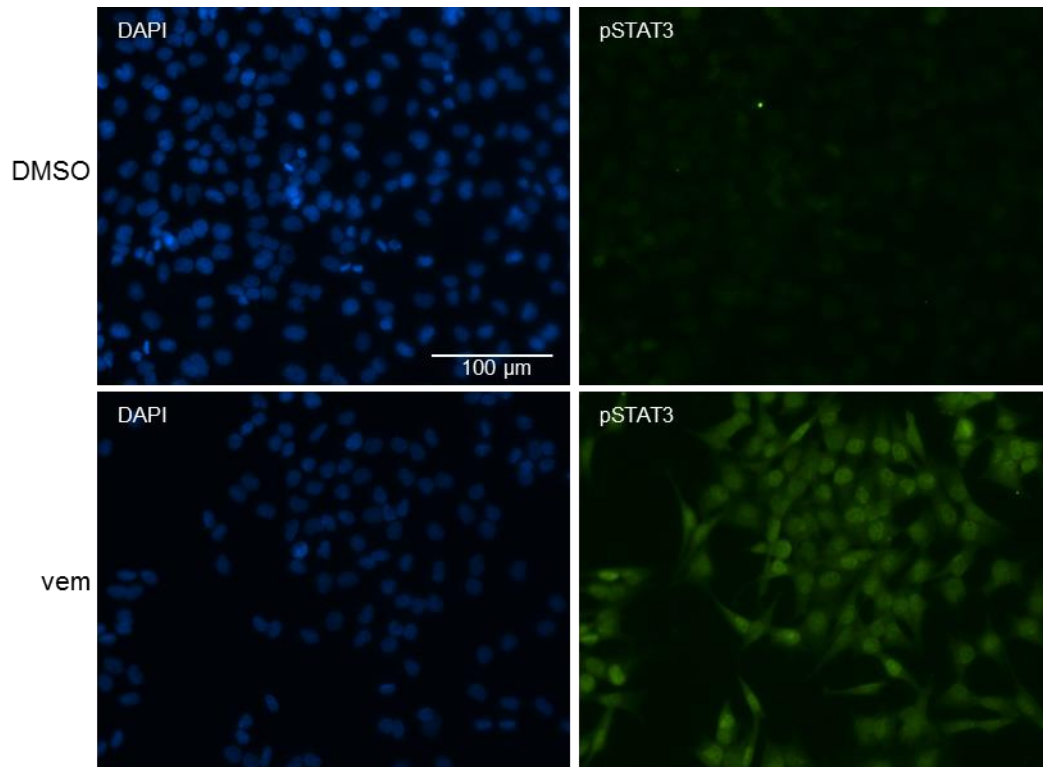
Figure 16: Phosphorylated STAT3 is increased and transferred to the nucleus upon vemurafenib treatment. DAPI (blue) stains the nucleus of all cells. pSTAT3 was stained with an antibody which specifically detects STAT3 phosphorylated at tyrosine 705 (green). A375 cells treated with vemurafenib [3µM; 24h] showed an increase in pSTAT3 mainly located in the nucleus.
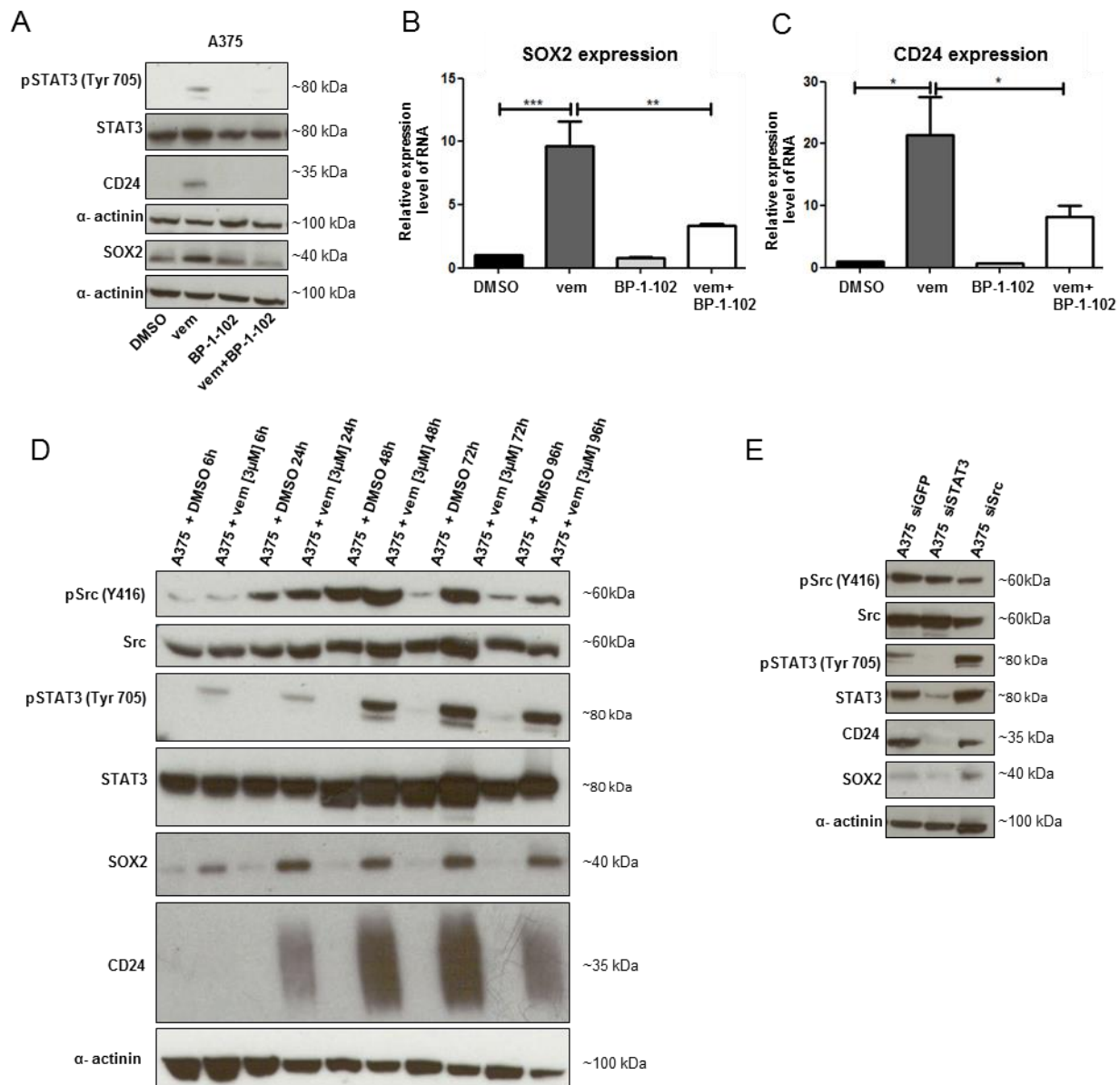
Figure 17: STAT3 activation by vemurafenib is essential for increased SOX2 and CD24 expression.
A: WB of A375 cells treated for 24h with DMSO, vemurafenib [3 μM], BP-1-102 [15 μM], vemurafenib [3 μM] + BP-1-102 [15 μM]. The WB shows that the increased STAT3 activation upon vemurafenib treatment could be inhibited in the presence of the STAT3 inhibitor BP-1-102. Furthermore the vemurafenib induced SOX2 and CD24 expression was reduced when the STAT3 inhibitor was present in addition to vemurafenib **B, C:** qPCR data confirming the WB results for SOX2 (B) and CD24 (C) on the mRNA level. qPCR showing relative expression level of mRNA, which is normalized to 18S. **D:** WB of A375 cells treated for the indicated times with 3 μM vemurafenib or DMSO as control. The STAT3 activation is depicted by pSTAT3 and was increased after 6h of vemurafenib treatment. Furthermore, SOX2 was also increased after 6h vemurafenib treatment while a high increase in CD24 was detected after 24h of vemurafenib treatment. Src was slightly activated after 24h vemurafenib treatment as depicted by the increase in pSrc. **E:** A375 cells were treated with siRNA against GFP as control, STAT3 and Src. SOX2 and CD24 were downregulated by siRNA knockdown (KD) of STAT3 but were unchanged after Src KD. (p < 0.05 *; p < 0.01 **; p < 0.001 ***)

4.8 Vemurafenib-induced NF-kappa B activation is an early event and sheddases play an important role in STAT3 activation

To study how vemurafenib can activate STAT3 the activation of NF-kappa B was examined as it was previously shown that NF-kappa B is able to activate STAT3 promoting a more dedifferentiated phenotype (Agarwal & Zambidis 2014). The results revealed an NF-kappa B activation already after 30 min of vemurafenib treatment while STAT3 was activated 6h after treatment (Figure 18A). As NF-kappa B activation can cause the release of soluble factors (Kulms & Schwarz 2006) which then might activate STAT3 it was studied if the supernatant alone was able to activate STAT3. Therefore, cells were pulsed for 6h with vemurafenib or DMSO as control. Next, the cells were washed and fresh medium was added over night. At the next day, the supernatant was transferred to naive cells and the cells were incubated with this medium for the indicated time. The results revealed that the supernatant of the vemurafenib pulsed cells alone was able to activate STAT3 (Figure 18B). Thus, soluble factors were the reason for the vemurafenib-induced STAT3 activation. To investigate which are the factors responsible for the STAT3 activation a cytokine array was performed. The cytokine array showed that cytokines present on the human cytokine profiler such as IL-6 or CCL2 were not the reason for the increased STAT3 activation in these settings (data not shown). Hence, it still needs to be investigated which soluble factors activate STAT3. Interestingly, the vemurafenib-induced STAT3 activation as well as the increased expression of SOX2 and CD24 could be diminished by using TAPI-2, which is an inhibitor of ADAMs (a disintegrin and metalloproteinase) (Figure 18C). ADAMs shed transmembrane domains of extracellular proteins (i.e. different receptor ligands and cytokines) and are therefore classified as sheddases. Recently, it was published that vemurafenib induces TNFα (tumor necrosis factor alpha) which then activates NF-kappa B (Lehraiki et al. 2015). For this reason, it was investigated if TNFα was present in the supplement and responsible for the increased STAT3 activation and the induction of expression of SOX2 and CD24. The administration of recombinant TNFα did not activate STAT3 or increase the expression of SOX2 and CD24 (Figure 18C). Moreover, a TNFα Elisa showed no increase in TNFα in the supernatant after vemurafenib treatment (data not shown). Hence, TNFα was not the player mediating the vemurafenib-induced STAT3 activation

and therefore not responsible for the increase in SOX2 and CD24 expression upon vemurafenib treatment. In summary, these data suggest that the vemurafenib-induced activation of STAT3 was triggered most likely by soluble factors cleaved by ADAMs.
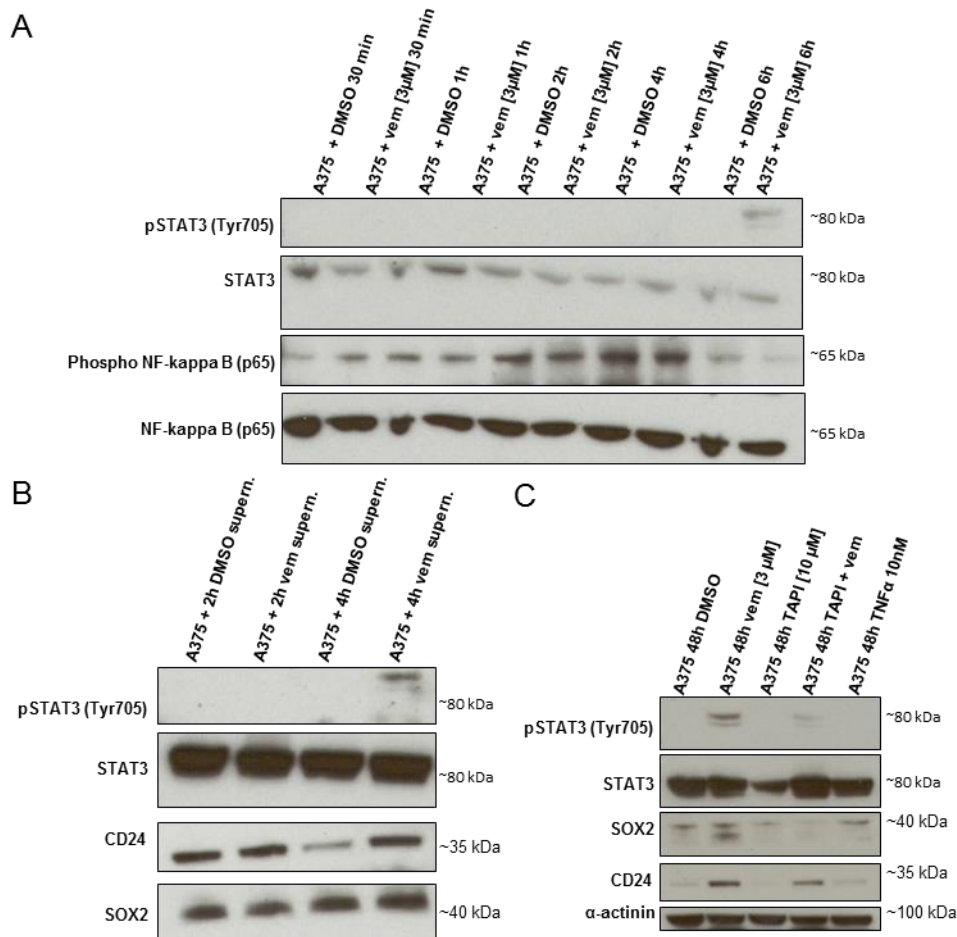
Figure 18: NF-kappa B (p65) activation is an early event after vemurafenib treatment followed by STAT3 activation. STAT3 is activated by a soluble factor cleaved by a sheddase. A: NF-kappa B (p65) showed an increased activation upon 30 min of vemurafenib treatment while STAT3 was activated by vemurafenib after 6h of treatment. **B:** A375 cells were pulsed for 6h with vemurafenib [3 µM] or DMSO as control. Then the medium containing vemurafenib or DMSO was exchanged with fresh medium after washing the cells. The next day the supernatant was transferred to fresh cells for the times indicated in the WB. STAT3 could be activated with the vemurafenib-pulsed supernatant after 4h. CD24 and SOX2 also showed a slight increase. **C:** The vemurafenib-induced STAT3 activation after 48h could be inhibited by the addition of TAPI-2 [10 µM] which inhibits sheddases while TNFα could not activate STAT3. Moreover, vemurafenib increased the expression of SOX2 and CD24. This increase was reduced by adding TAPI-2 [10 µM] to vemurafenib [3 µM].

4.9 Receptor tyrosine kinase (RTK) activation can be influenced by vemurafenib treatment

To investigate if RTKs are differentially activated after vemurafenib treatment an array screening different RTKs was performed. Figure 19 shows an increased activation of ErbB3 (Erb-B2 receptor tyrosine kinase 3) and M-CSF R (monocyte colony stimulating factor receptor) while Dtk (TYRO3 protein tyrosine kinase), EphA2, EphA4, EphA7 (ephrin receptors) and DDR1 (discoidin domain receptor tyrosine kinase 1) are less phosphorylated in comparison to the DMSO control. Most interesting was the ErbB3 activation upon vemurafenib treatment as this was already shown to play an important role in adaptive resistance (Kugel & Aplin 2014). Hence, ErbB3 activation might be responsible for the vemurafenib induced STAT3 activation and thereby cause an increased SOX2 and CD24 expression after vemurafenib treatment.
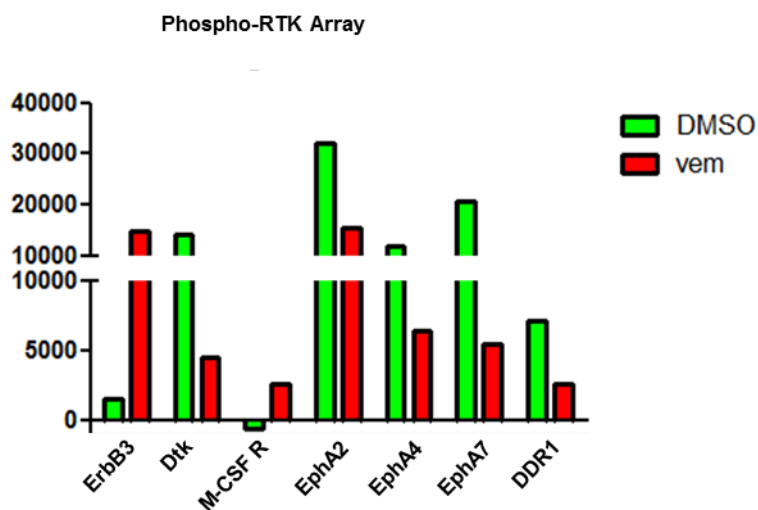
Figure 19: Vemurafenib-treatment can change the RTK phosphorylation. Phosphorylation of receptor tyrosine kinases (RTK) after 24h of vemurafenib [3 µM] treatment was compared to DMSO control treatment by using a Phospho-RTK array (bars represent mean of technical duplicates, SEM< 5%)

4.10 SOX2 and CD24 are not crucial in acquired therapy resistance

To investigate if SOX2 or CD24 play also an important role in acquired resistance, resistant cell lines were established. Figure 20A illustrates the higher drug tolerance of the resistant cells in comparison to their parental cell lines to confirm their resistance. During the acquisition of resistance some cell lines changed their morphology as shown

in Figure 20B while others showed the same morphology as their parental counterparts (data not shown). Microarray analysis was performed to investigate the differential gene expression in resistant and parental cells. In terms of SOX2 or CD24 only an increased expression of SOX2 could be detected in resistant HT144 cells (HT144 res cells) (FC>1) while CD24 was only upregulated in resistant SK Mel 28 cells (SK Mel 28 res cells) (Figure 21A&B). The CD24 and SOX2 expression was also analyzed on mRNA level via qPCR showing a significantly increased SOX2 expression in HT144 res cells in comparison to parental cells while SK Mel 28 res cells displayed a significant downregulation of SOX2 (Figure 21 C). In contrast, CD24 was significantly increased in SK Mel 28 res cells and vemurafenib-resistant A375 res 7 µM vem cells (Figure 21D). The analysis on protein level confirmed the results obtained from qPCR for SOX2 while an upregulation of CD24 was observed in trametinib resistant A375 res 130 nM tra cells instead of in A375 res 7 µM vem cells (Figure 21E). Thus, no correlation between SOX2 and CD24 expression in cells with acquired resistance was observed.

Furthermore, it was investigated if siRNA KD of SOX2 in cells with acquired resistance could restore sensitivity towards the inhibitor since in naive cells a KD of SOX2 resulted in an increased sensitivity. Figure 21F&G show that siRNA-mediated SOX2 KD did not change the sensitivity towards the BRAFi. Interestingly, it was observed that when the resistant cells were treated with a higher concentration of the BRAFi no significant increase in SOX2 or CD24 expression could be detected (Figure 21H&I). Taken together, these results reveal a role of SOX2 and CD24 in adaptive resistance but not in acquired resistance.
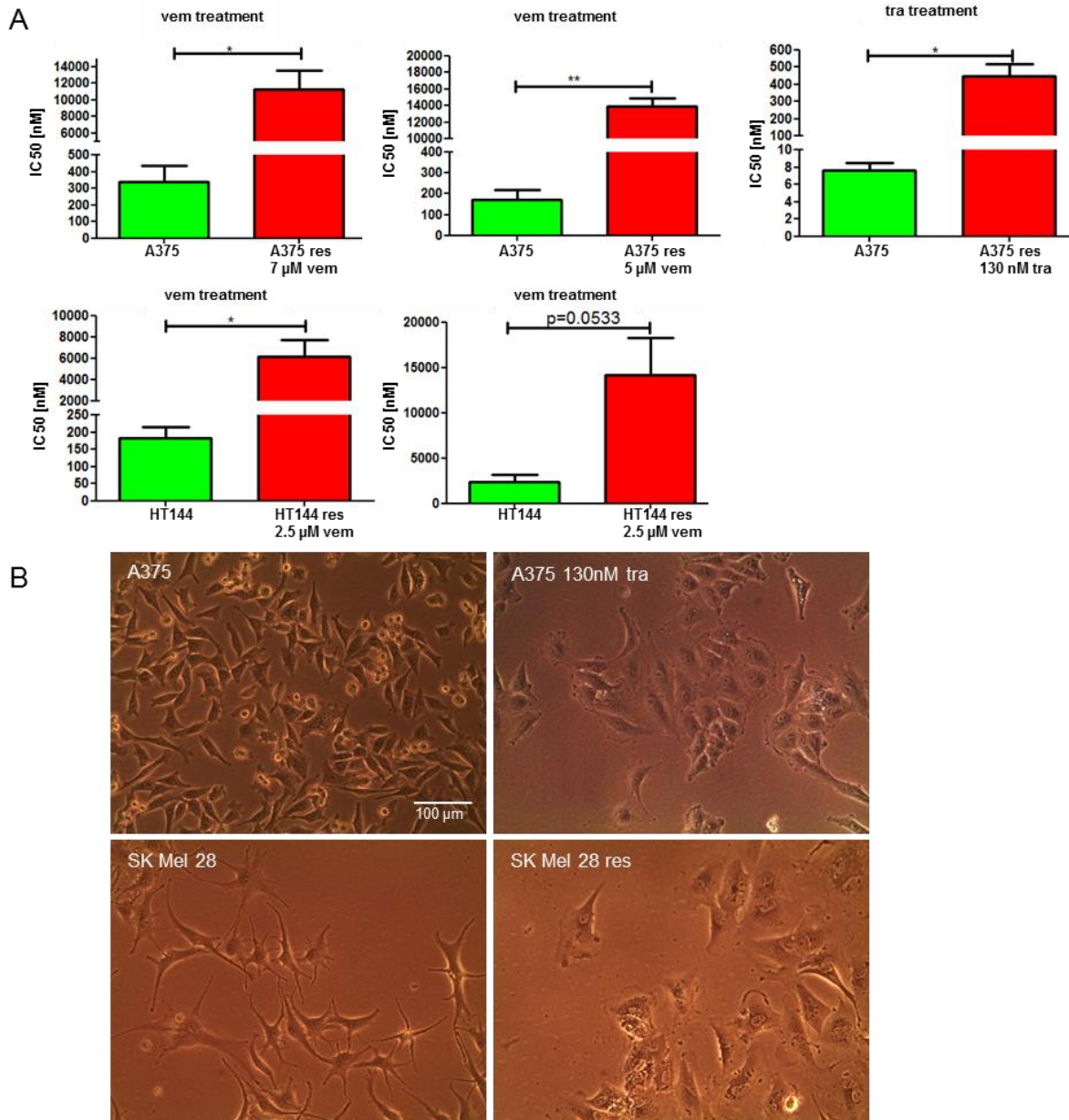
Figure 20: Resistant cells can tolerate a higher dose of the inhibitor they are resistant to and some change their morphology. A: Resistant (res) and parental cells were treated with increasing concentrations of the inhibitor they were resistant to. The res cells could tolerate a higher dose of the inhibitor as indicated by the higher IC50 value confirming their resistance. **B:** Some of the resistant cells changed their morphology. ($p < 0.05$ *; $p < 0.01$ **; $p < 0.001$ ***)
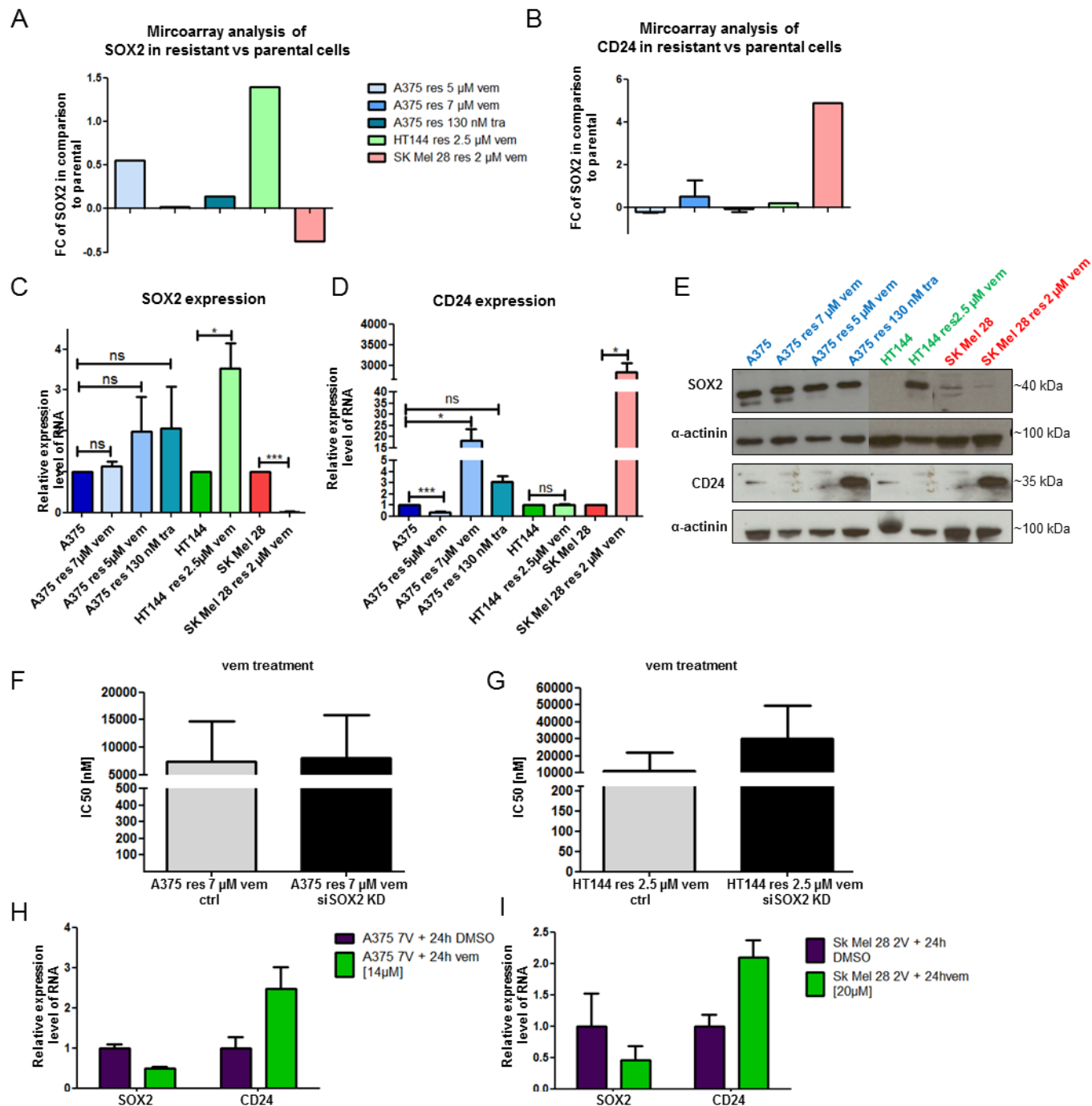
Figure 21: SOX2 and CD24 do not play a role in acquired resistance. A: Microarray analyses revealed that the level of SOX2 was only changed (FC: >1; <-1) in vemurafenib-resistant HT144 cells (HT144 res), in comparison to parental cells. **B:** CD24 was only changed in SK Mel 28 res cells in comparison to parental cells. **C:** qPCR data showed a significant SOX2 upregulation in vemurafenib-resistant HT144 cells and downregulation in vemurafenib-resistant SK Mel 28 cells in comparison to parental cells. **D:** CD24 was significantly increased in A375 res 7 µM vem cells and in SK Mel 28 res cells. **E:** WB showing the expression of SOX2 and CD24 in parental and resistant cells. **F/G:** siRNA KD of SOX2 could not restore sensitivity in the resistant A375 (F) and HT144 (G) cells. **H/I:** Treating the resistant cells with a higher dose of vemurafenib (as indicated) for 24h did not lead to a significant change in the SOX2 and

CD24 expression in A375 (H) and SK Mel 28 (I) res cells. A375 7V= A375 res 7 µM vem cells; SK Mel 28 2V=SK Mel 28 res 2 µM vem cells. (p < 0.05 *; p < 0.01 **; p < 0.001 ***)

4.11 Deregulated pathways and molecules in cells with acquired resistance

To further characterize the cells that acquired resistance, different pathways and molecules which might be deregulated were analyzed. First, the ERK activation in the resistant cells was examined showing an increased activity of ERK in all resistant cell lines in comparison to the parental cells. AKT activity was only increased in HT144 res cells and SK Mel 28 res cells. Interestingly, Src showed an increased activity in HT144 res cells while it was decreased in A375 res 7 µM vem cells. Moreover, STAT3 activity was high in A375 res 5 µM vem cells as well as in A375 res 130 nM tra and SK Mel 28 res cells (Figure 22A).

As the modified expression of Axl, MITF and SOX10 were shown to play a role in resistance (Müller et al. 2014; Sun et al. 2014) the expression of these molecules was examined. A decreased MITF and SOX10 expression in SK Mel 28 res cells was observed on mRNA and protein level while the Axl expression was increased. The MITF expression was also slightly downregulated in all other resistant cell lines while the SOX10 expression was also downregulated in A375 res 7 µM vem and A375 res 130nM tra cells as well as in HT144 res cells (Figure 22B-E). Hence, some resistant cells showed a modified expression of Axl, SOX10 and MITF.

As a change in EGRF expression was also shown to be involved in the establishment of resistance (Sun et al. 2014; Manzano et al. 2016), the EGFR expression in resistant cells in comparison to their parental counterpart was analyzed. No significant changes were noticed (Figure 22F).

Interestingly, microarray data of resistant and parental cells analyzed with Ingenuity Pathways Analysis revealed an altered activity of the TGFβ pathway in nearly all resistant cell lines (except A375 res 130nM tra cells). Moreover, this analysis also showed a change in cell survival as well as cellular movement and proliferation in the resistant cells. The genes changed in the majority of the resistant cell lines (all except A375 res 5 µM vem cells) were among others upregulated NUPR1 (nuclear protein 1), which promotes tumor repopulation and cell growth, as well as downregulated anti-tumor genes SFRP1 (secreted frizzled-related protein 1) and RUNX3 (runt-related transcription

factor 3) and the inhibitor of cell growth, metastasis and invasion AGPAT9 (1-Acyl-Sn-glycerol-3-phosphate O-acyltransferase 9).
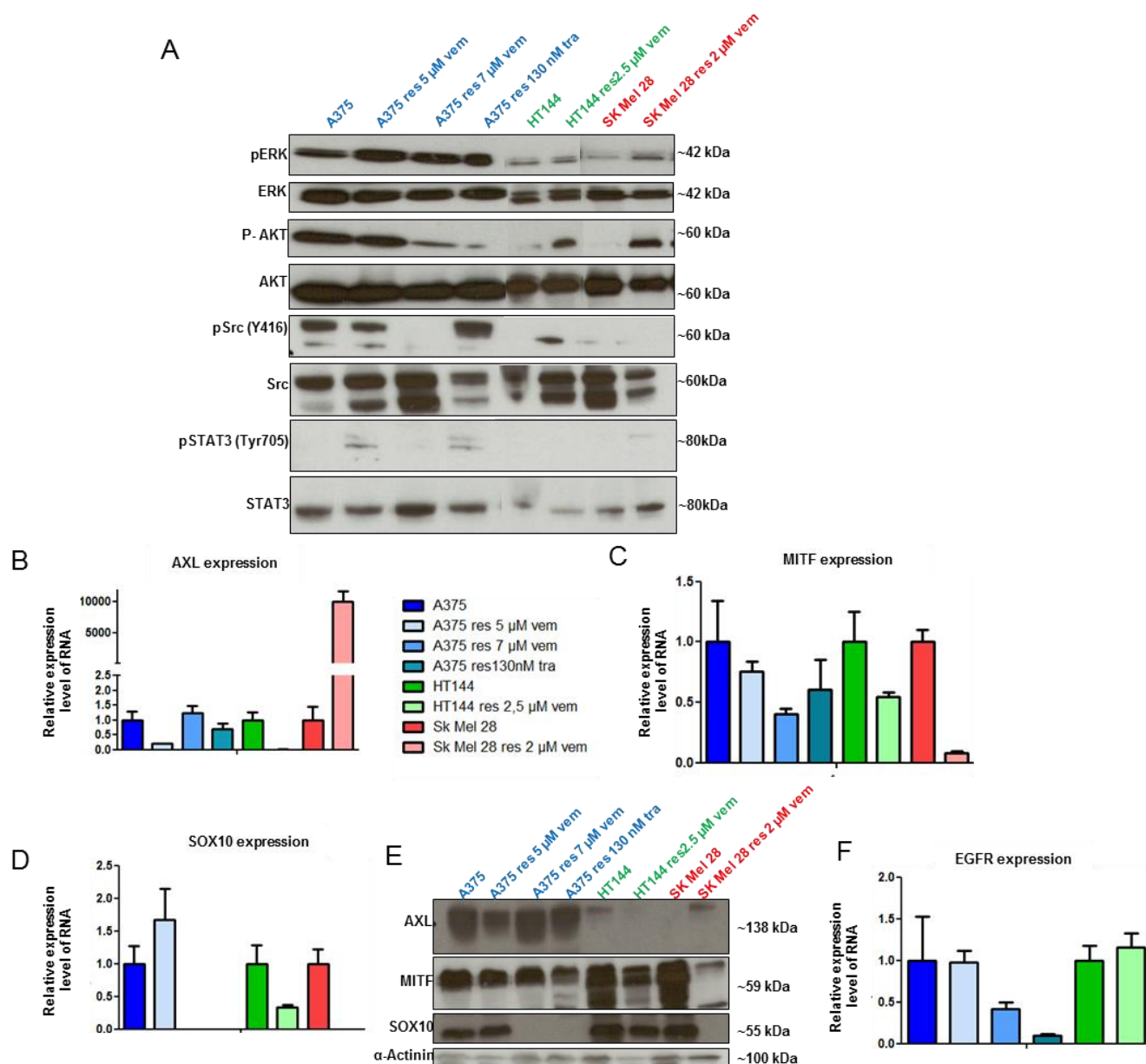
Figure 22: Characterization of resistant cells. A: WB analyses of pathways which might be deregulated after acquiring resistance. ERK is more activated in resistant cells in comparison to parental cells. AKT is more strongly activated in HT144 res cells and in SK Mel 28 res cells in comparison to parental cells while in A375 res 7 µM vem and A375 res 130 nM tra AKT is even inactivated. Src is activated in HT144 res cells and inhibited in A375 res 7 µM vem cells and SK Mel 28 res cells. STAT3 activation is increased in A375 res 5 µM vem, A375 res 130 nM tra and SK Mel 28 res cells. **B/C/D:** Determination of Axl, MITF and SOX10 expression by qPCR showing relative expression level of mRNA, normalized to 18S. **E:** Protein expression of Axl, MITF and SOX10 in resistant and parental cells. **F:** Change in EGFR RNA expression in resistant cells in comparison to parental cells.

4.12 Cell cycle analysis reveals an increased expression of the cyclin-dependent kinase inhibitors p27 and p21

To further investigate if the resistant cells have an altered cell cycle regulation, the expression of p27 and p21 was examined. Figure 23 illustrates that some of the resistant cell lines showed a change in the expression of the cell cycle regulators p27 and p21. In A375 res 5 µM vem as well as in A375 res 130nM tra, HT144 res and SK Mel 28 res cells an increased expression of p27 in comparison to their parental cells was visible. Moreover, an increase in p21 was detected in SK Mel 28 res cells compared to the parental cell line. Both, p27 and p21, are inhibitors of cyclin-dependent kinases (CDKs). CDKs regulate together with cyclins the transition from G1 phase to S phase or if the cells are in G2 they initiate mitosis. Hence, CDKs promote proliferation. As inhibitors of CDKs, p27 and p21 inhibit proliferation and thus the resistant cells have a less proliferative phenotype. Furthermore, p27 and p21 have also been demonstrated to play a role in apoptosis (Coqueret 2003).
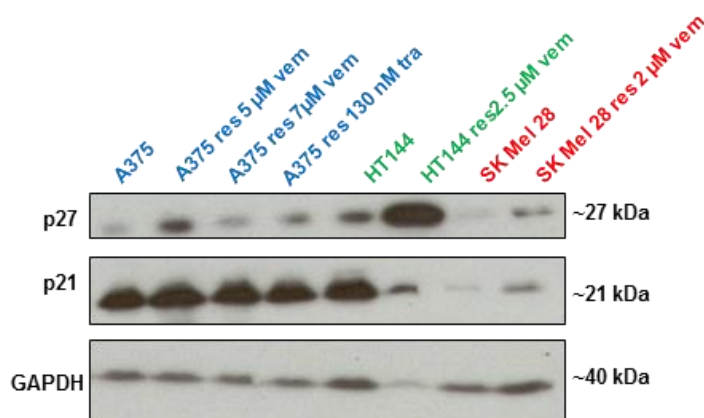

Figure 23: Cell cycle analysis of parental and resistant cells. Increased expression of p21 or p27 revealed a less proliferative phenotype because the cell cycle is arrested in G1. In A375 res 5 µM vem cells, A375 res 130 nM tra cells and in HT144 and SK Mel 28 res cells p27 is more strongly expressed than in parental cells. Only SK Mel 28 res cells show an increased expression of p21.

5 Discussion

Melanoma is one of the most aggressive types of skin cancer leading to the majority of skin cancer-related deaths. Targeted therapies are initially a very effective treatment but resistance occurs (Manzano et al. 2016). Therefore, understanding the mechanisms of resistance became the major topic of my study.

In the present work I show that i) SOX2 and CD24 were upregulated upon short-term BRAFi treatment of melanoma cells and a similar upregulation was observed in iPCCs that are resistant to targeted therapy; ii) there was a positive correlation between SOX2 and CD24 expression based on the analysis of IHC stainings of tissue sections of metastatic melanoma specimens; iii) SOX2 could directly bind and activate the CD24 promoter as revealed in luciferase reporter assays; iv) overexpression of SOX2 led to an increase in resistance towards BRAFi treatment which was attenuated by CD24 KD; v) CD24 overexpression could mimic the effect of SOX2 overexpression; vi) SOX2 KD resulted in a similarly decreased resistance towards BRAFis; vii) SOX2 OE and CD24 OE activated STAT3 and Src, viii) Inhibition of Src or STAT3 could overcome the resistance mediated by SOX2 OE or CD24 OE ;ix) STAT3 was activated by soluble factors and activated STAT3 was required for the induction of SOX2 expression forming a feedback loop. The mechanism found in this study is summarized in Figure 24 demonstrating that the activation of STAT3 by a soluble factor cleaved by sheddases promotes the expression of SOX2. SOX2 then binds to the CD24 promoter resulting in an upregulation of CD24 leading to an increased activity of Scr and STAT3. This mechanism helps tumor cells to circumvent the action of BRAF inhibitors.
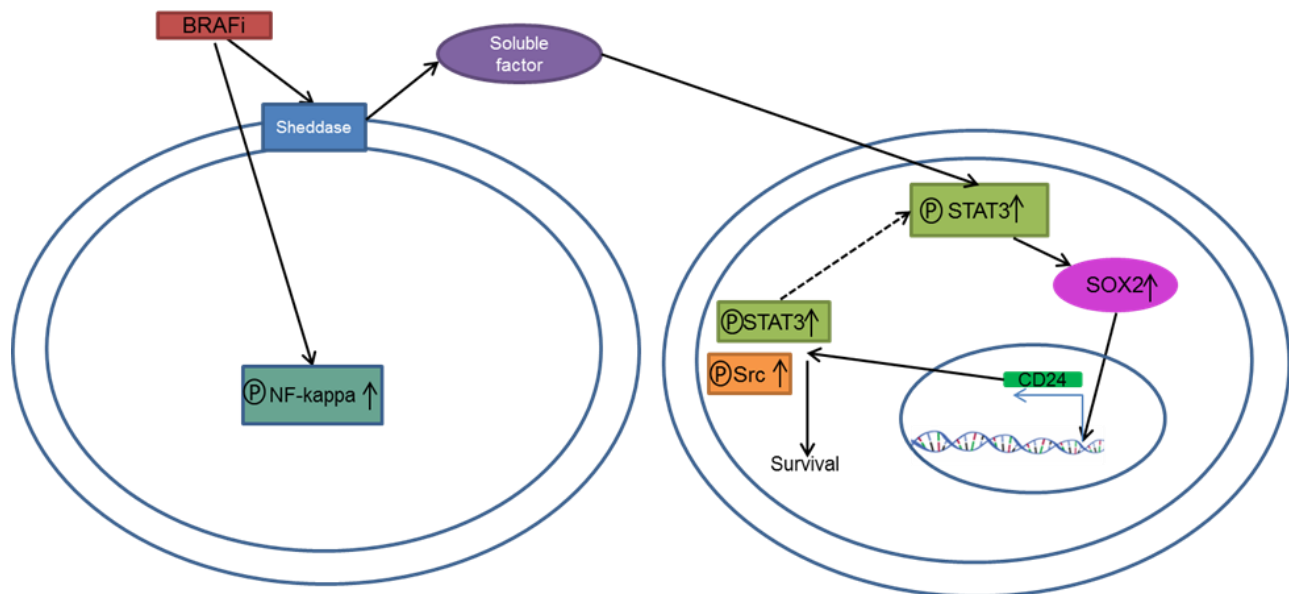
Figure 24: Schematic overview of the SOX2 and CD24-mediated adaptive resistance. The treatment with BRAFi leads to an activation of NF-kappa B and sheddases. This leads to a secretion of soluble factors. These factors induce STAT3 activity that induces a higher expression of SOX2. SOX2 promotes the expression of CD24 by binding to its promotor. The increased CD24 expression causes a higher Src and STAT3 activation contributing to cell survival. STAT3 might provide an autocrine stimulus for further SOX2 expression.

5.1 SOX2 and CD24 in adaptive resistance

Here, I show that the expression of SOX2 and CD24 was increased in iPCCs which are resistant to targeted therapy (Bernhardt et al., 2017) as well as in short-time inhibitor treated melanoma cells (Figure 8 and Figure 9). Additionally, I could show that the melanoma cells treated with BRAFis as well as melanoma cells overexpressing SOX2 reveal a more dedifferentiated phenotype (Figure 11). CD24 and SOX2 were already associated with a less differentiated and more cancer stem cell-like phenotype (Zhang 2014; Lundberg et al. 2016; Yang et al. 2014; Santini et al. 2014; Ke et al. 2012) for which also a higher resistance towards therapy was shown (Fallahi-Sichani et al. 2017). Interestingly, the later study by Fallahi-Sichani et al. (2017) reported some new observations regarding the cellular response to vemurafenib in melanoma. It was observed on a single-cell level that the exposure of tumor cells to BRAFi caused a heterogeneous response in which some cells die, some arrest, and the remainders adapt to the drug. Drug-adapted cells upregulate neural crest markers (e.g., NGFR), a melanocyte precursor marker, and grow slowly.

This is in good agreement with the study of Sachindra et al. (2017) who showed a link between adaptive resistance and dedifferentiation in melanoma. Moreover, the study of Marzagalli et al. (2018) demonstrated that cells which survived treatment with vemurafenib formed more often spheres in comparison to control cells. These cells also showed an increased expression of stemness genes like SOX2. Therefore the authors claimed that these cells build the cancer stem cell population.

Furthermore, both SOX2 and CD24 have also been linked to an increased therapy resistance (Song et al. 2016; Piva et al. 2014; Pietrobono et al. 2016; Deng et al. 2017; Surowiak et al. 2006; Ono et al. 2015; Jiao et al. 2013). This is in line with the data presented here that in melanoma cells an increased expression level of SOX2 or CD24 resulted in a higher tolerance towards BRAFis (Figure 13A&B), while the depletion of SOX2 via KD led to higher sensitivity (Figure 15A-C). Similarly, the KD of CD24 in the more drug resistant SOX2 OE cells led to a restoration of sensitivity (Figure 15D). These findings indicate that SOX2 expression induced a higher resistance towards BRAFis via the upregulation of CD24, since overexpression of CD24 showed the same effect as SOX2 overexpression. Moreover, the data even reveal a direct regulation of CD24 by SOX2 as SOX2 is able to bind to the CD24 promotor activating CD24 expression (Figure 12). Accordingly, in published CHIP-Seq data on the overexpression of SOX2 in human embryonic stem cells and human skin fibroblasts a binding of SOX2 to the CD24 promotor at position -1342 in relation to the transcription start site can be found (Tsankov et al. 2015; Soufi et al. 2012; GEO acession number: GSM1505768; GSM896986). Hence, SOX2 regulated CD24 expression by a direct binding to its promotor.

Additionally, to corroborate the SOX2 and CD24 expression data in clinical samples, I showed that both their expressions were correlated in metastatic melanoma patient samples (Figure 12C). As it is described that targeted therapy resistance can be due to selection of clones (Hong et al. 2017) I wanted to investigate if the increased expression of CD24 was due to selection of CD24-high clones or due to an increase in expression. Figure 10 shows that the increased expression of CD24 upon vemurafenib treatment was due to an upregulation of expression rather than selection. Previous work had demonstrated that CD24 has an influence on oncological properties such as cell proliferation and survival via an increased activity of Src and STAT3 (Baumann et al.

2012; Bretz et al. 2012). Therefore, I speculated that the upregulation of Src and STAT3 activity might be the reason for the SOX2/ CD24-associated resistance. Indeed, I could show that a KD of CD24 resulted in a decreased activity of Src and STAT3 (Figure 15E) and CD24 overexpression activated Src and STAT3 (Figure 13D), confirming the study of Bretz et al. (2012) on malignant melanoma. Additionally, I could show that cells overexpressing SOX2 had a higher activity of Src and STAT3 (Figure 13C). These results are in good agreement with the study of Wang et al. showing that SOX2 regulates the activity of Src in ovarian cancer (Wang et al. 2014). In addition, Figure 14B&C shows that Src inhibition could hamper the SOX2/CD24-dependent resistance towards vemurafenib. This is consistent with recent studies showing that Src inhibition can overcome resistance (Girotti et al. 2015; Girotti et al. 2013). Moreover, Fallahi-Sichani et al. (2017) showed that drugs targeting the c-Jun/ECM/FAK/Src cascade can increase the maximum effect of BRAFi by promoting cell killing. Thus, the analysis at the single-cell level identifies signaling pathways and inhibitory drugs missed by assays that focus on cell populations.

Additionally, I could demonstrate that the more resistant SOX2 or CD24 overexpressing cells were still sensitive to STAT3 inhibition (Figure 14E&F). This result is in good agreement with the study of Liu and colleagues (2013) showing that STAT3 inhibition can overcome targeted therapy resistance. Interestingly, the STAT3 inhibitor WP1066 is tested in a phase 1 clinical trial on patients with malignant glioma and brain metastasis from melanoma with an estimated completion in 2022.

Furthermore, Lee et al. (2011) observed that CD24 drives tumor initiation via STAT3 and Wang et al. (2010) showed that CD24 can regulate the MAPK pathway, demonstrating the importance of CD24 in tumor cell survival and proliferation. Interestingly, I could also show that patients which survived longer had a lower CD24 expression compared to patients with a shorter survival time (Figure 15F). Hence, CD24 had a negative impact on survival. This is good agreement with several studies in different carcinomas summarized by Fang et al. (2010). In breast cancer, for instance; Kristiansen et al. (2003) could show that high CD24 expression correlates with poor prognosis and the same could be shown for cholangiocarcinoma (Agrawal et al. 2007).

These findings suggest that SOX2 and CD24 play an important role in mediating adaptive resistance via upregulating Src and STAT3.

5.2 Are the CD24 mediated activation of Src and STAT3 interrelated?

Bretz et al. (2012) have shown in carcinoma cells that CD24 KD impaired STAT3 phosphorylation and similar results were obtained when Src was depleted. The authors suggested that Src was the kinase linking CD24 to the activation of STAT3. Similar findings were presented by Niu et al. (2002) for malignant melanoma. In contrast, we did not observe any effect of the Src kinase inhibitors on the vemurafenib-mediated phosphorylation of STAT3 in our experiments (Figure 14D). Likewise, in SOX2 OE A375 cells that showed strong STAT3 activation the Src inhibitor treatment did not alter this status (Figure 14A). Moreover, Src KD via siRNA had no effect on the STAT3 activation as demonstrated in Figure 17E. In addition, we could observe an upregulation of STAT3 already after 6 h of vemurafenib treatment while Src needed a longer time to get activated (Figure 17D). Consequently, I conclude that in our melanoma cell line model Src is not the kinase driving activation of STAT3. A recent study on colorectal cancer has shown that Hsp90 can serve as a signal-transmitting link between CD24 and STAT3 (Wang et al. 2016). Another study demonstrated that CD24 OE upregulates β-catenin expression (Lubeseder-martellato et al. 2016). Together with the studies of Anand et al. (2011) and Hao et al. (2006) who showed that β-catenin upregulates and activates STAT3 this reveals a potential STAT3 activation by CD24 via β-catenin. But more research is necessary to determine how CD24 activates STAT3 during vemurafenib treatment.

5.3 STAT3 activation is required for vemurafenib-induced SOX2 and CD24 expression

Several studies have already shown that STAT3 activation plays an important role in drug resistance (Liu et al. 2013; Zhao et al. 2016; H. J. Lee et al. 2014) as well as in the CD24-mediated tumor initiation (Lee et al. 2011).

I could show that early activation of STAT3 was required to obtain an increased expression of SOX2 and CD24 upon vemurafenib treatment (Figure 17A-C). Additionally, a KD of STAT3 with siRNA resulted in a decreased expression of SOX2 and CD24 (Figure 17E) while Src KD had no effect on the expression of SOX2 and CD24. Therefore, the STAT3 activation must be upstream of SOX2 which then regulates

the CD24 expression. That STAT3 is able to initiate the expression of SOX2 by directly binding to its promotor was already shown in two studies (Foshay & Gallicano 2008; Pietrobono et al. 2016). Foshay and Gallicano (2008) could show this in neural precursor cells while Pietrobono et al. (2016) even could show the binding of STAT3 to the SOX2 promotor in melanoma cells.

Taken together, these results suggest that the vemurafenib-induced expression of SOX2 and CD24 was due to vemurafenib-mediated activation of STAT3.

5.4 How is STAT3 activated upon vemurafenib treatment?

Here I showed that STAT3 was not activated by Src as reported by others (Bretz et al. 2012; Niu et al. 2002) but rather by soluble factors since the supernatant of vemurafenib-pulsed cells alone was able to activate STAT3 (Figure 18B). Haferkamp et al. (2013) could already show that vemurafenib induces senescence in melanoma cells. In combination with the observation of Ohanna et al. (2013) showing that the secretome, especially CCL2 and IL-6, of senescent melanoma cells drives basal melanoma cells towards a mesenchymal phenotype and activates the STAT3 pathway, STAT3 activation might be due to secreted factors. Moreover, Sos et al. (2014) could even show that vemurafenib-induced IL-6 secretion can lead to resistance via the activation of STAT3. To test this hypothesis in our settings, a cytokine array was performed which did not show a significant upregulation of any cytokine present on the array upon vemurafenib treatment. As CCL2 and IL-6 were part of the array I conclude that the vemurafenib-induced STAT3 activation is not due to their secretion. Pietrobono et al. (2016) showed another possible mechanism of STAT3 activation in melanoma. They could demonstrate that gentian violet (GV), a cationic triphenylmethane, can repress melanoma stem cell self-renewal through inhibition of SOX2. The authors suggested that GV suppressed STAT3 activation through an EGFR-dependent mechanism. Hence, EGFR activation by its ligands might be the reason for the vemurafenib-induced STAT3 activation. Therefore, a phospho-RTK array was performed (Figure 19). The most striking result was the activation of ErbB3. Interestingly, it was already shown that ErbB3 activation plays an important role in adaptive resistance (Abel et al. 2013) and is connected to STAT3 activation (Yu et al. 2014). Moreover, it could be shown that ADAMs lead to the cleavage of ErbB3 ligands such as heregulin 1β (Kirkegaard et al. 2014; Finigan et al.

2011). Additionally, Capparelli et al. (2015) showed that fibroblast derived heregulin 1β promotes resistance via the activation of ErbB3. This is in good agreement with my observation showing that if TAPI-2, an inhibitor of ADAMs, is present in addition to vemurafenib, STAT3 was less activated and the vemurafenib induced expression of SOX2 and CD24 was less pronounced (Figure 18C). Thus, it can be concluded that vemurafenib might activate STAT3 by ligands binding ErbB3 i.e. heregulin 1β which are cleaved by ADAMs. Hence, vemurafenib might have an influence on the activity of ADAMs or their accessibility to their substrate molecule like heregulin 1β. Further research is necessary to investigate how vemurafenib regulates ADAMs cleavage of molecules and to find out which ligand activates ErbB3. Moreover, it has to be proven in our system that ErbB3 is responsible for the vemurafenib-induced activation of STAT3.

Another interesting finding is the early activation of NF-kappa B after vemurafenib treatment (Figure 18A). This is in line with the observation of Lehraiki et al. (2015) who could show that vemurafenib induces the activation of NF-kappa B promoting melanoma cell survival and vemurafenib resistance. While Lehraiki and collegues (2015) showed that the vemurafenib-induced activation of NF-kappa B is mediated by TNFα, which is highly secreted after administration of vemurafenib, I did not observe any change in the amount of TNFα in the supernatant after vemurafenib treatment. Moreover, TNFα treatment of cells did not change STAT3 activation or SOX2/CD24 expression (Figure 18C). Hence, my results do not confirm the results by Lehraiki et al. (2015). However, there are other publications which also show that NF-kappa B activation is an important event/ prerequisite for STAT3 activation (Bretz et al. 2013; Agarwal & Zambidis 2014). Moreover, Hinohara et al. (2012) even showed that in mammosphere formation NF-kappa B activation plays an very important role as it promotes ErbB3 activation via heregulin. Thus, it might be possible that the vemurafenib-induced NF-kappa B activation could lead to an ErbB3 activation via heregulin resulting in a STAT3 activation. As heregulin needs to be cleaved from the cell surface via ADAMs this would also explain the role of ADAMs in the vemurafenib-induced STAT3 activation.

Thus, it is quite possible that diverse signaling pathways can lead to STAT3 activation which in turn can trigger SOX2 expression. It is becoming clear that feedback activation of STAT3 plays a prominent role in mediating drug resistance to a broad spectrum of targeted cancer therapies and chemotherapies including melanoma therapy.

5.5 The role of SOX2 and CD24 in acquired resistance in melanoma

To examine if SOX2 and CD24 also play a role in acquired resistance, resistant cell lines were established (Figure 20). Apparently neither SOX2 nor CD24 played a major role in acquired resistance as in the established resistant cell lines HT144 res, A375 res and SK Mel 28 res SOX2 and CD24 expression were not permanently upregulated and vemurafenib exposure could not upregulate SOX2 or CD24 anymore (Figure 21A-E&H&I). Moreover, a siRNA-mediated KD of SOX2 in cells that acquired resistance did not lead to a retrieval of sensitivity (Figure 21F&G). These observations are in agreement with a recent publication demonstrating that SOX2 has no oncogenic function during melanoma development and is not required for the acquisition of resistance to BRAFi treatments (Cesarini et al. 2017).

Therefore, I conclude that SOX2-mediated upregulation of CD24 and the activation of Src and STAT3 are only instrumental in establishing resistance shortly after the start of vemurafenib treatment. It most likely acts as an emergency plan to rescue many cancer cells from death induced by BRAFi treatment.

5.6 Melanoma cell lines with acquired resistance

To further characterize the resistant cell lines, several signaling pathways were investigated. ERK phosphorylation was strong in all resistant cell lines, although they were still treated with the MAPK pathway inhibitors (vemurafenib or trametinib) (Figure 22A). This finding is consistent with other studies showing that ERK is more strongly phosphorylated in resistant cell lines even if they are treated with MAPK pathway inhibitors (Herreros-Villanueva et al. 2013; Ahn et al. 2015). As increased activation of AKT is a possible mechanism promoting acquired resistance (Perna et al. 2015; Villanueva et al. 2011; Manzano et al. 2016), AKT activation in resistant cell lines in comparison to their parental counterparts was examined. Indeed, HT144 res and in SK Mel 28 res cells showed an increased activation of AKT (Figure 22A). Since I could show that Src and STAT3 signaling play an important role in adaptive resistance, I studied if their activation was changed in cells that acquired resistance. Interestingly, I found Src to be upregulated in HT144 res cells while STAT3 was upregulated in A375 res 5 µM vem, A375 res 130 nM tra and SK Mel 28 res cells (Figure 22A). That Src and

STAT3 activity also play an important role in acquired resistance was shown by several studies (Sinnberg et al. 2011; Liu et al. 2013; Girotti et al. 2013; Girotti et al. 2015).

The expression levels of MITF and Axl were shown to play an important role in conferring resistance to melanoma cells in several studies. The study of Müller et al. (2014) showed a relationship between early resistance and a low MITF/Axl ratio. Here, an elevated amount of Axl was only detected in SK Mel 28 res cells in comparison to the parental cells. These cells also showed a decreased expression of MITF (Figure 22B, C, E). Thus, these results are in good agreement with the study of Müller et al. (2014). Furthermore, a lower expression of MITF was detected in all resistant cell lines in comparison to their parental counterparts (Figure 22C&E). This is consistent with the findings from a great number of studies (Konieczkowski et al. 2014; Müller et al. 2014; Sun et al. 2014). Interestingly, some other studies reported the opposite, demonstrating that a high expression of MITF favors resistance (Van Allen et al. 2014; Johannessen et al. 2013). These discrepancies might be due to the different approaches used in the studies. Moreover, the majority of the resistant cells show a decrease in the expression of SOX10 (Figure 22D&E). This is in good agreement with the study of Sun et al. (2014) that demonstrated a loss of SOX10 in samples from patients that did not respond to targeted therapy. Another study revealed an increased expression of shRNA targeting SOX10 mRNA in resistant cells. Since SOX10 is important for differentiation in melanocytes less SOX10 leads to a more dedifferentiated and slower growing phenotype. This phenotype is associate with an increased resistance (Zhang & Herlyn 2014). This is in line with my observation that in the majority of the resistant cell lines the CDK inhibitors p27 and p21 were increased favoring a less proliferative phenotype (Figure 23). Carlino et al. (2014) also showed that p27 is accumulated upon BRAF and MEK inhibitor resistance. Moreover, resistance to targeted therapy was also linked to an increased expression of EGFR (Sun et al. 2014; Zhang & Herlyn 2014). However, no increase in the EGFR expression in resistant cells was observed in this study (Figure 22F). Further analysis of the microarray expression data revealed an altered activation of TGFβ signaling in the resistant cells. This is consistent with previous studies (Sun et al. 2014; Zhang & Herlyn 2014) showing that an altered TGFβ signaling plays an important role in resistance. Moreover, the microarray data also showed a change in cell survival, proliferation and cellular motility. These all are important feature in resistance.

Interestingly, I saw a downregulation of the tumor suppressor RUNX3 in the microarray data of resistant cells. RUNX3 downregulation was already shown previously to play a role in resistance (Zheng et al. 2013). AGPAT9, which I also found to be downregulated in the resistant cells, was already shown to be an important tumor suppressor and downregulated upon drug resistance in breast cancer (Fan et al. 2015). In contrast NUPR1 which has already been shown to induce resistance in different cancers is upregulated in resistant cells (Chowdhury et al. 2009). Taken together, these results suggest that the development of acquired resistance is accompanied by a broad spectrum of pathway alterations as well as changes in the expression of different proteins.

6 Conclusion

Taken together, this work contributes to the understanding of the various steps involved in the development of vemurafenib-resistance, especially the adaptive resistance. Here, I report that BRAFi treatment led to an increase in STAT3 activation shortly after treatment with vemurafenib. This might be mediated by an increased shedding of for example heregulin 1β which then could bind to specific receptors (i.e. ErbB3) which are able to activate STAT3. The increased activation of STAT3 promoted SOX2 expression. SOX2 in turn upregulated the expression of CD24 by binding to its promotor. CD24 activated Src and STAT3 signaling leading to increased cell survival. In accordance with this I showed that SOX2 or CD24 overexpressing cells can tolerate a higher dose of BRAFi treatment. Since inhibition of STAT3 or Src was still effective in the more resistant SOX2 and CD24 overexpressing cell lines, it might be beneficial to use Src or STAT3 inhibitors together with MAPK pathway inhibitors in order to block this escape pathway and thereby prevent adaptive resistance in clinical settings. Another possibility is to target CD24 directly by the use of monoclonal antibodies. Due to its high importance for different cellular functions targeting SOX2 might lead to a lot of unwanted side effects.

While in adaptive resistance SOX2 and CD24 played an important role they seemed to be of minor impact in acquired resistance. Hence, other molecules and pathways which are yet to identify play a key role in acquired resistance.

7 References

Abel, E. V. et al., 2013. Melanoma adapts to RAF/MEK inhibitors through FOXD3-mediated upregulation of ERBB3. *Journal of Clinical Investigation*, 123(5), pp.2155–2168.

Adameyko, I. et al., 2012. Sox2 and Mitf cross-regulatory interactions consolidate progenitor and melanocyte lineages in the cranial neural crest. *Development*, 139(2), pp.397–410.

Agarwal, J.R. & Zambidis, E.T., 2014. The Role of an NFκB-STAT3 Signaling Axis in Regulating the Induction and Maintenance of the Pluripotent State. *Pluripotent Stem Cell Biology - Advances in Mechanisms, Methods and Models*. Available at: http://www.intechopen.com/books/pluripotent-stem-cell-biology-advances-in-mechanisms-methods-and-models/the-role-of-an-nf-b-stat3-signaling-axis-in-regulating-the-induction-and-maintenance-of-the-pluripot.

Agrawal, S. et al., 2007. CD24 expression is an independent prognostic marker in cholangiocarcinoma. *Journal of Gastrointestinal Surgery*, 11(4), pp.445–451.

Ahn, J.H., Han, B.I. & Lee, M., 2015. Induction of resistance to brafinhibitor is associated with the inability of spry2 to inhibit BRAF-V600E activity in BRAF mutant cells. *Biomolecules and Therapeutics*, 23(4), pp.320–326.

Aigner, S. et al., 1997. CD24, a mucin-type glycoprotein, is a ligand for P-selectin on human tumor cells. *Blood*, 89(9), pp.3385–95. Available at: http://www.bloodjournal.org/content/89/9/3385.abstract.

Aigner, S. et al., 1998. CD24 mediates rolling of breast carcinoma cells on P-selectin. *The FASEB journal : official publication of the Federation of American Societies for Experimental Biology*, 12(12), pp.1241–1251.

Van Allen, E.M. et al., 2014. The genetic landscape of clinical resistance to RAF inhibition in metastatic melanoma. *Cancer Discovery*, 4(1), pp.94–109.

Alonso, M.M. et al., 2011. Genetic and epigenetic modifications of Sox2 contribute to the invasive phenotype of malignant gliomas. *PLoS ONE*, 6(10).

Anand, M., Lai, R. & Gelebart, P., 2011. β-catenin is constitutively active and increases STAT3 expression/activation in anaplastic lymphoma kinase-positive anaplastic large cell lymphoma. *Haematologica*, 96(2), pp.253–261.

Baumann, P. et al., 2005. CD24 expression causes the acquisition of multiple cellular properties associated with tumor growth and metastasis. *Cancer Research*, 65(23), pp.10783–10793.

Baumann, P. et al., 2012. CD24 interacts with and promotes the activity of c-src within lipid rafts in breast cancer cells, thereby increasing integrin-dependent adhesion. *Cellular and Molecular Life Sciences*, 69(3), pp.435–448.

Bensimon, J. et al., 2016. Forced extinction of CD24 stem-like breast cancer marker alone promotes radiation resistance through the control of oxidative stress. *Molecular Carcinogenesis*, 55(3), pp.245–254.

Bernhardt, M. et al., 2017. Melanoma-Derived iPCCs Show Differential Tumorigenicity and Therapy Response. *Stem Cell Reports*, 8. Available at: http://linkinghub.elsevier.com/retrieve/pii/S2213671117301133.

Bhatia, S., Tykodi, S.S. & Thompson, J.A., 2009. Treatment of metastatic melanoma: an overview. *Oncology (Williston Park, N.Y.)*, 23(6), pp.488–96. Available at: http://www.ncbi.nlm.nih.gov/pubmed/19544689%5Cnhttp://www.pubmedcentral.nih.gov/articlerender.fcgi?artid=PMC2737459.

Börner, K. et al., 2013. Robust RNAi enhancement via human Argonaute-2 overexpression from plasmids, viral vectors and cell lines. *Nucleic Acids Research*, 41(21), p.e199.

Bretz, N.P. et al., 2013. Body fluid exosomes promote secretion of inflammatory cytokines in monocytic cells via Toll-Like receptor signaling. *Journal of Biological Chemistry*, 288(51), pp.36691–36702.

Bretz, N.P. et al., 2012. CD24 controls Src/STAT3 activity in human tumors. *Cellular and Molecular Life Sciences*, 69(22), pp.3863–3879.

Capparelli, C. et al., 2015. Fibroblast-derived neuregulin 1 promotes Compensatory ErbB3 receptor signaling in mutant BRAF melanoma. *Journal of Biological Chemistry*, 290(40), pp.24267–24277.

Carlino, M.S. et al., 2014. Differential activity of MEK and ERK inhibitors in BRAF inhibitor resistant melanoma. *Molecular Oncology*, 8(3), pp.544–554. Available at: http://dx.doi.org/10.1016/j.molonc.2014.01.003.

Cesarini, V. et al., 2017. Sox2 is not required for melanomagenesis, melanoma growth and melanoma metastasis in vivo. *Oncogene*, (January), pp.1–8. Available at: http://dx.doi.org/10.1038/onc.2017.53.

Chen, G.-Y. et al., 2009. Supporting Online Material for CD24 and Siglec-10 Selectively Repress Tissue Damage-Induced Immune Responses. *Science*, 885(March), pp.1722–1726.

Chen, S. et al., 2014. SOX2 regulates apoptosis through MAP4K4-Survivin signaling pathway in human lung cancer cells. *Carcinogenesis*, 35(3), pp.613–623.

Chowdhury, U.R. et al., 2009. Emerging role of nuclear protein 1 (NUPR1) in cancer biology. *Cancer and Metastasis Reviews*, 28(1–2), pp.225–232.

Colombino, M. et al., 2014. Targeted Therapies in Melanoma: Knowledge, Resistance and Perspectives. *Journal of Carcinogenesis & Mutagenesis*, S4, p.4. Available at: http://omicsonline.org/open-access/targeted-therapies-in-melanoma-knowledge-resistance-and-perspectives-maria-colombino-2157-2518-S4-004.php?aid=27244.

Coqueret, O., 2003. New roles for p21 and p27 cell-cycle inhibitors: A function for each cell compartment? *Trends in Cell Biology*, 13(2), pp.65–70.

Cufí, S. et al., 2012. Metformin-induced preferential killing of breast cancer initiating CD44+CD24-/low cells is sufficient to overcome primary resistance to trastuzumab in HER2+ human breast cancer xenografts. *Oncotarget*, 3(4), pp.395–398. Available at: http://www.oncotarget.com/fulltext/488.

Darnell, J.E., 1997. STATs and gene regulation. *Science*, 277(5332), pp.1630–1635.

Deng, X. et al., 2017. CD24 Expression and differential resistance to chemotherapy in triple-negative breast cancer. *Oncotarget*, 5(0), p.10.18632/oncotarget.16203. Available at: http://www.oncotarget.com/abstract/16203.

Dogan, I. et al., 2014. SOX2 expression is an early event in a murine model of EGFR mutant lung cancer and promotes proliferation of a subset of EGFR mutant lung adenocarcinoma cell lines. *Lung Cancer*, 85(1), pp.1–6. Available at:

http://dx.doi.org/10.1016/j.lungcan.2014.03.021.

Emery, C.M. et al., 2009. MEK1 mutations confer resistance to MEK and B-RAF inhibition. *Proceedings of the National Academy of Sciences of the United States of America*, 106(48), pp.20411–20416.

Fajuyigbe, D. & Young, A.R., 2016. The impact of skin colour on human photobiological responses. *Pigment Cell and Melanoma Research*, 29(6), pp.607–618.

Fallahi-Sichani, M. et al., 2017. Adaptive resistance of melanoma cells to RAF inhibition via reversible induction of a slowly dividing de-differentiated state. *Molecular Systems Biology*, 13(1), p.905. Available at: http://msb.embopress.org/lookup/doi/10.15252/msb.20166796.

Fan, S.-H. et al., 2015. AGPAT9 suppresses cell growth, invasion and metastasis by counteracting acidic tumor microenvironment through KLF4/ LASS2/V-ATPase signaling pathway in breast cancer. *Oncotarget*, 6(21). Available at: www.impactjournals.com/oncotarget%5Cnwww.impactjournals.com/oncotarget/.

Fang, X. et al., 2010. CD24: From A to Z. *Cellular and Molecular Immunology*, 7(2), pp.100–103.

Finigan, J.H. et al., 2011. Neuregulin-1-human epidermal receptor-2 signaling is a central regulator of pulmonary epithelial permeability and acute lung injury. *Journal of Biological Chemistry*, 286(12), pp.10660–10670.

Flaherty, K.T. et al., 2012. Combined BRAF and MEK Inhibition in Melanoma with BRAF V600 Mutations. *New England Journal of Medicine*, 367(18), pp.1694–1703. Available at: http://www.nejm.org/doi/abs/10.1056/NEJMoa1210093.

Foshay, K.M. & Gallicano, G.I., 2008. Regulation of Sox2 by STAT3 initiates commitment to the neural precursor cell fate. *Stem cells and development*, 17(2), pp.269–278.

Gandini, S. et al., 2005. Meta-analysis of risk factors for cutaneous melanoma: II. Sun exposure. *European Journal of Cancer*, 41(1), pp.45–60.

Gibney, G.T. & Smalley, K.S.M., 2013. An unholy alliance: Cooperation between BRAF and NF1 in melanoma development and BRAF inhibitor resistance. *Cancer Discovery*, 3(3), pp.260–263.

Girotti, M.R. et al., 2013. Inhibiting EGF receptor or SRC family kinase signaling overcomes BRAF inhibitor resistance in melanoma. *Cancer Discovery*, 3(2), pp.158–167.

Girotti, M.R. et al., 2015. Paradox-breaking RAF inhibitors that also target SRC are effective in drug-resistant BRAF mutant melanoma. *Cancer Cell*, 27(1), pp.85–96. Available at: http://dx.doi.org/10.1016/j.ccell.2014.11.006.

Girouard, S.D. et al., 2012. SOX2 contributes to melanoma cell invasion. *Laboratory Investigation*, 92(3), pp.362–370. Available at: http://dx.doi.org/10.1038/labinvest.2011.188.

Goldman, A. et al., 2015. Temporally sequenced anticancer drugs overcome adaptive resistance by targeting a vulnerable chemotherapy-induced phenotypic transition. *Nature Communications*, 6, pp.1–13. Available at: http://dx.doi.org/10.1038/ncomms7139.

Haferkamp, S. et al., 2013. Vemurafenib Induces Senescence Features in Melanoma Cells. *Journal of Investigative Dermatology*, 133(6), pp.1601–1609. Available at: http://linkinghub.elsevier.com/retrieve/pii/S0022202X15362801.

Han, X. et al., 2012. Silencing SOX2 induced mesenchymal-epithelial transition and its expression predicts liver and lymph node metastasis of CRC patients. *PLoS ONE*, 7(8).

Hanahan, D. & Weinberg, R.A., 2011. Hallmarks of cancer: The next generation. *Cell*, 144(5), pp.646–674. Available at: http://dx.doi.org/10.1016/j.cell.2011.02.013.

Hao, J. et al., 2006. WNT/β-catenin pathway up-regulates Stat3 and converges on LIF to prevent differentiation of mouse embryonic stem cells. *Developmental Biology*, 290(1), pp.81–91. Available at: http://dx.doi.org/10.1016/j.ydbio.2005.11.011.

Herreros-Villanueva, M. et al., 2013. SOX2 promotes dedifferentiation and imparts stem cell-like features to pancreatic cancer cells. *Oncogenesis*, 2(8), p.e61. Available at: http://dx.doi.org/10.1038/oncsis.2013.23.

Hinohara, K. et al., 2012. ErbB receptor tyrosine kinase / NF-κB signaling controls mammosphere formation in human breast cancer. *Proceedings of the National Academy of Sciences of the United States of America*, 109(17), pp.6584–6589.

Hong, A. et al., 2017. Exploiting drug addiction mechanisms to select against MAPKi-resistant melanoma. *Cancer Discovery*, (January 2018), p.CD-17-0682. Available at: http://cancerdiscovery.aacrjournals.org/lookup/doi/10.1158/2159-8290.CD-17-0682.

Hough, M.R. et al., 1994. Mapping of CD24 and homologous sequences to multiple chromosomal loci. *Genomics*, 22(1), pp.154–161.

Jaggupilli, A. & Elkord, E., 2012. Significance of CD44 and CD24 as cancer stem cell markers: An enduring ambiguity. *Clinical and Developmental Immunology*, 2012.

Jia, X. et al., 2011. SOX2 promotes tumorigenesis and increases the anti-apoptotic property of human prostate cancer cell. *Journal of Molecular Cell Biology*, 3(4), pp.230–238.

Jiao, X.L. et al., 2013. Downregulation of CD24 inhibits invasive growth, facilitates apoptosis and enhances chemosensitivity in gastric cancer AGS cells. *European Review for Medical and Pharmacological Sciences*, 17(13), pp.1709–1715.

Johannessen, C.M. et al., 2013. A melanocyte lineage program confers resistance to MAP kinase pathway inhibition. *Nature*, 504(7478), pp.138–142. Available at: http://dx.doi.org/10.1038/nature12688.

Johannessen, C.M. et al., 2010. COT drives resistance to RAF inhibition through MAP kinase pathway reactivation. *Nature*, 468(7326), pp.968–972. Available at: http://dx.doi.org/10.1038/nature09627.

Kay, R., Rosten, P.M. & Humphries, R.K., 1991. CD24, a signal transducer modulating B cell activation responses, is a very short peptide with a glycosyl phosphatidylinositol membrane anchor. *Journal of immunology (Baltimore, Md. : 1950)*, 147(4), pp.1412–1416.

Ke, J. et al., 2012. A subpopulation of CD24+ cells in colon cancer cell lines possess stem cell characteristics. *Neoplasma*, 59(6), pp.622–630.

Keysar, S.B. & Jimeno, A., 2010. More than Markers: Biological Significance of Cancer Stem Cell-Defining Molecules. *Molecular Cancer Therapeutics*, 9(9), pp.2450–2457. Available at: http://mct.aacrjournals.org/cgi/doi/10.1158/1535-7163.MCT-10-0530.

Kim, H.J. et al., 2007. Isolation of CD24high and CD24low/- cells from MCF-7: CD24

expression is positively related with proliferation, adhesion and invasion in MCF-7. *Cancer Letters*, 258(1), pp.98–108.

Kirkegaard, T. et al., 2014. The broad-spectrum metalloproteinase inhibitor BB-94 inhibits growth, HER3 and Erk activation in fulvestrant-resistant breast cancer cell lines. *International Journal of Oncology*, 45(1), pp.393–400.

Kitaura, Y. et al., 2011. Transforming growth factor ??1 contributes to the invasiveness of pancreatic ductal adenocarcinoma cells through the regulation of CD24 expression. *Pancreas*, 40(7), pp.1034–1042.

Klinac, D. et al., 2013. Advances in personalized targeted treatment of metastatic melanoma and non-invasive tumor monitoring. *Frontiers in oncology*, 3(March), p.54. Available at: http://www.pubmedcentral.nih.gov/articlerender.fcgi?artid=3601325&tool=pmcentre z&rendertype=abstract.

Konieczkowski, D.J. et al., 2014. A melanoma cell state distinction influences sensitivity to MAPK pathway inhibitors. *Cancer Discovery*, 4(7), pp.816–827.

Kristiansen, G. et al., 2003. CD24 Expression Is a New Prognostic Marker in Breast Cancer. *Clin. Cancer Res.*, 9(13), pp.4906–4913. Available at: http://clincancerres.aacrjournals.org/content/9/13/4906.short.

Kristiansen, G. et al., 2010. Molecular and clinical dissection of CD24 antibody specificity by a comprehensive comparative analysis. *Laboratory Investigation*, 90(7), pp.1102–1116.

Kristiansen, G., Sammar, M. & Altevogt, P., 2004. Tumour biological aspects of CD24, a mucin-like adhesion molecule. *Journal of Molecular Histology*, 35(3), pp.255–262.

Kugel, C.H. & Aplin, A.E., 2014. Adaptive resistance to RAF inhibitors in melanoma. *Pigment Cell and Melanoma Research*, 27(6), pp.1032–1038.

Kulms, D. & Schwarz, T., 2006. NF-κB and Cytokines. *Vitamins and Hormones*, 74(6), pp.283–300.

Lee, H.J. et al., 2014. Drug resistance via feedback activation of stat3 in oncogene-addicted cancer cells. *Cancer Cell*, 26(2), pp.207–221. Available at: http://dx.doi.org/10.1016/j.ccr.2014.05.019.

Lee, S.H. et al., 2014. SOX2 regulates self-renewal and tumorigenicity of stem-like cells of head and neck squamous cell carcinoma. *British Journal of Cancer*, 111(11), pp.2122–2130.

Lee, T.K.W. et al., 2011. CD24 + Liver Tumor-Initiating Cells Drive Self-Renewal and Tumor Initiation through STAT3-Mediated NANOG Regulation. *Cell Stem Cell*, 9(1), pp.50–63. Available at: http://dx.doi.org/10.1016/j.stem.2011.06.005.

Lehraiki, A. et al., 2015. Increased CD271 expression by the NF-kB pathway promotes melanoma cell survival and drives acquired resistance to BRAF inhibitor vemurafenib. *Cell Discovery*, 1, p.15030. Available at: http://www.nature.com/articles/celldisc201530.

Liu, F. et al., 2013. Stat3-Targeted Therapies Overcome the Acquired Resistance to Vemurafenib in Melanomas. *Journal of Investigative Dermatology*, 133(8), pp.2041–2049. Available at: http://linkinghub.elsevier.com/retrieve/pii/S0022202X15363806.

Long, G. V. et al., 2014. Combined BRAF and MEK Inhibition versus BRAF Inhibition Alone in Melanoma. *New England Journal of Medicine*, 371(20), pp.1877–1888. Available at: http://www.nejm.org/doi/10.1056/NEJMoa1406037.

Long, G. V. et al., 2017. Dabrafenib plus trametinib versus dabrafenib monotherapy in patients with metastatic BRAF V600E/K-mutant melanoma: long-term survival and safety analysis of a phase 3 study. *Annals of oncology : official journal of the European Society for Medical Oncology*, 28(7), pp.1631–1639.

Lubeseder-martellato, C. et al., 2016. Membranous CD24 drives the epithelial phenotype of pancreatic cancer. *Oncotarget*, 7(31).

Lundberg, I. V et al., 2016. SOX2 expression is associated with a cancer stem cell state and down-regulation of CDX2 in colorectal cancer. *BMC cancer*, 16, p.471. Available at: http://www.ncbi.nlm.nih.gov/pubmed/27411517%5Cnhttp://www.pubmedcentral.nih.gov/articlerender.fcgi?artid=PMC4944515.

Manzano, J.L. et al., 2016. Resistant mechanisms to BRAF inhibitors in melanoma. *Annals of Translational Medicine*, 4(12), pp.237–237. Available at: http://atm.amegroups.com/article/view/10777/11428.

Marzagalli, M. et al., 2018. Targeting melanoma stem cells with the Vitamin E derivative δ-tocotrienol. *Scientific Reports*, 8(1), p.587. Available at:

http://www.nature.com/articles/s41598-017-19057-4.

Mierke, C.T., Bretz, N. & Altevogt, P., 2011. Contractile forces contribute to increased glycosylphosphatidylinositol- anchored receptor CD24-facilitated cancer cell invasion. *Journal of Biological Chemistry*, 286(40), pp.34858–34871.

Miller, A.J. & Mihm, M.C., 2013. Review Article. , 2(2), pp.156–171.

Moloney, F.J. et al., 2006. A population-based study of skin cancer incidence and prevalence in renal transplant recipients. *British Journal of Dermatology*, 154(3), pp.498–504.

Müller, J. et al., 2014. Low MITF/AXL ratio predicts early resistance to multiple targeted drugs in melanoma. *Nature communications*, 5, p.5712. Available at: http://www.pubmedcentral.nih.gov/articlerender.fcgi?artid=4428333&tool=pmcentre z&rendertype=abstract.

Muñoz-Couselo, E. et al., 2015. Recent advances in the treatment of melanoma with BRAF and MEK inhibitors. *Annals of translational medicine*, 3(15), p.207. Available at: http://www.ncbi.nlm.nih.gov/pubmed/26488003%5Cnhttp://www.pubmedcentral.nih. gov/articlerender.fcgi?artid=PMC4583602.

Nathanson, K.L. et al., 2013. Tumor genetic analyses of patients with metastatic melanoma treated with the BRAF inhibitor dabrafenib (GSK2118436). *Clinical Cancer Research*, 19(17), pp.4868–4878.

Nazarian, R. et al., 2010. Melanomas acquire resistance to B-RAF(V600E) inhibition by RTK or N-RAS upregulation. *Nature*, 468(7326), pp.973–977. Available at: http://dx.doi.org/10.1038/nature09626.

Niu, G. et al., 2002. Roles of activated Src and Stat3 signaling in melanoma tumor cell growth. *Oncogene*, 21(46), pp.7001–7010. Available at: http://www.nature.com/doifinder/10.1038/sj.onc.1205859.

Ohanna, M. et al., 2013. Secretome from senescent melanoma engages the STAT3 pathway to favor reprogramming of naive melanoma towards a tumor-initiating cell phenotype. *Oncotarget*, 4(12), pp.2212–2224. Available at: http://www.oncotarget.com/fulltext/1143.

Ono, Y.J. et al., 2015. Met Signaling Cascade Is Amplified by the Recruitment of Phosphorylated Met to Lipid Rafts via CD24 and Leads to Drug Resistance in Endometrial Cancer Cell Lines. *Molecular Cancer Therapeutics*, 14(10), pp.2353–2363. Available at: http://mct.aacrjournals.org/cgi/doi/10.1158/1535-7163.MCT-15-0187.

Overdevest, J.B. et al., 2012. CD24 expression is important in male urothelial tumorigenesis and metastasis in mice and is androgen regulated. *Proceedings of the National Academy of Sciences of the United States of America*, 109(51), pp.E3588-96. Available at: http://www.pubmedcentral.nih.gov/articlerender.fcgi?artid=3529071&tool=pmcentrez&rendertype=abstract.

Overdevest, J.B. et al., 2011. CD24 offers a therapeutic target for control of bladder cancer metastasis based on a requirement for lung colonization. *Cancer Research*, 71(11), pp.3802–3811.

Perna, D. et al., 2015. BRAF inhibitor resistance mediated by the AKT pathway in an oncogenic BRAF mouse melanoma model. *Proceedings of the National Academy of Sciences*, 112(6), pp.E536–E545. Available at: http://www.pnas.org/lookup/doi/10.1073/pnas.1418163112.

Pietrobono, S. et al., 2016. Down-Regulation of SOX2 Underlies the Inhibitory Effects of the Triphenylmethane Gentian Violet on Melanoma Cell Self-Renewal and Survival. *Journal of Investigative Dermatology*, 136(10), pp.2059–2069. Available at: http://dx.doi.org/10.1016/j.jid.2016.06.610.

Piva, M. et al., 2014. Sox 2 promotes tamoxifen resistance in breast cancer cells. *EMBO Molecular Medicine*, 6(1), pp.66–79.

Poulikakos, P.I. et al., 2011. RAF inhibitor resistance is mediated by dimerization of aberrantly spliced BRAF(V600E). *Nature*, 480(7377), pp.387–390. Available at: http://dx.doi.org/10.1038/nature10662.

Rastrelli, M. et al., 2014. Melanoma: epidemiology, risk factors, pathogenesis, diagnosis and classification. *In vivo (Athens, Greece)*, 28(6), pp.1005–11.

Read, J., Wadt, K.A.W. & Hayward, N.K., 2015. Melanoma genetics. *Journal of Medical Genetics*, 53(1), pp.1–14.

Ribeiro, C.S. et al., 2016. Melanoma associated with congenital intermediate common

blue nevus of the scalp - Case report. *Anais Brasileiros de Dermatologia*, 91(4), pp.514–516.

Runz, S. et al., 2008. CD24 induces localization of β1 integrin to lipid raft domains. *Biochemical and Biophysical Research Communications*, 365(1), pp.35–41.

Sachindra et al., 2017. New role of ID3 in melanoma adaptive drug-resistance. *Oncotarget*, 8(66), pp.110166–110175.

Sagiv, E. et al., 2008. Targeting CD24 for treatment of colorectal and pancreatic cancer by monoclonal antibodies or small interfering RNA. *Cancer Research*, 68(8), pp.2803–2812.

Samatar, A.A. & Poulikakos, P.I., 2014. Targeting RAS–ERK signalling in cancer: promises and challenges. *Nature Reviews Drug Discovery*, 13(12), pp.928–942. Available at: http://www.nature.com/doifinder/10.1038/nrd4281.

Sammar, M. et al., 1997. Mouse CD24 as a signaling molecule for integrin-mediated cell binding: Functional and physical association with src-kinases. *Biochemical and Biophysical Research Communications*, 234(2), pp.330–334.

Sanlorenzo, M. et al., 2014. Melanoma immunotherapy. *Cancer Biology and Therapy*, 15(6), pp.665–674.

Santini, R. et al., 2014. SOX2 regulates self-renewal and tumorigenicity of human melanoma-initiating cells. *Oncogene*, (August 2013), pp.1–12. Available at: http://www.ncbi.nlm.nih.gov/pubmed/24681955.

Sarkar, A. & Hochedlinger, K., 2013. The Sox family of transcription factors: Versatile regulators of stem and progenitor cell fate. *Cell Stem Cell*, 12(1), pp.15–30. Available at: http://dx.doi.org/10.1016/j.stem.2012.12.007.

Senner, V. et al., 1999. CD24 Promotes Invasion of Glioma Cells in Vitro.

Shi, H. et al., 2012. Melanoma whole-exome sequencing identifies V600EB-RAF amplification-mediated acquired B-RAF inhibitor resistance. *Nature Communications*, 3, p.724. Available at: http://www.nature.com/doifinder/10.1038/ncomms1727.

Sinnberg, T. et al., 2011. ??-Catenin Signaling Increases During Melanoma Progression and Promotes Tumor Cell Survival and Chemoresistance. *PLoS ONE*, 6(8).

Smalley, K.S.M. et al., 2008. Increased cyclin D1 expression can mediate BRAF inhibitor resistance in BRAF V600E–mutated melanomas. *Mol Cancer Ther*, 7(9), pp.2876–83.

Smith, S.C. et al., 2006. The metastasis-associated gene CD24 is regulated by Ral GTPase and is a mediator of cell proliferation and survival in human cancer. *Cancer Research*, 66(4), pp.1917–1922.

Song, W.S. et al., 2016. Sox2, a stemness gene, regulates tumor-initiating and drug-resistant properties in CD133-positive glioblastoma stem cells. *Journal of the Chinese Medical Association*, 79(10), pp.538–545. Available at: http://dx.doi.org/10.1016/j.jcma.2016.03.010.

Sos, M. et al., 2014. Oncogene Mimicry as a Mechanism of Primary Resistance to BRAF Inhibitors. , 8(4), pp.1037–1048.

Soufi, A., Donahue, G. & Zaret, K.S., 2012. Facilitators and impediments of the pluripotency reprogramming factors' initial engagement with the genome. *Cell*, 151(5), pp.994–1004. Available at: http://dx.doi.org/10.1016/j.cell.2012.09.045.

Spagnolo, F. et al., 2015. BRAF-mutant melanoma: Treatment approaches, resistance mechanisms, and diagnostic strategies. *OncoTargets and Therapy*, 8, pp.157–168.

Sun, C. et al., 2014. Reversible and adaptive resistance to BRAF(V600E) inhibition in melanoma. *Nature*, 508(7494), pp.118–122. Available at: http://www.ncbi.nlm.nih.gov/pubmed/24670642%5Cnhttp://www.nature.com/doifinder/10.1038/nature13121.

Sun, C. et al., 2013. Sox2 expression predicts poor survival of hepatocellular carcinoma patients and it promotes liver cancer cell invasion by activating Slug. *Medical Oncology*, 30(2).

Surowiak, P. et al., 2006. CD24 expression is specific for tamoxifen-resistant ductal breast cancer cases. *Anticancer Research*, 26(1 B), pp.629–634.

Takahashi, K. & Yamanaka, S., 2006. Induction of Pluripotent Stem Cells from Mouse Embryonic and Adult Fibroblast Cultures by Defined Factors. *Cell*, 126(4), pp.663–

676.

Topalian, S.L. et al., 2017. New England Journal. , pp.1311–1320.

Tsankov, A.M. et al., 2015. Transcription factor binding dynamics during human ES cell differentiation. *Nature*, 518(7539), pp.344–349. Available at: http://dx.doi.org/10.1038/nature14233.

Tsao, H. et al., 2012. Melanoma: From mutations to medicine. *Genes and Development*, 26(11), pp.1131–1155.

Villanueva, J., Vultur, A. & Herlyn, M., 2011. Resistance to BRAF inhibitors: Unraveling mechanisms and future treatment options. *Cancer Research*, 71(23), pp.7137–7140.

Wagner, N.B. et al., 2015. Diminished levels of the soluble form of RAGE are related to poor survival in malignant melanoma. *International Journal of Cancer*, 137(11), pp.2607–2617.

Wang, Q. et al., 2009. Oct3/4 and Sox2 are significantly associated with an unfavorable clinical outcome in human esophageal squamous cell carcinoma. *Anticancer research*, 29(4), pp.1233–41. Available at: http://www.ncbi.nlm.nih.gov/pubmed/19414369.

Wang, W. et al., 2010. CD24-dependent MAPK pathway activation is required for colorectal cancer cell proliferation. *Cancer Science*, 101(1), pp.112–119.

Wang, X. et al., 2016. CD24 promoted cancer cell angiogenesis via Hsp90-mediated STAT3/VEGF signaling pathway in colorectal cancer. *Oncotarget*, 7(34), pp.55663–55676. Available at: http://www.ncbi.nlm.nih.gov/pubmed/27494878%0Ahttp://www.pubmedcentral.nih.gov/articlerender.fcgi?artid=PMC5342444.

Wang, X. et al., 2014. SOX2 enhances the migration and invasion of ovarian cancer cells via Src kinase. *PLoS ONE*, 9(6).

Wang, X., 2012. STAT3 mediates resistance of CD44+CD24-/low breast cancer stem cells to tamoxifen in vitro. *Journal of Biomedical Research*, 26(5), pp.325–335. Available at: http://www.jbr-pub.org/ch/reader/view_abstract.aspx?file_no=JBR120504&flag=1.

Weina, K. et al., 2016. TGF- *β* induces SOX2 expression in a time-dependent manner in human melanoma cells. *Pigment Cell & Melanoma Research*. Available at: http://doi.wiley.com/10.1111/pcmr.12483.

Weina, K. & Utikal, J., 2014. SOX2 and cancer: current research and its implications in the clinic. Available at: http://www.clintransmed.com/content/pdf/2001-1326-3-19.pdf [Accessed August 14, 2015].

Wilbertz, T. et al., 2011. SOX2 gene amplification and protein overexpression are associated with better outcome in squamous cell lung cancer. *Modern Pathology*, 24(7), pp.944–953. Available at: http://www.nature.com/doifinder/10.1038/modpathol.2011.49.

Wuebben, E.L. & Rizzino, A., 2017. The dark side of SOX2 : cancer - a comprehensive overview.

Yang, C.-H. et al., 2014. Identification of CD24 as a cancer stem cell marker in human nasopharyngeal carcinoma. *PloS one*, 9(6), pp.e99412–e99412. Available at: http://www.pubmedcentral.nih.gov/articlerender.fcgi?artid=4067285&tool=pmcentrez&rendertype=abstract.

Yu, Z. et al., 2014. Downregulation of both EGFR and ErbB3 improves the cellular response to pemetrexed in an established pemetrexed-resistant lung adenocarcinoma A549 cell line. *Oncology Reports*, 31(4), pp.1818–1824.

Zarn, J.A. et al., 1996. Association of CD24 with the kinase c-fgr in a small cell lung cancer cell line and with the kinase lyn in an erythroleukemia cell line. *Biochemical and Biophysical Research Communications*, 225(2), pp.384–391.

Zhang, C. et al., 2015. RAF inhibitors that evade paradoxical MAPK pathway activation. *Nature*, 526(7574), pp.583–6. Available at: http://www.nature.com/doifinder/10.1038/nature14982%5Cnhttp://www.ncbi.nlm.nih.gov/pubmed/26466569.

Zhang, G. & Herlyn, M., 2014. Linking SOX10 to a slow-growth resistance phenotype. *Cell Research*, 24(8), pp.906–907. Available at: http://dx.doi.org/10.1038/cr.2014.67.

Zhang, S., 2014. Sox2, a key factor in the regulation of pluripotency and neural differentiation. *World Journal of Stem Cells*, 6(3), p.305. Available at: http://www.wjgnet.com/1948-0210/full/v6/i3/305.htm.

Zhao, C. et al., 2016. Feedback Activation of STAT3 as a Cancer Drug-Resistance Mechanism. *Trends in Pharmacological Sciences*, 37(1), pp.47–61. Available at: http://dx.doi.org/10.1016/j.tips.2015.10.001.

Zheng, Y. et al., 2013. Epigenetic downregulation of RUNX3 by DNA methylation induces docetaxel chemoresistance in human lung adenocarcinoma cells by activation of the AKT pathway. *International Journal of Biochemistry and Cell Biology*, 45(11), pp.2369–2378. Available at: http://dx.doi.org/10.1016/j.biocel.2013.07.013.
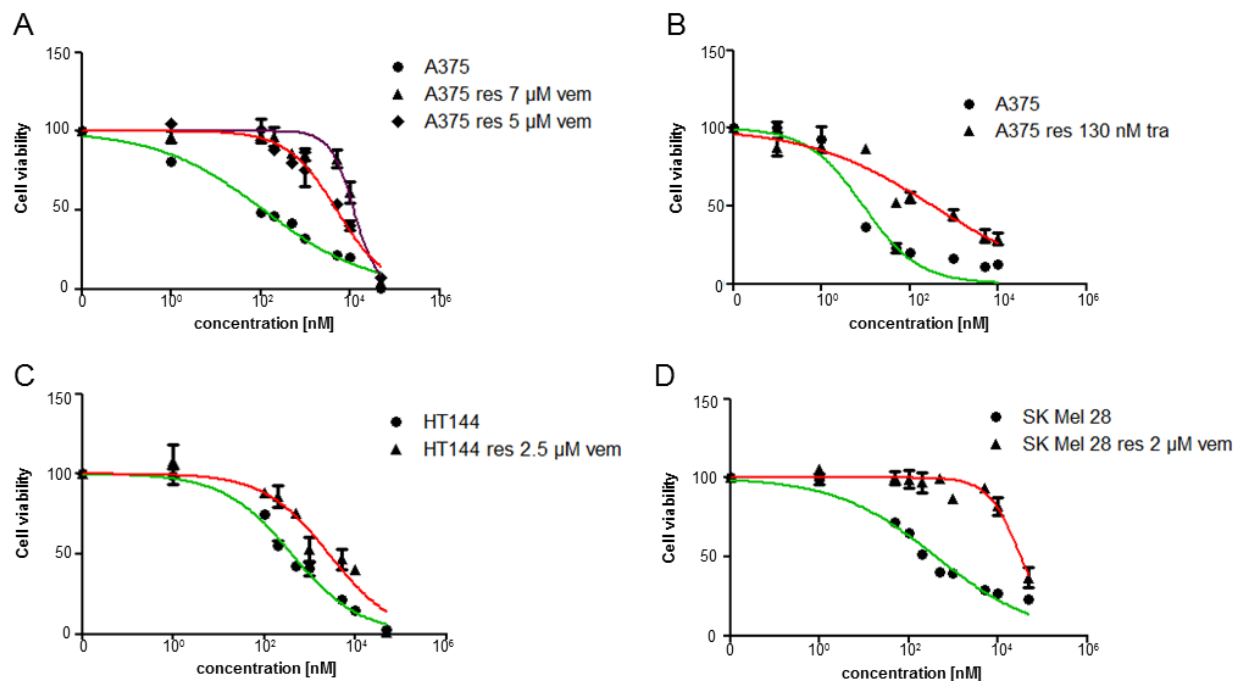
Appendix

Figure 25: Representative viability curves of cells that acquired resistance. A: A375, A375 res 7 µM vem and A375 res 5 µM vem cells treated with various concentrations of vemurafenib as indicated. **B:** A375 in comparison to A375 res 130 nM tra treated with different concentrations of trametinib as indicated. **C:** Viability curves of HT144 and HT144 res 2.5 µM vem treated with various concentrations of vemurafenib. **D:** Viability curves of SK Mel 28 cells in comparison to SK Mel 28 res 2µM vem treated with different vemurafenib concentrations.
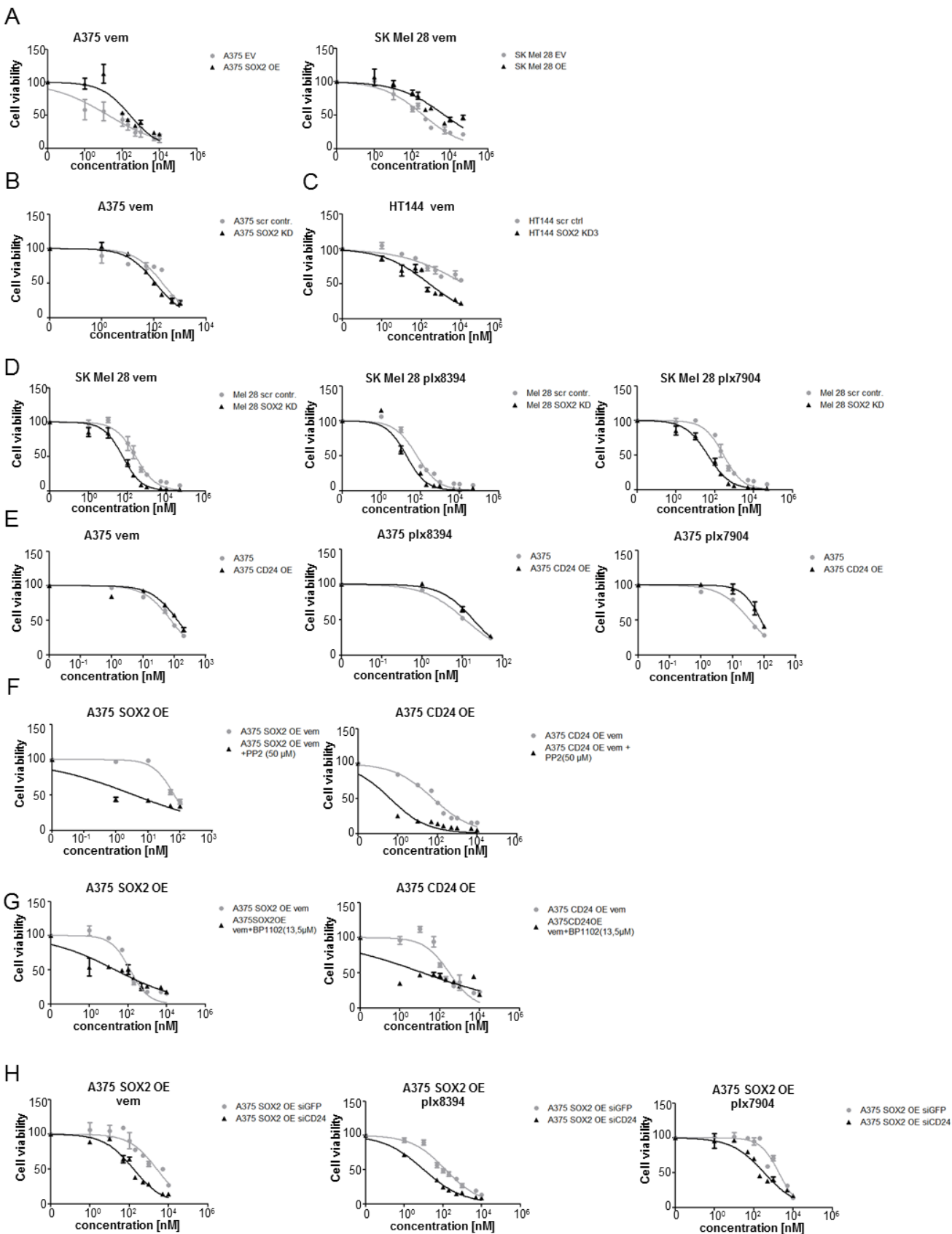
Figure 26: Representative viability curves. A: Viability curves for A375 and SK Mel 28 EV and SOX2 OE cells treated with different concentrations of vemurafenib are shown as indicated. **B:** A375 scramble control and SOX2 KD cells treated with different concentrations of vemurafenib to obtain a viability curve. **C:** KD of SOX2 made HT144 cells more sensitive as revealed by treatment with various concentrations of vemurafenib. **D:** Viability curves of SK Mel 28 scramble control and SOX2 KD cells treated with various concentrations of vemurafenib, plx8394 and plx7904. **E:** A375 EV and CD24 OE cells treated with vemurafenib, plx8394 and plx7904. **F:** A375 SOX2 OE and CD24 OE cells treated with different concentrations of vemurafenib and DMSO (grey curve) or PP2 [50 µM] (black curve) in addition. **G:** A375 cells with SOX2 or CD24 OE were treated with different concentrations of vemurafenib and DMSO (grey curve) or BP-1-102 [13.5 µM] (black curve) in addition. **H:** Viability curves of A375 SOX2 OE cells with siGFP (as control) or siCD24 knockdown treated with vemurafenib, plx8394, plx7904.

Acknowledgement

At the end of my thesis I want to thank serval people which made it possible for me to achieve this.

First, I want to thank **Prof. Dr. Jochen Utikal** who gave me the opportunity to work on this project in his lab. Especially, I am thankful for the great working atmosphere he created in the group. Moreover, I am highly appreciating the freedom to create and follow my own ideas while he was still making sure to not lose track.

I would like to thank **Prof. Dr. Peter Altevogt** for all the fruitful discussions and the plenty of brainstorming sessions. I enjoyed this lot. I am really thankful that he gave me a very good guidance with all his ideas and knowledge.

Moreover, I would like to thank **Prof. Dr. Viktor Umansky**, for being my first examiner as well as one of my TAC members. I am highly appreciating his scientific input thought my thesis to help to make it better. I also want to express my gratitude to my other TAC members, **Dr. Martin Sprick** and **Prof. Dr. Jonathan Sleeman**, for their suggestions and guidance in my PhD project.

I want to thank all my colleagues I worked with in the lab. I want to thank **Dr. Daniel Novak** for his guidance and supervision thought my thesis especially in cloning. Moreover, I want to thank him for proofreading my thesis as well as all the abstracts, posters etc. Especially, I want to thank **Sachindra** for his constant help and for sharing his knowledge with me. You were a great lab partner and made this a real fun place. My sit neighbor and very nice college **Nello** I want to thank for his help and advises and for providing me so often with sweets. **Karol** I want to thank for her help and advice especially in FACS and for always taking care that everybody gets a birthday present. We are a great social event team. I want to thank **Dr. Lionel Larribère** for scientific input. **Huizi** and **Maike** I want to thank for their constructive feedback and the nice times. My special thanks go to **Jenny** for being such a great technician. I know without you our lab would end up in chaos. Moreover, I want to thank **Sayran** for her help with the TMAs. I also want to thank **Dr. Kasia Weina** for getting me started in the lab. **James** and **Sunee** I want to thank for being such nice colleagues and all the fun moments. All in all I am very thankful for all my awesome colleagues who made this a great experience.

I also want to thank all my friends and my brother who always supported and believed in me. Especially, I want to thank **Robert** for being on my side for the whole time of my PhD. Last but not least, I want to thank my parents who made this way possible. You always made me strong by believing in me. I am really grateful that you were always there for me no matter what.